CATÓLICA
ESCOLA SUPERIOR DE BIOTECNOLOGIA
PORTO

EXPLORING THE POTENTIAL OF PORTUGUESE THERMAL SPRING WATER AS AN INGREDIENT FOR COSMETIC FORMULATIONS

by
Pedro Emanuel de Almeida Rocha

July 2025

CATÓLICA
ESCOLA SUPERIOR DE BIOTECNOLOGIA
PORTO

EXPLORING THE POTENTIAL OF PORTUGUESE THERMAL SPRING WATER AS AN INGREDIENT FOR COSMETIC FORMULATIONS

Dissertation presented to *Escola Superior de Biotecnologia* of the *Universidade Católica Portuguesa* to fulfil the requirements of Master of Science degree in **Applied Microbiology**

by
Pedro Emanuel de Almeida Rocha

Supervisor (Company): Ana Raquel Madureira
Co-supervisor (Company/University): Sílvia Santos Pedrosa

July 2025

Agradecimentos

Antes de mais queria agradecer, de forma sincera, à minha orientadora, Doutora Ana Raquel Madureira, e à minha co-orientadora, Doutora Sílvia Santos Pedrosa, por todo o apoio prestado no decorrer deste último ano. Pela vossa orientação e escolha permitiram-me prosseguir com este mestrado conciliando o trabalhando com o estudo, contribuindo decisivamente para o meu desenvolvimento académico e profissional. Tudo isto num ambiente onde nunca me faltaram nem recursos, nem apoio para a realização do meu trabalho. Agradeço, de forma especial, todo o tempo que me dedicaram, mesmo em agendas tão preenchidas, orientando-me no trabalho de laboratório, integrando-me na equipa e revendo cuidadosamente o meu trabalho, permitindo assim a concretização desta tese.

Gostaria também de agradecer aos meus colegas de laboratório, que foram uma ajuda fundamental na execução do trabalho aqui apresentado, bem como uma companhia constante e uma fonte de boa disposição durante as nossas pausas e almoços. Obrigado por me acolherem no vosso grupo e por tornarem as minhas horas de trabalho mais leves e menos solitárias. Em especial, deixo uma palavra de profundo agradecimento à Doutora Margarida Faustino, que foi das primeiras pessoas a auxiliar-me no meu projeto, demostrando sempre disponibilidade para me auxiliar, mesmo em períodos com mais carga de trabalho, e com uma preocupação constante com o meu progresso.

Gostaria de expressar a minha profunda gratidão aos meus pais e avó, pelo apoio incondicional que sempre demonstraram, nomeadamente aquando do meu ingresso neste mestrado. Sempre manifestaram uma preocupação genuína não apenas com o meu percurso académico e profissional, mas, sobretudo, com a minha realização pessoal e felicidade. Sem vocês nada do que atualmente alcancei seria possível. Agradeço-vos de coração por todos os esforços que fizeram para me ver crescer. Agradeço também ao meu irmão por estar do meu lado e por demonstrar preocupação e um interesse genuíno pelo meu percurso e atividades, mesmo no meio de uma grande fase de adaptação que foi a sua entrada na faculdade. Desejo-lhe muita força e sucesso neste novo caminho, na esperança de um dia poder ler também a sua tese.

Por fim, mas não menos importante, quero agradecer à minha namorada, Sofia. Nestes últimos anos, passámos ambos por fases marcantes, que evidenciam o quanto crescemos juntos. O meu mais profundo obrigado por ter sido – e continuar a ser - o meu pilar de apoio, por todas as horas em que me ouviu, pelos desabafos partilhados e por todos os momentos em que me retirou um sorriso e uma gargalhada mesmo quando eu próprio acreditava que tal não seria possível. Sem o seu apoio, esta última etapa teria sido, sem dúvida, muito mais difícil de superar.

A todos os mencionados acima e a todos aqueles que de alguma forma contribuíram para esta conquista,

MUITO OBRIGADO

Resumo

As águas termais, tradicionalmente empregues pelos seus benefícios à saúde, são progressivamente reconhecidas pela comunidade científica, pelo seu relevante potencial terapêutico. Tais características devem-se em grande parte às suas composições minerais únicas, resultantes de interações prolongadas entre a água e as rochas. têm impulsionado o interesse nas TSW na indústria cosmética, impulsionado pela procura dos consumidores por ingredientes naturais e eficazes. Esta tese tem como objetivo investigar o potencial cosmético da água termal de Chaves, Portugal, uma nascente historicamente reconhecida pelas suas propriedades cujas propriedades permaneciam cientificamente pouco exploradas.

Inicialmente, foi feita a caracterização da água termal de Chaves e a avaliação do seu potencial bioativo na pele. Resultados *in vitro* revelaram um potencial anti-inflamatório, evidenciado pela redução dos níveis de IL-6 em queratinócitos humanos expostos a poluentes urbanos, evidenciando a sua capacidade imunomodeladora. Para além disso, demonstrou ainda efeito anti-envelhecimento através da inibição da atividade da elastase. Um estudo clínico em 23 voluntários humanos demonstrou que a água termal melhorou significativamente a hidratação da pele quando desidratada e reduziu a perda transepidérmica de água, sugerindo uma melhoria da barreira cutânea sem perturbar a microbiota residente.

Com o objetivo de desenvolver uma formulação que incorporasse a água termal de Chaves e atendesse às expectativas dos consumidores, foi desenvolvida uma formulação com elevado índice de naturalidade (96% com base na ISO 16128:2:2017). O âmbito da investigação foi alargado para avaliar os efeitos desta na fibra capilar, uma aplicação que até ao momento, é cientificamente menos explorada no âmbito das águas termais. Embora a água termal de Chaves por si só não tenha alterado significativamente as propriedades da fibra capilar, a formulação melhorou a sua penteabilidade, provavelmente devido aos tensioativos incluídos. Por outro lado, a formulação diminuiu a temperatura de desnaturação térmica da queratina capilar, potencialmente ligada às interações surfactante-queratina observadas através das análises de DSC e ATR-FTIR.

Por fim, visando a melhoria da formulação desenvolvida, explorou-se a adição de extratos bioativos capazes de evidenciar as propriedades da formulação e da água termal de Chaves. Assim, foram selecionados os extratos de Malva (Malva sylvestris), endémico da região; e Pepino (Cucumis sativus), conhecidos pelos seus benefícios para a pele e pelo seu potencial antioxidante. Foram desenvolvidas três formulações contendo os extratos individuais e uma com a respetiva mistura. As relações sinérgicas dos seus componentes revelaram uma forte capacidade quelante do ião Fe^{2+}, sendo superior à do agente quelante integrado na formulação, isoladamente. Isto poderá estar associado ao aumento da atividade antioxidante e da significativamente maior inibição das enzimas colagenase e tirosinase, provavelmente devido à quelatação dos seus cofatores. A combinação de ambos o extrato conduziu também uma acrescida e potente inibição da elastase. Além disso, os efeitos anti-inflamatórios foram reavaliados utilizando-se uma mistura contendo a água termal, os extratos e o fitato de sódio (agente

quelante), que demonstrou, propriedades anti-inflamatórias semelhantes, no entanto reduzindo os níveis de IL-1α.

Em conclusão, este trabalho valida as propriedades benéficas da água termal de Chaves para os cuidados da pele, particularmente os seus efeitos anti-inflamatórios e de reforço da barreira cutânea. Além disso, demonstra que a formulação de água termal, especialmente quando reforçada com extratos naturais sinérgicos como a malva e o pepino, pode criar uma formulação multifuncional com atividades antioxidantes, anti-enzimáticas e anti-inflamatórias significativamente amplificadas, que representa uma promessa para os cuidados da pele e potencialmente do couro cabeludo.

Palavras-chave: Formulação cosmética, água termal, cosmecêuticos, condicionamento da fibra capilar, propriedades dermatológicas

Abstract

Thermal spring waters (TSW), utilized for centuries for their health benefits, are increasingly recognized scientifically for their therapeutic potential. These are largely attributed to their unique mineral compositions derived from long-term water-rock interactions. Properties like immunomodulation, antioxidant activity, and skin barrier reinforcement have spurred interest in TSW within the cosmetics industry, driven by consumer demand for natural and effective ingredients. This thesis aims at investigating the cosmetic potential of TSW from Chaves, Portugal, a historically recognized spring whose properties remained scientifically underexplored.

The initial phase characterized Chaves TSW and evaluated its dermatological bioactivities. *In vitro* studies revealed anti-inflammatory potential, evidenced by reduced IL-6 levels in human keratinocytes (HaCaT) exposed to urban pollutants, alongside with anti-elastase activity. A clinical study on 23 human volunteers demonstrated that Chaves TSW significantly improved skin hydration on dry skin volunteers and reduced transepidermal water loss (TEWL), suggesting skin barrier enhancement without disrupting the resident skin microbiota. Based on these positive skin findings, a cosmetic formulation incorporating Chaves TSW was developed with a high natural index (96% based on ISO 16128). The research scope was extended to evaluate the effects on hair, a less common application for TSW. While Chaves TSW alone did not significantly alter bleached hair fiber's properties, the formulation improved hair combability, likely due to included surfactants. Conversely, the formulation decreased the thermal denaturation temperature of hair keratin, potentially linked to surfactant-keratin interactions observed via DSC and ATR-FTIR analyses.

Finally, the base formulation's potential was further explored by incorporating Mallow (*Malva sylvestris*); endemic to the region; and Cucumber (*Cucumis sativus*) extracts, known for their skin benefits, such as antioxidant potential. Three formulations containing both extracts and a mixture of both were developed, and subsequent testing revealed significantly improved bioactivities. Notably, a strong synergistic Fe^{2+} chelating capacity emerged, exceeding that of the formulation's chelating agent alone. This correlated with enhanced antioxidant activity and significantly increased inhibition of the age-related enzymes collagenase and tyrosinase, likely due to cofactor chelation. The combination of extracts also yielded potent elastase inhibition. Furthermore, the anti-inflammatory effects were re-evaluated using a mixture containing TSW extracts, and sodium phytate (chelating agent), which nonetheless exhibited anti-inflammatory properties like those of water but effectively reducing IL-1α levels.

In conclusion, this work validates the beneficial properties of Chaves TSW for skincare, particularly its anti-inflammatory and barrier-reinforcing effects. It further demonstrates that formulating TSW, especially when enhanced with synergistic natural extracts like Mallow and Cucumber, can create multifunctional cosmetic ingredients with significantly amplified antioxidant, anti-enzyme, and anti-inflammatory activities, offering promise for advanced skin and potentially scalp care applications.

Key-words: Cosmetic formulation, thermal spring water, cosmeceuticals, hair fiber conditioning, dermatological properties

Contents

Figure index

Table Index

Supplementary figures index

Supplementary tables index

Abbreviation list

Abbreviation	Definition
18-MEA	18-Methyleicosanoic Acid
ABTS	2.2′-Azino-Bis (3-Ethylbenzothiazoline-6-Sulphonic Acid) Diammonium Salt
AGA	Androgenetic Alopecia
ATR-FTIR	Attenuated Total Reflection Fourier-Transform Infrared Spectroscopy
CAPB	Cocoamidopropyl Betaine
CFU	Colony-Forming Units
Ctrl	Control
DHT	Dihydrotestosterone
DMEM	Dulbecco's Modified Eagle Medium
DP	Dermal Papilla
DPPH	2,2-Diphenyl-1-Picrylhydrazyl
DSC	Differential Scanning Calorimeter
EC	Enzyme Control
ECM	Extracellular Matrix
ER	Endoplasmic Reticulum
FBS	Fetal Bovine Serum
FChv	Base Chaves' Thermal Spring Water Formulation
FM	Chaves' Thermal Spring Water Formulation Supplemented With Cucumber Extract
FMP	Chaves' Thermal Spring Water Formulation Supplemented With Both Extracts
FP	Chaves' Thermal Spring Water Formulation Supplemented With Cucumber Extract
FPHL	Female Pattern Hair Loss
HaCaT	Human Keratinocytes
nHDF	Human Dermal Fibroblasts
HFSCs	Hair Follicle Stem Cells

Abbreviation	Definition
IF	Intermediate Filament
IL-1α	Interleukin-1α
IL-6	Interleukin 6
IRS	Inner Root Sheath
KAPs	Keratin Associated Proteins
MMP1	Metalloproteinases 1
MHB	Mueller Hinton Broth
OD	Optical Density
ORS	Outer Root Sheath
PP	Pollution Particles
qPCR	Quantitative Real-Time PCR
ROS	Reactive Oxygen Species
SDA	Sbouraud Dextrose Agar
TACs	Transient Amplifying Matrix Cells
TEWL	Trans-Epidermal Water Loss
TSA	Tryptic Soy Agar
TSW	Thermal Spring Waters
UVR	Ultraviolet Radiation

Introduction

1. Thermal Spring Waters

Thermal springs are geological structure where water at elevated temperatures originates from subterranean depths where it is typically heated by volcanic activity and local geothermal gradient beneath the Earths' crust. Due to their origin, these waters are rich in dissolved minerals [1] and their composition may vary according to the geological profile of the spring's location. Since this composition is a consequence of the prolonged water-rock interactions, pH, temperature, and sediment mineralogy [2, 3], the mineral profile of these waters is substantially different from more superficial waters [4, 5]. Common elements such as chloride, bicarbonate, sulfate, sulfide and carbo-dioxide are present in combination with soluble minerals such as like magnesium, calcium, sodium, iron compounds, silicates, and trace minerals such as selenium, zinc, boron, among many others [6]. They therefore tend to exhibit a composition that reflects both the geological and geographical characteristics of the area.

These minerals are major key elements considered responsible for the beneficial health properties reported for these waters. Therefore one important parameter for the classification of these waters is their dry residue measurement at 180ºC [7]. This measures the amount of residual mineral salts present after the water evaporation and is an indicator of the water mineralization [8]. Temperature is another hallmark of TSWs, ranging from temperatures as low as 34ºC to temperatures as high as 255ºC [9, 10], allowing for further classification.

The remarkable diversity and unique properties of these waters enable them to produce a wide range of therapeutic effects, warranting their thorough investigation for potential health benefits. This thesis focuses on the well-known thermal spring waters (TSW) from the Chaves region in northern Portugal. Used as a local spa since Roman times, Chaves TSW emerge from its source at approximately 76 °C, contains a total dissolved solids of 1 600–1 800 mg/L, have a neutral pH, and is rich in bicarbonate, sodium, and CO_2 [11]. A comprehensive understanding of the interplay between these chemical and physical properties provides a scientific basis for validating their application in health and wellness.

1.1 Health Benefits of Thermal Spring Waters

In accordance to their variable mineral and thermal composition, TSWs possess a range of therapeutic benefits, that can positively impact dermatological conditions such as atopic and seborrheic dermatitis, psoriasis, and many other [6]. As an example, waters that exhibit high salt or sulfur content, are valuable for dermatological treatments due to their keratolytic, regenerative, antioxidant and anti-inflammatory properties [7].

These properties can even extend beyond skincare. Due to their antioxidant and anti-inflammatory effects, TSW can be used to tackle certain allergic disorders as well as exerting a positive impact on respiratory ailments, affecting both the upper and lower respiratory tract functions [12, 13]. Thermal waters may exhibit inherent antimicrobial properties, with potential benefits for both cutaneous and respiratory health. In dermatological contexts, immersion in these waters has been shown to aid in the

removal of microbial peptides implicated in certain skin disorders [7]. Additionally, thermal spring water (TSW) has demonstrated the ability to reduce populations of pathogenic bacteria, promote the restoration of beneficial microbiota, and inhibit biofilm formation in the respiratory tract [13].

In addition to the mineral composition, the temperature has also been regarded as an important factor. Although not interfering with its immunomodulatory properties, TSWs with a temperature similar to the human body have been reported to stimulate increased heart rate and cardiac flow, resulting in reduced blood pressure, alleviation of muscle spasms, pain control in soft tissues, treatment of osteoarticular infections and rebalancing of the neurovegetative system [14].

These waters have proven to have multiple benefits, nonetheless, it is possible to observe that the major organ affected by these properties is the skin, which is in direct contact with the water.

2. Impact of the Thermal Spring water on the skin

2.1. Skin structure

The skin is the biggest organ in the human body, which plays a pivotal role in various biological processes. It is constituted by different layers such as the epidermis, dermis and hypodermis. [15, 16]. The primary function of the skin is to act as a barrier to the entry of pathogens, to protect the body against solar radiation, as well as other physical and chemical harms, and to prevent water and extracellular fluids loss. Not only that but the skin also plays a role in regulating the body temperature, sensory perception, immunological reactions, hormone synthesis, and many other different functions [16].

Among the three layers, that constitute the skin, the epidermis is its outermost layer with thickness ranging from 0.5-1.5 mm. It is formed by a stratified squamous epithelial layer, where keratinocytes and melanocytes are the major constitutes. Analyzing deeply the structure of the skin, the epidermis can be further divided into four other layers. At the base, it is possible to observe the basal layer which is formed in part by the rapidly proliferating cells, where upon leaving the layer, they ascend, and some cells continue their differentiation until the stratum spinosum. This layer is proceeded by the stratum granulosum, which is the last layer that contains living cells, being then followed by the stratum corneum. It's in between these two structures that keratinocytes pass through their final step of differentiation, where they form flat, anucleated dead cells, named corneocytes which are the main components of the stratum corneum [16]. Through this differentiation process the skin gets continuously renewed, with the outermost cells being shed to maintain the total number cells in the epithelium constant [16, 17].

Beneath the epidermis, it's possible to observe the dermis. This thick layer is composed of fibrous and elastic tissue providing structural and nutritional support to the skin. Similar to the epidermis, the dermis is composed of two other smaller layers the thin and superficial papillary dermis, and a thicker and deeper reticular dermis. In the junction between the dermis with the epidermis is located the papillary dermis that is composed of loosely arranged collagen fibers. As for the reticular dermis, it is formed by thicker bundles of collagen parallel to the skin surface. In this layer there is a larger variety of cells containing fibroblasts, fibrocytes and structural cells of the blood and lymph vessels. In addition there

are many different populations of myeloid and lymphoid immune cells that either reside in or traffic through the dermis [16].

The final and deeper layer is the hypodermis. This layer serves as an energy reservoir, protects the skin and allows mobility by sliding over underlying structures. The major constituents of the hypodermis are the adipocytes which are organized in lobules defined by the fibrous connective tissue (septa). It's in the septa that the nerves, blood and lymphatic vessels are located [16].

Between these three layers, epidermis is the first layer that is in direct contact with the water's surface. However, the minerals present in the water might reach the dermis, passing through the hydrophobic barrier of the stratum corneum, and exerting their beneficial effect towards the skin [18].

2.2. Skin Aging

Skin aging is one of the most visible signs of human aging being dependent on intrinsic and extrinsic factors that define its exposome and are responsible for the emergence of the biological and clinical signs of aging. Solar radiation, air pollution, tobacco smoke and poor nutrition are some of the external factors of the skin exposome [19], that interact with the human body, and therefore their internal factors [20]. The exposome of the skin is responsible for the rearrangement of elastin and collagen in the skin, being also responsible for the reduction of skin moisture content, vessel walls thinning, lower production of sebum, increase in the skin pH, changing therefore the characteristics of the skin [21].

Skin accumulates an excessive number of senescent cells, leading to the gradual loss of cellular functions. These cells are metabolically active and are able to secrete pro-inflammatory cytokines, chemokines, proteases and growth factors. Immunological alterations are associated with ageing, turning progressively more hyperresponsive, with increased levels of pro-inflammatory cytokines such as IFN-α, TNF-α, IL-1, IL-6, leading to an imbalance between inflammatory and anti-inflammatory responses [22].

In addition, epidermal skin's barrier function gradually deteriorates. Epidermal stem cells are responsible for the replenishment of keratinocytes in the upper layer. During ageing, although the normal number of these cells is maintained their capacity to migrate and respond to proliferative signals declines, leading to a lower production rate of new keratinocytes. Since the stratum corneum serves as the primary component of the skin barrier a progressive degradation of its structure leads to a loss of its function [23]. This dysfunction may further exacerbate this chronic inflammation, increasing even further the levels of pro-inflammatory cytokines [22]. Such progressive disequilibrium of the immune system as well as the loss of the skin's barrier function, are responsible for the onset of skin conditions such as atopic dermatitis, prutius, rosacea, among others [22-24].

2.3. Health impact of TSW in the skin

2.3.1. Anti-inflammatory properties

Being the first line of defense against pathogens and noxious substances, the skin is a tissue characterized by having a significantly active immunological activity, with several resident immune cells

and recirculating lymphocytes. Dysregulations of this system caused by pathogens or other external factors such as physical and chemical aggressions, lead to the development of inflammatory conditions on the skin [25]. One of the most reported properties of the TSW is their capacity to modulate the immune response being crucial for the management of inflammatory skin conditions [7].

Dendritic cell differentiation and maturation, was reported to be affected by TSW, also impacting their cytokine production. TSW has revealed the ability to reduce the expression of differentiation and maturation markers on the surface of these cells upon stimulation by lipopolysaccharides, peptidoglycan and lipoteichoic acid, attenuating the activation of T cells [25]. Additionally, TSW revealed the capacity to promote IL-10 production from these cells. This cytokine known for its anti-inflammatory role, which protects the organism from exacerbated immune responses [26-28], may lead to the reduction of IL-12 and IL-23 which are known pro-inflammatory cytokines.

The pathway beneath the observed properties has not been disclosed yet. However, since the differential of these waters resides in their mineral composition, it is possible that they play a role in these immunomodulatory effects. Different minerals such as magnesium, zinc, copper, iron and selenium have different supporting roles in the immunologic system, regulating systemic inflammation. For instance, magnesium plays a crucial role in modulating the immune response, due to its influence on multiple immune cells, cytokines and signaling pathways. Zinc, for example, is involved in the development and function process of multiple immune cells with regulatory functions that range from the activation and differentiation of immune cells to their maintenance, playing also a crucial role in proinflammatory reactions by generation of cytokines [29]. Other minerals such as calcium, inhibit mast cell's release of histamine [7], modulating allergic responses and mediating autoimmune conditions and hematopoiesis, playing a key role in body inflammatory responses [30].

Other possible explanation for these properties might be associated with the microbial life that inhabits the geological zone of the spring. For an instance *Aquaphilus dolominae* extract, that is present in Avène's TSW aquifer revealed to be capable of inhibiting inflammatory mediators like IL-8, IL-4R, IL-18, macrophage inflammatory protein-3a, among other immune system components [31]. These waters host a multitude of microbial taxa as Aquificae, Proteobacteria, Firmicutes, Bacteroidetes, and Cyanobacteria [32-34] with each spring exhibiting a characteristic microbiota related with its geographical location and physicochemical properties [35, 36]. As an example, some species of Cyanobacteria such as *Nostoc spp.* or *Microcystis spp.*, are known to exert similar benefits through different metabolites [37].

By presenting a significant impact in modulating the inflammatory process, understanding the anti-inflammatory properties of TSW has been a focus of research in the area, leading to a consequent variety of reports in the topic.

2.3.2. Reinforcement of the skin barrier

As a physical and biological barrier, the skin is in continuous contact with the environment. Further than protecting the body from environmental insults, it also plays a crucial role in the regulation of water and solute loss.

TSW has been reported as an agent capable of reinforcing the skin barrier due to its capacity of modulating the expression of key markers such as filaggrin and human β-defensin 2. This regenerative activity according to Cauche, et al. [15], may be due to the presence of calcium in these water, since this ion is responsible for being a key regulator in keratinocyte differentiation and proliferation. Additionally, it has been reported that the presence of calcium also influences the expression of β-defensin 2, a antimicrobial peptide that contributes to microorganism defense through the skin, therefore playing a crucial role in the skin barrier function [15, 38].

Hydration of the skin is also an important characteristic required to maintain the normal function activity of enzymes that participate in desquamation. A deficient hydration turns the skin drier leading to the accumulation of corneocytes in the stratum corneum. With application of TSW it was reported an improvement in the hydration levels of the epidermis, being also possible to observe an increase in collagen I synthesis which in turn led to an increased epidermal thickness, enhancing the cellular renewing of this layer [15].

Additionally, TSW has been reported as capable of improving wound healing. Due to its exposure to external factors it is only natural that the skin is very susceptible to lesions, being thereafter subject to the healing process that is achieved through a complex interplay of biological components separated into a sequence of four phases:1) coagulation and haemostasis, which begins after injury; 2) inflammation, which begins shortly after; 3) proliferation, being the major healing process and 4) wound remodeling where scar tissue is formed. This process takes time, depending on the type of wound, however a complete recovery is not always possible [39]. Therefore, a therapeutic approach that is aimed at enhancing this process is highly sought after, and TSW's properties have been reported as a potential strategy in this regard.

3. Potential impact of Thermal Spring Water on the hair fiber

3.1. Hair fiber structure and growth

Similar to the skin, hair undergoes rapid stem cell division and differentiation, resulting in keratinocytes that migrate, flatten and die, giving rise to keratinized cells.

Its growth can be divided into three phases: anagen (growth), catagen (transition) and telogen (rest). They alternate with periods of rapid growth and elongation with quiescence and regression driven by apoptotic signals [40].

The anagen phase is the active phase where the entire hair shaft is produced, and the time in this phase varies depending on the type of hair follicle. Scalp hair follicles, for example, reside in this phase for 2-8 years, whereas eyebrow hair follicles reside for only two to three months. During ageing the proportion of follicles in this phase declines [41].

The catagen phase represents the transitory phase from anagen to telogen, lasting for approximately two weeks. During this phase, hair follicles regress and detach from the dermal papilla – the population of mesenchymal cell in hair follicles – which results in epithelial cell apoptosis in the bulb of the follicle. Afterwards, the dermal papilla moves upward towards the hair follicle bulge - where the majority of stem

cells are located in the hair's follicle bulb – whereas if it is unable to reach it, the follicle cycling terminates resulting in hair loss [41].

Finally, the telogen phase is a resting phase ranging from two to three months. At any time, about 9% of the total scalp hair resides in the telogen phase. During this period, new hair begins to develop at the base of the hair follicle, eventually pushing the old hair out [41].

The final product of all these phases is a hair fiber fully composed of keratin. However, this is not an unstructured agglomeration of keratin. Instead, the hair fiber exhibits an organized structure.

3.1.1. Hair follicle

The hair follicle is the primary structure responsible for hair growth. It is divided into three segments the infundibulum, the isthmus and the inferior segment, that represents the growing proportion of the follicle. At its base the bulb is formed by invagination of a tuft of vascularized loose connective tissue called the dermal papilla, responsible for the active production of hair [42].

3.1.1.1. Dermal Papilla (DP)

The dermal papilla is a specialized mesenchymal compartment located at the base of the hair follicle. It functions as a signaling center which regulates hair growth, shape, size and color.

Its formation begins upon release signals from dermal mesenchymal cells to the epithelial cells that lead to epithelium thickening in order to form the placode. The placode then promotes further mesenchymal cells proliferation that induces invagination and a downward extension of the basal cell of the placode into a mature DP. During the hair follicule formation, the inner basal cells differentiate into the inner root sheath (IRS), which encapsulates the future hair shaft, while the outer basal cells differentiate into the outer root sheath (ORS). Its in the ORS that the hair follicle stem cells (HFSCs) and melanocyte stem cells are located. The ORS cells then, differentiate into highly proliferative matrix cells at the bulb region, which surround the DP [43].

The mature DP serves as the signaling center for the hair follicles regulating the growth cycle. It's at the anagen phase that the DP cells release signals for the differentiation of transient amplifying matrix cells (TACs) – germ cells derived directly from the HFSCs that begin proliferating during anagen phase – into hair shafts. At the catagen phase, the DP cells remain intact although two-thirds of the lower follicle undergo apoptosis. During this phase these cells migrate upwards along the epithelium. It's at the telogen phase that the DP once again exhibits a signaling role. At this resting phase, the epithelial cells of the hair follicle remain in a quiescent state, and the DP is located at the tip of the hair follicle, being in direct contact with the hair germ cells. DP, can then signal these cell to rapidly proliferate into progenitor cells and differentiate into various mature cells, initiating the new hair growth cycle [43].

3.1.1.2. The Bulge

At the end of the catagen phase, the epithelial cells from the lower follicle suffered from apoptosis, reducing their size. The epithelial bulge is the region in the hair follicle where the HFSCs are located serving as a reservoir. These cells are typically slow-cycling - meaning they don't divide frequently during

normal homeostasis – and possess the capacity to self-renew and become activated upon signaling of, for example the DP [44].

The main purpose of the bulge is to continuously regenerate the hair follicle during cycling. Upon activation these cells proliferate and mi grate downwards to repopulate the matrix, allowing for the formation of a new hair bulb, and contributing for the formation of new ORS [44, 45].

3.1.2. Hair shaft

The hair shaft as mentioned is the visible component of the hair. It is thin, flexible and composed of non-living keratinized epithelial cells. It is comprised by three distinct layers, the outermost cuticle, the cortex and sometimes the central medulla found in thicker hair [40].

3.1.2.1. Cuticle

The cuticle is the primary protective shield of the hair fiber. It is composed of multiple layers of flattened, overlapping, dead keratinized cells, often referred to as scales. These scales are arranged towards or downward, away from the scalp with approximately a thickness of approximately 0.5 μm.

This structure can be further subdivided into sub layers denominated the epicuticle, the A-layer, the B-layer (Exocuticle) and the endocuticles.

The epicuticle is a thin lipo-protein membrane that is the absolute outermost sub-layer of the cuticle, crucial to establish the hydrophobic nature of the hair surface as it is covalently bound to the fatty acid 18-Methyleicosanoic acid (18-MEA). Right beneath the epicuticle is the A-layer which contains the highest concentration of cysteine and the B-layer, both contributing to the hair's mechanical resilience [46, 47]. Finally, the endocuticle is the innermost sub-layer and is adjacent to the cortex. This is the layer with least cystine content compared to both the above layers[48] .

The primary function of the cuticle is to protect the inner cortex from the damage caused by various external factors, and its appearance is dependent on their impact on the hair fiber. A healthy cuticle presents smooth flat scales that minimizes the friction between the hair fibers, it regulates the moisture in and out of the hair shaft which allows for proper hydration and flexibility [49].

3.1.2.2. Cortex

The cortex is responsible for the main bulk of the hair fiber, being the primary determinant of the mechanical properties of the hair, such as its strength, elasticity, texture and natural color [40]. It is composed of densely packed, elongated, spindle-shaped cells known as cortical cells. Most of these cells are composed by α-keratin, a helical protein that can be divided in two types: type I with acidic amino acid residues and type II with basic aminoacidic residues. Both type I and type II strands spiral together forming coiled-coil dimers that further coil with other similar dimers in an antiparallel manner forming tetramers. These tetramers when fully connected, are known as protofilaments. The interaction of 7 of these protofilament creates the intermediate filament (IF) that further aggregates to form macro-filaments/macro-fibrils. Additionally, between the intermediate filaments exists a matrix consisting of keratin associated proteins (KAPs) that exhibit an irregular structure [48]. Due to the presence of

cysteine residues in both the IFs and KAPs, the matrix proteins function as disulfide crosslinkers holding the cortical superstructure together [50].

3.1.2.3. Medulla

The medulla is a loosely packed, disordered region near the center of the hair fiber being surrounded by the cortex [48]. It's presence is variable being frequently absent with exception of thicker hairs, where it sometimes appears [40]. This structure is formed as a column of cells which, upon hair formation, collapse forming a network of cellular connections and spaces filled with hair [51]. Additionally, its aspect may vary in thickness, continuity and opacity [51]. Contrary to the cortex where keratin adopts an α-helix conformation, the keratin in this structure exhibits a β-sheet conformation [52].

3.2. Impact of ageing on the hair

Although part of the integumentary system, the ageing process of hair exhibits several distinct physiological changes compared to that of skin. While scalp ageing generally follows the same principles as skin ageing - although with a reduced impact from UV radiation depending on hair coverage - the ageing of the hair fiber itself involves additional, specific changes. An ageing hair fiber tends to become grayer, its synthesis and numbers get reduced, it gets progressively thinner and its lipid composition also tends to become scarcer [53].

Hair loss is one of the most common signs of an ageing hair. As an example, female pattern hair loss (FPHL) also denominated as androgenic alopecia, mainly occurs on the emergence of menopause where estrogen levels decrease abruptly [54]. The hallmark of the condition is the progressive shortening of the anagen phase duration which leads to a small number of hairs in this phase of hair growth. This results in an increased number of hair follicles in the stationary telogen phase which firstly leads to the onset of hair shedding prior to the gradual hair thinning that occurs throughout the years [55]. Androgens - sex steroid hormones that are produced in adrenal glands, the gonads, the brain and in the placenta in pregnant women – are described as possibly playing a role in hair growth acting through intracellular androgen receptor in the cells of the hair follicle [54]. However, women with FPHL have neither clinical nor biochemical features of hyperandrogenism making the role of elevated androgen levels controversial, bringing the hypothesis that androgens act through unknown mechanisms. One possible hypothesis relies on the equilibrium of both estrogen and androgen levels as upon menopause estrogen levels drastically reduce, while androgen secretion only gradually declines being maintained until the later stages of life [56, 57].

Hair graying (canities) is another common and visible sign of ageing. It has been hypothesized that this change in the hair pigmentation is due to a decrease in the number of follicular melanocyte stem cells or their dysfunction. These cells are located at the bulge of the follicle, which upon signaling from surrounding HFSCs and the inferior DP, proliferate and migrate to the bulb where they differentiate into melanocytes. These melanocytes are responsible for synthesizing melanin which is subsequently transported to adjacent precortical keratinocytes of the hair shaft [58]. The accumulation of highly reactive oxygen species (ROS) is hypothesized as being the main possible cause of canities. ROS production can be exacerbated by external factors, but the intrinsic biochemical pathways can also

naturally produce these reactive chemical species. Melanocytes melanogenic activity can generate vast amounts of ROS via the oxidation of tyrosine during the melanin synthesis, but with the progressive weakening of defense mechanisms against ROS, characteristic of ageing, leads to an inevitable increase in their levels. Melanocytes are then damaged disrupting their melanogenesis activity, interfering with important enzymes such as tyrosinase and even leading to their apoptosis [59].

The ageing process also inherently changes the mechanical properties of the hair fiber. With the passage of time, hair starts to exhibit reveals a reduced mass, with a thinner diameter and lower density. It has been reported that the mRNAs that encode the hair keratins also declines with age affecting the cortex organization [59, 60]. Lipids such as the 18-MEA, that cover the hair fiber and are crucial to the hair's hydrophobicity, the fibers also play an important role in this loss of structural quality. With a reduction of the amount of cuticle-bound 18-MEA it is possible to observe a diminution in the hair diameter , and an increased damage potential to the cortex via external factors [60]. The removal of this layer also affect the lubrification of the hair fibers increasing their contact friction and altering their mechanical properties leading to more brittle hair fibers [60, 61].

Hair ageing involves a complex interplay of various biochemical pathways and, together with skin ageing, constitutes one of the most visible outward signs of ageing

3.3. Possible impacts of a TSW formulation on the hair

Faced with the dramatic changes associated with the ageing process, consumers are consistently searching for ways to prevent, attenuate or even revert these alterations. Therefore, it has been an increased focus of the cosmetic industry in addressing such necessities.

Most of the products targeted at the hair are mainly targeted at improving the mechanical properties that change during the ageing process. Thinning of the hair is masked by frequently shampooing the hair fiber, which turns it fluffier giving the illusion of thicker hair. Dry hair, which cannot retain moisture due to increased porosity from cuticle weathering, relies on conditioners to help restore its ability to retain hydration. Cationic polymers, hydrolyzed proteins, and silicones, such as dimethicone, are useful in this process. Other agents such as panthenol are absorbed into the shaft and acts as a humectant improving hair moisture levels [62].

Although having a growing interest, with the a projected to growth of 7% in the cosmetic market with a size of value of USD 312.33 billion [63], hair care products employing thermal spring water in their composition have not been fully explored.

Hair, being a porous structure allows solutes to penetrate into the hair fiber [64]. Some of these components can even be deposited upon the surface of the hair fiber and change the aspect of the hair as well as its physical properties.

TSW has already discussed is enriched in dissolved minerals [1] such as sodium, calcium, zinc, selenium, magnesium, and silicates [6], that are positively charged. Since the main content of the hair fiber is keratin, which carries a negative surface charge under most pH conditions [65], these ions are attracted to the hair fiber and can accumulate on the hair cuticle.

Some of these interactions might prove detrimental for the hair quality over the long term, as in the case of prolonged exposure to hard water rich in $CaCO_3$ and $MgSO_4$. These minerals can deposit on the hair surface reducing hair fiber thickness due to the abrasiveness nature of the deposited film upon washing [66]. On the other hand, other compounds may present benefits when deposited in the hair fiber. Silicone for example is the most used conditioning agent. It spreads over the hair surface forming a thin hydrophobic layer that increases luster and gloss which reduces the combing force [65].

By integrating the water in formulation, it's possible to change and improve these electrostatic interactions through pH adjustment. Alkaline cosmetics further intensify the net negative charge of the hair promoting even further the attraction of these cationic molecules that can be found in conditioners [65]. Therefore, an alkaline formulation that might contain naturally higher levels of silicon due to the presence of TSW as its main component might exhibit an improved conditioner effect.

These formulations typically consist of a mixture of substances that are intended to be placed in contact with external parts of the human body. Due to the addition of other substances that can play a crucial role in enhancing its delivery, efficacy and safety [67], the presence of other substances such as surfactants and moisturizing agents might help improving hair health and appearance, by retaining the humidity that is lost through the continuous degradation of the hair fiber across the years [68, 69].

Additionally, by providing beneficial effects onto the skin, the impact of TSW can also be translated into potential benefits for the scalp. However, while sharing the basic structure of epidermis, dermis and hypodermis, the scalp exhibits significant differences regarding its appendages and physiological functions [70]. Scalp contains increased levels of surface lips [70], is densely populated by hair follicles and is protected by a vast amount of hair fibers [53, 71]. Different products applied to, for example, facial skin might exhibit a different outcome regarding the scalp or may need a different delivery strategy since hair might present a challenge in effectively applying the active compounds [72]. For example, salicylic acid (SA), in the facial skin can be applied for the treatment of acne vulgaris due to its comedolytic – capacity for breaking up clogged pores - and anti-inflammatory properties [73], as well as its exfoliating effect that improve skin texture [60]. As for the scalp SA is mainly used for the management of hyperkeratotic and scaling conditions like scalp psoriasis, seborrheic dermatitis and dandruff [72]. Both approaches rely on the keratolytic activity of SA for removal of the scales in a Psoriasis scalp [72] or exfoliating the skin in the case of Acne Vulgaris [60]. However having in account the difficulty that is to efficiently treat the scalp due to the dense hair population, SA differently to acne treatment can be applied in a shampoo where it's keratolytic activity can be used to enhance the penetration of other topical medications such as corticosteroids [72].

The fundamental structural homology between the scalp and the skin throughout the body strongly suggests that known TSW benefits may be applicable to the scalp, highlighting a promising opportunity to expand the use of TSW-based products.

Chapter I: Assessing the potential cosmetic properties of Chaves' TSW

Since ancient times, TSW has been used due to its association with therapeutic benefits. However only more recently, some of these effects have been scientifically verified [74] with the World Health Organization officially recognizing hydrotherapy and balneotherapy's efficiency [7, 75].

With its main function being the body's protection against external environment, the skin is the most impacted organ by TSW properties. Such benefits are mainly attributed to the water's chemical, thermal and immunological effects that might impact dermatological conditions such as atopic dermatitis, seborrheic dermatitis, psoriasis, and many other [6].

Nowadays there is a growing emphasis on the use of more natural and sustainable solutions. This is mainly due to the fact that natural components might exhibit a higher biocompatibility which results in a safer outcome, being its production eco-friendlier compared to synthetic components [76]. For such a reason a noticeable increase in the interest and demand on these waters and TSW based cosmetic products has been observed.

Chaves thermal spring water is located in the north of Portugal, and it has been used as a local spa since Roman times. Its waters present a range of temperatures that varies from 55 to 76 °C, with total diluted solids of 1600–1800 mg/L and a neutral pH, being bicarbonated, sodium and CO_2-rich [11]. Although the Chaves thermal spa has been in operation since 1726 and is reputed for its medicinal waters, as evidenced by longstanding user satisfaction [77, 78], there is a lack of scientific evidence specifically supporting its effects on skin health.

Being a well-known thermal spring, it is the goal of this chapter to analyze the properties of these waters in the skin in order to develop a cosmetic formulation that makes use of its potential benefits.

1. Material and Methods

1.1. Water samples collection and transportation

Thermal spring water was provided by *Caldas de Chaves* (Chaves, Portugal) being retrieved directly at its source at 76 ºC. The water samples were bottled in 1-liter glass containers and transported at room temperature for approximately 1 hour. Upon arrival three batches were stored at 2-8 ºC.

1.2. Chaves TSW characterization

Since the water properties' arise mainly from their chemical composition [6], a previous characterization of the TSW was performed.

The pH value and electrical conductivity (EC) were first determined by using a multiparameter SevenExcellence™ Mettler-Toledo AG (Greifensee, Switzerland) at 20 ºC. The pH was measured with a precision of ± 0.002 pH units, and the electric conductivity was expressed in µS/cm.

The procedure for Total dissolved solids (TDS) determination was based on standard method 2540C present in *Standard Methods for the Examination of Water and Wastewater*™ [79]. In brief, the water

was filtered and well-mixed through a standard glass fiber filter, evaporating the filtrate to dryness in a weighted dish at 180ºC. The increase in the dish weight therefore represents the total dissolved solids.

Mineral determination was performed by ICP analysis. For that, 2 mL of Chaves TSW was mixed with 5 mL of 65% HNO_3 and 1 mL 30%H_2O_2 in a Teflon reaction vessel and digested in a microwave system (Speedwave, Germany). Digestion was conducted at 160 °C for 5 min; 190 °C for 10 min; and 100 °C for 4 min. The resulting solutions were brought up to 10 mL with ultrapure water for analysis. Mineral concentrations were analyzed inductively coupled plasma argon spectrometry through Model Optima 7000 DV ™ (PerkinElmer, United States of America). Triplicates were used during the analysis and the concentrations were expressed in mg/L.

Microbial control was performed according to ISO 6222:1999 [80] "Water quality—Enumeration of culturable micro-organisms—Colony count by inoculation in a nutrient agar culture medium", for total germs. 1 mL of Chaves' TSW was diluted in 9 mL of sterile peptone water and mixed in a vortex. Afterwards, several dilutions were carried out and samples were plated by spread plate in Tryptic soy agar (TSA) and Sbouraud dextrose agar (SDA). TSA plates were incubated at 37 ºC for 24 h and SDA plates at 30ºC for 48 h. Triplicates were used during the analysis and colony-forming units (CFUs) were calculated in order to determine the total aerobic bacteria and total yeasts and molds following the formula below transcribed:

$$\mathrm{CFU} = \mathrm{n°colonies} \times \frac{1}{\mathrm{v}} \times \frac{1}{\mathrm{df}}$$

1.3. Analysis of Chaves' TSW properties

1.3.1. Evaluation of the Antioxidant Capacity of Chaves' TSW

For the testing of the antioxidant properties of the water two surveys were performed. The 2.2′-azino-bis (3-ethylbenzothiazoline-6-sulphonic acid) diammonium salt radical cation (ABTS) decolorization assay was first performed as described by Gonçalves, et al. [81]. To initialize, a 20 mL ABTS solution was obtained by addition of 7 mmol/L of ABTS (Sigma-Aldrich, USA) to a 2.45 mM of potassium persulfate ($K_2S_2O_8$) solution (Merck, Darmstadt, Germany) at a 1:1 (*v*/*v*) proportion. This solution was then left in the dark for 16 hours being promptly diluted with deionized water and the absorbance was measured at 734 nm to obtain an optical density (OD) of 0,700 ± 0.020. The assay was carried out on a 96-well plate, with 15 µL of each sample and 200 µL of the diluted ABTS solution. The reaction mixture was then incubated for 5 min at 30 ºC. At the same time, a calibration curve with Trolox standard solutions (0.0125–0.14 g/L), was included. After incubation, the OD was again measured at 734 nm using Synergy H1 microplate reader (Biotek, USA) and the results were expressed as the percentage of inhibition of the free radicals generated.

2,2-diphenyl-1-picrylhydrazyl (DPPH) salt radical cation decolorization assay was also performed as already reported by Gonçalves, et al. [81]. A 100 mL solution of 600 µM DPPH was prepared by combining 24 mg of DPPH salt (Sigma-Aldrich, USA) with methanol. This solution was then diluted with its solvent until reaching an OD of 0,600 ± 0,100 at 515 nm. Then, in a 96-well plate, 25 µL of each sample was incubated for 30 min with 175 µL of DPPH solution. This method also included a calibration

curve prepared with Trolox standard solutions (0.001875–0.060 g/L). The OD was then measured at 515 nm and the results were also expressed as the percentage of inhibition of the free radicals generated.

1.3.2. Skin enzymes inhibition assays

1.3.2.1. Elastase

For Elastase enzyme, the Neutrophil Elastase Inhibitory assay kit (abcam-AB118971, United Kingdom) was used. For that, a 96-well plate was used to mix 25 µL of the samples with 50 µL of Elastase solution, being left to incubate for 5 min at 37 ºC. Then, the substrate solution was added to each well, and the fluorescence was measured at Excitation (Ex) and emission (Em) wavelength of 400 and 505 nm in kinetic mode for 30 min at 37 °C using Synergy H1 (Biotek, Portugal). Each assay included the blank and 5.0 × 10^{-4} g/L of peptide succinyl-alanyl-alanyl-prolyl-valine chloromethyl ketone (SPCK) as a positive control of inhibition.

The RFU of the fluorescence produced by substrate hydrolysis was determined by ΔRFU = R2 − R1. It is advised to read kinetically and select R1 and R2 in the linear range. The percentage inhibition was calculated using the following equation:

$$\text{Enzyme inhibition activity } (\%) = \frac{\Delta\text{RFU test inhibitor}}{\Delta\text{RFU enzyme control}} \times 100$$

1.3.2.2. Tyrosinase

Regarding Tyrosinase enzyme, the colorimetric tyrosinase inhibitor assay kit (abcam-AB204715, United Kingdom) was used. In brief, in 96-well plate, 20 µL of the three formulations and their respective extracts were mixed with 50 µL of tyrosinase solutions and were incubated at 25 ºC for 10 min. Upon incubation, the substrate solution was added, followed by the absorbance measure of each well at 510 nm using Synergy H1 (Biotek, Portugal). This reading was deployed in kinetic mode for 30 min and the data was monitored at 2 min intervals. For each assay included a blank and a 0,021 g/L Kojic acid solution as positive control of inhibition.

From this data a linear plot was traced, and the slopes were computed for each sample (S), inhibition control and enzyme control (EC). The percentage of inhibition activity was then calculated using the following equation:

$$\text{Enzyme inhibition activity } (\%) = \frac{\text{Slope}_{\text{EC}} - \text{Slope}_{\text{S}}}{\text{Slope}_{\text{EC}}} \times 100$$

1.3.2.3. Collagenase

For collagenase Inhibition Assay, the colorimetric metalloproteinases 1 (MMP1) inhibitor screening kit (abcam-AB196999, United Kingdom) was used following the manufacturer's instruction. In brief, the 0.75 U/L MMP1 enzyme was introduced to a flat-bottom 96-well microplate (Thermo Scientific, United States of America) followed by the addition of Chaves' TSW samples, vitamin C - used as benchmark– (Sigma-Aldrich, Germany), N-Isobutyl-N-(4-methoxyphenylsulfonyl)glycyl hydroxamic acid (NNGH) as

a positive control, and the blank to the respective wells. The microplate was then incubated at 37 °C for 30 to 60 min, promoting the interaction between the test samples and controls with the enzyme. Finally, 1 mM thiopeptide chromogenic substrate (Ac-PLG-[2-mercapto-4-methyl-pentanoyl]-LG-OC_2H_5) was added, and the absorbance was recorded at 412 nm using Synergy H1 (Biotek, Portugal). Data collection was done for 10-20 min in intervals of 1 min. The percentage of enzyme inhibition activity was calculated using the following equation, in which V describes the reaction velocity expressed in OD/min:

$$\text{Enzyme inhibition activity (\%)} = 1 - \left(\frac{\text{V inhibitor}}{\text{V enzyme control}} \times 100\right)$$

1.4. Cell culture Assays

For the following assays different cell types were used, including Human Keratinocyte (HaCaT) cell line (CLS, Lot No. 300493-4619) and Human Primary Dermal Fibroblasts (nHDFs) from adult skin (Lonza Bioscience, Cat. CC2511, Lot No. 0000577924). The cell lines were maintained in Gibco Dulbecco's Modified Eagle Medium (DMEM) - DMEM 41965062 for HaCaT and DMEM 11885084 - supplemented with FBS (BIOWEST, United States of America) – 10% FBS for HaCaT and 15% for nHDF – plus 1% penicillin (100 U/mL)–streptomycin (100 µg/mL) (Gibco, Thermo Fisher Scientific, United States of America) being maintained at 37 ºC in a 5% CO_2 humidified atmosphere. For HaCaT cells DMEM 41965062 supplemented with 10% FBS

1.4.1. Cytotoxicity Assay

Both HaCaT and nHDF lines were seeded at 1 × 10^4 cells/well in a 96-well plate and left to adhere overnight at 37 °C in a 5% CO_2 humidified atmosphere. The culture medium was then replaced by the test and control culture-supplemented media and cells were again incubated for 24 h at 37ºC in a 5% CO_2 humidified atmosphere. A 10% (v/v) of 10× PrestoBlue cell viability reagent (Invitrogen, Thermo Fischer Scientific, United States of America) was prepared for cytoxicity assessment. The solution was added to each well and incubated at 37 ºC in 5%CO_2 for one hours, protected from direct light. Fluorescence emission was measured through Synergy H1 (Biotek, Portugal) for cell viability determination. Experiments were performed in triplicates with HaCaT cell on the 20th and 22nd passages and nHDF cells on the 5th and 6th passages. The results were presented as the percentage of cell viability, where 100% viability corresponds to control cells and a reduction in the cell viability of more than 30% is considered a cytotoxic effect, according to ISO 10993-5 [82].

1.4.2. Quantification of Pro-Collagen I α1

For this test nHDFs were seeded in 12-well plates at 3 × 10^5 cells/well and allowed to adhere overnight at 37 °C in a 5% CO_2 humidified atmosphere. The culture medium was then replaced by test and control culture-supplemented media and cells were incubated for 24 h at 37 °C in a 5% CO_2 humidified atmosphere. Total protein was obtained using the extraction buffer of the ELISA kits and its concentration was determined by BCA kit (Thermo Fischer, United States of America). The amount of total protein was then normalized to 10 µg/mL and pro-collagen I α1 was quantified using Human Pro-Collagen I alpha 1 ELISA Kit (abcam, United Kingdom). As positive control 0,5 µM Palmitoyl Tripeptide-1 (Pal-GHK)

(Cayman Chemicals, United States of America) was used as positive control for both assays. The assay was performed in triplicate and the results were expressed in pg of Pro-Collagen I α1/mg of total protein.

1.5. Exposure to Urban Particulate Matter

HaCaT were used for this assay and seeded at 1 × 10^5 cells/well in a 24-well plate and maintained at 37 °C in a 5% CO_2 humidified atmosphere for 24 h. Afterwards, cells were incubated with and without 500 µg/mL of urban air pollution particles (SRM 1648a) (PP) resuspended in test- or control-supplemented medium for 24 h, following the literature [83]. As positive control, 20µM Dexamethasone (Dex) (Sigma-Aldrich, Germany), was used. Supernatants were collected and used to evaluate the levels of the proinflammatory cytokine IL-6 and IL-1α, by ELISA (Biolegend, United States of America). Cells were lysed with Radioimmunoprecipitation assay buffer (RIPA) Thermo Fischer, United States of America) and used for protein quantification through BCA kit (Thermo Fischer, United States of America). Duplicates were performed and the results were expressed in pg of cytokine/mg of total protein.

1.6. Population of the Study of Skin Microbiota

For this study female and male volunteers with more than 18 years old with or without skin diseases were recruited. As exclusion criteria for the test, pregnant women, women during the lactation period, individuals with tattoos or significant scars on the inner forearm; individuals that performed hair removal/exfoliation/skin cleansing on the inner forearm 3 to 4 weeks prior to the sampling and during the study period were not included. Individuals that applied cosmetic products onto the inner forearm prior to sampling and during the study as well and those who took pre- or probiotics, antibiotics, immunosuppressants, and chronic anti-inflammatory and chronic antihistamine drugs and/or systemic antifungals 1 month prior to the sampling and during the study period, were also excluded.

Based on this criteria, 23 participants were included (19 females and 4 males) that were separated according to their age in two groups: 26 to 35 years old (*n*= 17) and 36 to 45 years old (*n* = 6). Seven of the volunteers reported eczema, neurofibromatosis, psoriasis, and sensitive skin. Oral and written instructions were provided to all volunteers, who received a 50 mL vaporizer with Chaves' TSW to be used twice a day (in the morning and then in the afternoon) for 15 days. The control and test forearms were randomly chosen to eliminate the effect of the dominant arm.

1.6.1. Measurement of Skin Biometric Parameters

Measurements of the skin biometric parameters were taken on days 0, 8, and 16, from the inner forearms. Twelve hours before the measurement, the volunteers were instructed not to apply any cosmetic or test products. A Multi Probe Adapter MPA 6 (Courage and Khazaka, Germany) coupled with different probes was used: the Corneometer® CM 825 probe, to quantify the level of hydration; the Tewameter® TM Hex probe, to determine the transepidermal water loss (TEWL); and the probe Skin-pH-meter PH 905, to measure the pH.

1.6.2. Collection of Skin Microbiota

On days 0 and 16, samples of skin microbiota were collected from both inner forearms of 13 of the total selected volunteers following the protocol described by Carvalho, et al [84]. In brief, 4N6FLOQSwabs™

(Thermo Fisher Scientific, United States of America) moistened in a sterile solution of phosphate buffer solution (PBS) at 0.1 M (pH 7.3 ± 0.2 at 25 °C) plus 0.1% (*v*/*v*) Tween 80 were used to collect the skin microbiota samples from each inner forearm. The swab was then placed into a tube with RPMI 1640 medium (Gibco, Thermo Fisher ScientificUnited States of America) and was incubated for 2 h at 34 °C with agitation. The control of the collection method was performed by repeating the procedure without the skin microbiota sample. At the end, the tubes were centrifuged at 21,130× *g* for 10 min, and the pellet was recovered and stored at −20 °C until DNA extraction. The controls were processed similarly to the skin microbiota samples.

1.6.3. DNA Extraction and Quantitative Real-Time PCR (qPCR)

Total DNA from all pellets was extracted using QIAmpDNA Microbiome Kit (Qiagen, Germany), following manufacturer's instructions. After extraction DNA was quantified by Qubit 4 Fluorometer dsDNA HS Assay Kit (Life Technologies, United States of America), and the concentration was standardized at 10 ng/µL.

The qPCR assays were then used to determine relative abundances of the specific microbial genera and species. Universal primers were used to target a conserved region of the 16S rRNA gene for bacteria and the ITS2 region for fungi. For genus and species-specific assays, primers targeting genus- or species-specific genes were used. qPCR reactions were prepared as previously described by Carvalho, et al [84].

1.7. Statistical Analysis

Data was processed using GraphPad Prism software version 10.2.3 (Insight Partners, United States of America). For data that followed the necessary assumptions of normality and homogeneity of variables, parametric tests such as ANOVA supplemented with Tukey's HSD post-hoc test were used, for multiple comparisons. Differences were considered statistically significant at $p < 0.05$.

2. Results and Discussion

2.1. Chaves Thermal Water Chemical Properties

The mineral composition of TSWs is diverse being characteristic of the geological site they are situated since their enrichment in dissolved minerals is characteristics of prolonged water-rock [4, 5]. These minerals are the key responsible for the properties exhibited by these waters playing a crucial roles in many physiological processes such as enzyme systems and energy metabolism maintaining cellular integrity in cutaneous cells [85].

Since mineral composition majorly impacts the properties exhibited by TSWs, it was necessary to evaluate its composition in order to guide further research and justify possible benefic properties.

Chaves' TSW revealed a pH of 6,8 and a mineralization of 1 630 mg/L of total dissolved solids, being therefore characterized as a low mineralized water. The main minerals present in these waters are sodium, potassium, silicon and calcium (**Table 1.1**). A close to neutral pH as the one exhibited by Chaves' TSW is an important characteristic since skin pH regulates the maintenance of the stratum

corneum homeostasis and the skin barrier permeability [86]. With an acidic pH between 4 and 6, a disruption of the skin's pH may negatively impact on the aforementioned systems and therefore a close to neutral pH is ideal for a potential cosmetic as it may not significantly change its value.

Table 1.1 Characterization of Chaves' TSW

Chaves Thermal Spring Water	
Physicochemical characterization	
pH	6.84 ± 0.01
Conductivity (µS/cm)	2532 ± 2.12
Total dissolved solids (mg/L)	1630 ± 10
Minerals (mg/L) *	
Sodium (Na)	576 ± 16.91
Potassium (K)	74.02 ± 1.02
Silicon (Si)	37.20 ± 0.34
Calcium (Ca)	26.03 ± 0.46
Magnesium (Mg)	7.62 ± 0.10
Sulfur (S)	4.89 ± 0.05
Phosphor (P)	4.02 ± 0.05
Molybdenum (Mo)	0.04 ± 0.001
Manganese (Mn)	0.03 ± 0.0004
Cadmium (Cd)	0.02 ± 0.0003

2.2. Chaves' TSW exhibited potential antioxidant and anti-elastase activity

Skin aging is a complex process. However, one of primary agents involved in its ageing is the oxidative stress, caused by an excess of reactive oxygen species (ROS). These reactive species are capable of damaging skin cells, and therefore impacting its appearance, causing wrinkles, loss of elasticity and pigmentation [87, 88]. The exposure of the skin to air pollution or UV radiation, can even exacerbate the process of skin ageing as it has been reported that it increases ROS production [89].

Finding ways to minimize oxidative damage is therefore essential. Certain minerals exhibit potent antioxidant activity, and TSWs from Avène, Uriage, and Vichy are particularly notable for having mineral compositions proven to help in the removal of peroxides from the cytosol and cell membranes [6]. To

evaluate the potential antiaging effects of this water, the first assays employed were ABTS and DPPH, for determination of the antioxidant potential of these waters [6, 90-92].

Between both tests only ABTS allowed the evaluation of free radical's neutralization by Chaves' TSW (**Table 1.2**). Such outcomes have been previously reported [93], with ABTS revealing more strong results on low affinity DPPH scavenging antioxidants. This might be caused by the different mechanisms of action in which DPPH and ABTS radicals are affected by the antioxidant agent. ABTS radical being more chemically reactive, can interact with both lipophilic and hydrophilic antioxidants through hydrogen atom or electron transfer. On the other hand, DPPH only reacts on lipophilic compounds through hydrogen atom transfer. Therefore, compounds that might be weak radical scavengers in DPPH assay might show significant activity in the ABTS [93].

Table 1.2 Evaluation of the antioxidant activity of Chaves' TSW. nd stands for not detected

	Antioxidant Activity (%)	
	ABTS	**DPPH**
Chaves thermal spring water	9.09 ± 3.88 [b]	nd
Vitamin C (0.075 mg/mL)	91.94 ± 2.03 [b]	86.56 ± 0.48 [b]

The radical inhibition for Chaves' TSW exhibited an ABTS radical inhibition much lower than the inhibition caused by Vitamin C. However, such inhibition might be due to the presence of calcium and magnesium [94, 95]. Since both minerals are present in much lower concentrations the low antioxidant activity was expected.

Anti-ageing potential was also determined by the capacity of the water to inhibit ageing related enzymes such as Collagenase, elastase and tyrosinase (**Table 1.3**). These enzymes are responsible for degrading the components in the extracellular matrix (ECM) such as collagen which is the most abundant and provides structural support to the skin and elastin that provides elasticity to the tissues [96, 97]. As for tyrosinase, a copper-containing enzyme, it plays a crucial role in melanin biosynthesis. However with ageing its activity may become deregulated due to oxidative stress and inflammation being therefore responsible for disorders such as age spots and melasma [98, 99].The results observed can be viewed in the table bellow:

Table 1.3 Evaluation of Chaves' TSW potential to inhibit age related enzymes

	Enzyme Relative Inhibition (%)		
	Elastase	**MMP-1**	**Tyrosinase**
Chaves thermal spring water	14.22 ± 4.29 [b]	0.70 ± 0.25 [b]	0.005 ± 0.00 [b]
Vitamin C (8 mg/mL)	90.54 ±1.51 [a]	96.26 ± 0.31 [a]	99.26 ± 0.31 [a]

Between the three enymes, only elastase exhibited a significant inhibtory activity, suggesting that the TSW may contribute to the improvement of skin health and appearance by avoiding elastin degradation by the enzyme.

2.3. Collagen production remained stable upon application of Chaves' TSW

Fibroblasts represent the major cell type of connective tissue being the main responsible for the dermal extracellular matrix (ECM) synthesis and its homeostasis. These cells are embedded into the ECM they synthesized, exerting contractile forces that determine their morphology, the organization of cytoskeletal tissue, gene expression and signaling transduction. Type I collagen constitutes approximately 80-90% of total collagen in the dermis being an important component in this process [100].

Collagen is initially translated as a pre-propeptide containing an N-terminal signal sequence. This directs its translocation into the endoplasmic reticulum (ER), where it undergoes post-translational modifications that enable trimerization into a stable triple-helical procollagen molecule. The procollagen is then stabilized by the propeptide ends which are subsequently cleaved in the extracellular matrix [101]. The presence of these propeptide fragments makes them valuable biomarkers for rapidly assessing collagen synthesis levels.

It has been reported through *in vitro* studies that TSW can significantly increase collagen I α1 and I α2 levels in human epidermal keratinocytes and fibroblasts [12, 102]. Silicon content according to the literature is important for an optimal synthesis of collagen. Orthosilicic acid ($SiOH_4$) that is present in drinking water, is the most readily available silicon source for the human being, exhibiting the capacity to stimulate fibroblast secretion of collagen type I [103]. Therefore, although Chaves' TSW does not exhibit the capacity to inhibit MMP-1 – the matrix metalloproteinase (MMP) responsible for the gradual degradation of the ECM - it may still promote pro-collagen synthesis due to its rich silicon content.

For assess this property, pro-collagen I α1 levels were measured in nHDF cells. Prior to this assay, it was necessary to evaluate if Chaves' TSW did not exhibit any negative impact on nHDF cells viability and therefore influence the pro-collagen I α1 quantification assay

As observed in **Supplementary Figure 1**, the TSW did not significantly impact the cell viability of the nHDF cells maintaining their viability above 70%, which according to ISO 10993-5:2009, demonstrates that Chaves' TSW is biocompatible.Through Human Pro-Collagen I Alpha 1 ELISA Kit it was possible to verify both nHDF cells incubated with Chaves' TSW supplemented medium, did not reveal significant differences in pro-collagen I α1 levels compared to the control (**Figure 1.1)**.

Although Chaves' TSW contains silicon concentration of 32,70 mg/L, this level appears to be insufficient to promote collagen synthesis in nHDF cells. In contrast, Nitrodi's TSW, which has been reported to stimulate collagen synthesis, contains a silicon concentration more than twice that of Chaves' TSW [12, 102], supporting the hypothesis that the silicon content in Chave's TSW may be inadequate to eliciting such a biological response.

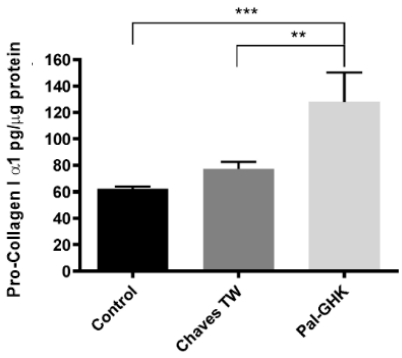

*Figure 1.1 Quantification of pro-collagen 1α1 in HDF cells treated with Chaves' TS. Palmitoyl Tripeptide-1 (Pal-GHK) was used as positive control. Statistical analysis was performed using the one-way ANOVA with Tuckey's multiple comparison. The results are represented as bar graphs (Average±SD). ** stand for p < 0,005 and *** stand for p < 0,0005*

2.4. The application of Chaves' TSW on HaCaT cells revealed a reduction of inflammation *upon exposure to pollution particles*

Anti-inflammatory and immunomodulatory properties are the most reported benefits of TSWs. Their capacity to decrease pro-inflammatory cytokines is often reported promoting their application in inflammatory conditions such as atopic dermatitis, psoriasis and rosacea [25, 74, 104, 105].

Keratinocytes are important players in the regulation of skin inflammation, responding to both environmental and immune cell stimuli. These cells are targeted by multiple cytokines that modulate their biological functions and behavior. In various skin conditions, several cytokines have been reported to induce, for example, a psoriasiform phenotype in normal human epidermal keratinocytes. Notably, IL-1α, IL-22, TNF-α, oncostatin M (OSM), and IL-6 are among the key cytokines involved [106].

During ageing it's possible to observe a progressive dysregulation of these interleukins which gradually evolves in a state of chronic low-grade inflammation. The persistent imbalance between pro- and anti-inflammatory signals not only sustains chronic skin inflammation but also accelerates tissue damage and functional decline over time. In addition, environmental aggressors are also able to induce the production of interleukins like IL-6 on the skin. As an example, continuous exposure to urban pollution further exacerbates these changes and contributes to the ageing process [107].

The complex interplay between the different immunological agents is extensive, making a comprehensive analysis of TSW's impact on their expression beyond scope of this thesis. Instead, this study focuses on two cytokines that are frequently reported in inflammatory skin responses, using healthy HaCaT keratinocytes as the *in vitro* model.

Interleukin-1α (IL-1α), is a cytokine that *in vitro* testing revealed to be a potent cytokine regulating of a vast ranges of genes [106]. This cytokine is constitutively expressed by keratinocytes and retained in intracellular stores. Due to its continuous expression, this cytokine has long been associated as having an alarmin role. In the event of cellular damage or programmed cell death, IL-1α is then released into the extracellular space, warning the surrounding cell of the damage or infection. It has revealed that IL-1α expression and secretion from keratinocytes play a role in chronic inflammation condition [108].

IL-6 is a multifunctional cytokine that plays a significant role in both acute and chronic inflammatory responses, being a key production stimulator of the majority of acute-phase proteins. This cytokine is rapidly synthetized upon detection of diverse danger signals and cytokines such as IL-1α/β and TNF-α and is capable of inducing systemic manifestations away from the site of inflammation through the bloodstream being essential for the acute-phase response. Although not the most potent pro-inflammatory cytokine [106], dysregulation and persistent IL-6 production is responsible for the state chronic inflammation observed in many inflammatory and autoimmune diseases [109].

Given their importance, the impact of application of Chaves' TSW in their expression was evaluated. Before proceeding with the cytokine quantification, it was necessary - similarly to the collagen quantification - to first assess any potential cytotoxic effect of the water on the cells.

Upon exposure of the HaCaT cells to the Chaves' TSW, no significant impact on cell viability was observed (**Supplementary figure 2**). Therefore, the water was deemed suitable for use in the subsequent assay.

For IL-6 and IL-1α quantification, urban air PP were used as a stress inducing agent according to the described materials and methods. Regarding IL-6, it was observed that the application of these particles led to a significant increase in IL-6 expression, exceeding a 10-fold rise compared to cells without particle treatment (**Figure 1.2-A (With Pollution particles**). Under both basal conditions and pollution-induced stress, Chaves' TSW significantly reduced IL-6 levels compared to the control.This reduction

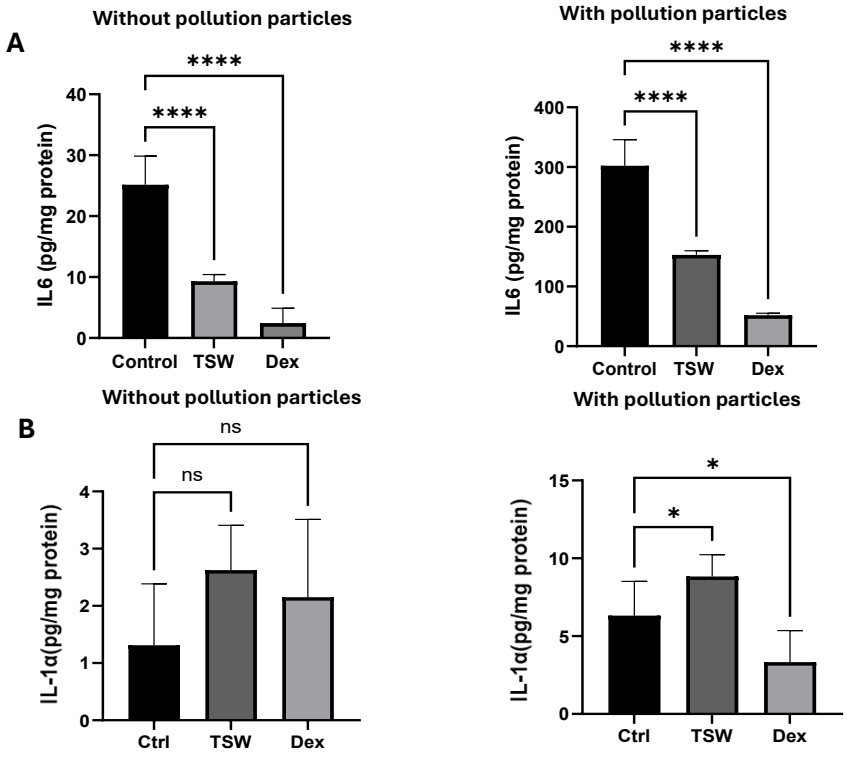

*Figure 1.2 Evaluation of anti-inflammatory potential of Chaves' TSW. Quantification of IL-6 (A) and IL-1α (B) levels in supernatants of HaCaT cells with and without urban air pollution. Statistical analysis was performed using the one-way ANOVA with Tukey's multiple comparison. The results are represented as bar graphs (Average±SD). * and *** stand for p<0,05 and p <0,0001*

might be explained due to the mineral composition of Chaves' TSW. Among the minerals contained in the water, Mg^{2+} recognized for exhibiting immunoregulatory action. Magnesium is one of the most abundant minerals present in the human body, being a cofactor for multiple enzymes that are involved in several metabolic and intracellular biochemical pathways. Both *in vitro* and *in vivo* studies revealed that Mg^{2+} is important for the modulation of the inflammatory response, affecting several cells of the immune system [110]. Magnesium deficiency for instance appears to promote an over function of the innate immune defense leading to an increase in the release of IL-6 and acute phase proteins [111]. It has been demonstrated that supplementation of Mg^{2+} decreases IL-6 levels [112] and the stimulation of intracellular magnesium through $MgSO_4$ also exhibited reduced cytokine production [113, 114].

As for IL-1α, TSW did not cause any significant pro-inflammatory response as IL-1α. Upon applying the particulate matter, it was possible to observe that Chaves' TSW did not reduce the interleukin levels, exhibiting a significant increase when compare to the control. However, this increase is attributable to the effects of the urban particles themselves, rather than to any potentiating interaction between the particles and the water, since Chaves' TSW does not exhibit a pro-inflammatory effect at baseline conditions without the particles.

Nonetheless, due to its anti-inflammatory effect on IL-6, Chaves' TSW, may present benefic results as a cosmetic ingredient, for a formulations target for people suffering from inflammatory dermatological conditions such as atopic dermatitis where there has been registered increased levels of IL-6 [115, 116]. This study therefore reveals the potential soothing effect of Chaves' TSW being in accordance with other published data regarding other TSWs [25, 74, 104, 105].

2.5. Applying Chaves' TSW improved skin barrier function by promoting a higher water retention

Skin is the physiological and biological barrier of our body with constant contact with the environment. It protects the body from various environmental factors such as UV radiation, allergens, chemicals and microbes [117], also displaying an important role in regulating water and solute loss from our body [118].

TSW skin barrier reinforcement properties have been reported in recent years promoting the expression of key markers such as filaggrin and human β-defensin 2. In addition, application of TSW has been reported as improving skin's hydration in its outermost layer and in the epidermis [15].

Parameters such as transepidermal water loss (TWEL) and hydration levels are associated with skin health and its ageing being frequently used in dermatology and cosmetology to evaluate the integrity of the skin barrier, being also important parameter to determine the efficacy of topical products [119, 120].

Having considered the potential benefits of Chaves' TSW these parameters were measured for 16 days by 23 participants.

Regarding hydration levels, measurements were made in both inner forearms of the volunteers. Similar values were obtained on the first day before thermal water application (day 0), day 8 and day 16 (**Figure**

1.3-A). However, when considering only the volunteers with a dry skin, whose hydration levels were below 30 a.u (arbitrary units) (n=7) [121], hydration levels where significantly higher in the 8th day being maintained until the 16th where there was no application of the TSW (**Supplementary figure 3**).

As for TEWL values, after 15 days applying Chaves' TSW, the water loss levels were significantly decreased under 10g/m^2/h in comparison to day 0, revealing a restorative effect on the skin barrier (**Figure 1.3-B**). This property leads to once again potential benefits for individuals with skin diseases that naturally exhibit an increase in TWEL values [122, 123]. As an example, individuals with psoriatic plaques and atopic dermatitis eczematous lesions revealed TWEL levels significantly higher than healthy individuals [122].

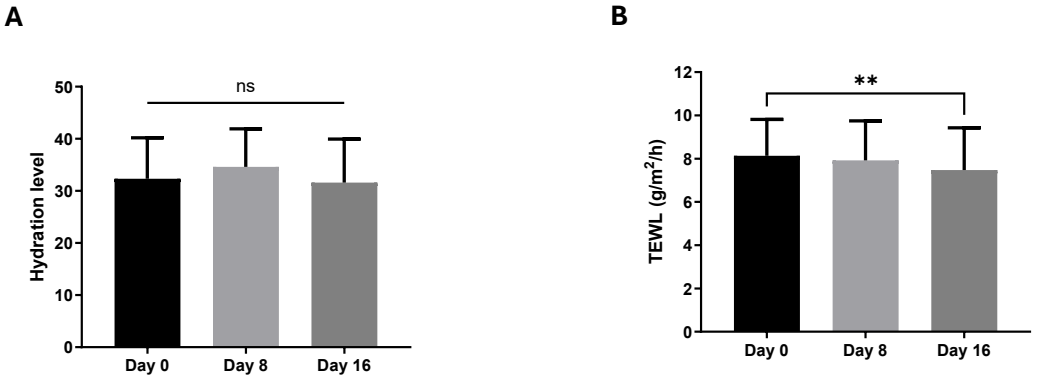

*Figure 1.3 Skin biometric parameters. The measurement of (A) hydration level, (B) transepidermal water loss (TEWL) was performed on Day 0 (before the application), 8 and 16 (after the application). Statistical analysis was performed using the one-way ANOVA with Tukey's multiple comparison. The results are represented as bar graphs (Average±SD). ** stand for p < 0,005. Ns, not significant*

This regenerative effect on the skin barrier, according to the literature, might be related to the high concentration of calcium presents in the water. Calcium (Ca^{2+}), which is one of the major components of Chaves' TSW is a key regulator in keratinocyte differentiation and proliferation [15]. Such properties once again reveal the beneficial impact that Chaves' TSW may have on the skin, endorsing its use on cosmetic formulation.

2.6. Chaves' TSW application does not destabilize skin's microbiota

A healthy human body is populated on average by 10^{14} microorganism cells. From bacteria, fungi and other eukaryotic microorganism, these microorganism play an essential function on everyday life by assisting in digestion, nutrient absorption and immune development [124].

Skin is a dynamic tissue composed of multiple cell types and structures, each with physical and biochemical properties. These complex and ever-changing dynamic environments naturally impact microbiome composition and behavior. Sebaceous sites of the skin that exhibit high lipid content led to colonization of taxa such as the bacteria *Cutibacterium* and the fungi *Malassezia*, that are lipophilic taxa. Areas with higher water content due to, for example, the presence of sweat glands are populated by

bacteria such as *Corynebacterium* and *Staphylococcus*. Dry sites in contrast are less populated by microorganism with bacteria such as *Corynebacterium*, *Cutibacterium*, and *Streptococcus* being the dominant bacterial species [125, 126].

Disturbances in this equilibrium might lead to prejudicial effects. The immune system is largely intertwined with the skin microbiota, with certain microorganisms improving the skin barrier function and healing ability of the skin, and other leading to disturbances, promoting inflammation and exacerbated skin diseases. Disbalances in this delicate balance are linked to dermatological conditions such as atopic dermatitis, acne and psoriasis [125, 127].

In cases of atopic dermatitis, characterized by its chronic and relapsing inflammation of the skin is associated with colonization of *Staphylococcus aureus*, due to the capacity of some virulence factors of the bacteria to promote inflammatory cytokines production in keratinocytes [127].

Since dysregulation on this sensible ecosystem between bacteria and human skin might lead to undesirable outcomes, understanding the impact of the water on skin's microbiome is an essential aspect to assess the quality and potential benefic effects of the TSW.

Skin's microbiota was characterized in a subset of 13 volunteers at days 0 and 16. The main bacterial genera that compose the human skin microbiota such as *Staphylococcus*, *Cutibacterium,* and *Corynebacterium* as well as the fungal genera *Malassezia* [125, 127]. The relative abundance of all these genera was determined demonstrating no statistically significant differences between skin microbiota before and after Chaves' TSW application (**Figures 1.4 A-D**).

Additionally, the relative abundances of two bacterial species *Staphylococcus epidermidis* and *Cutibacterium acne* were also determined since both bacteria represent two major sentinels of skin microbiota being important to determine the influence of cosmetic products. These species are usually considered commensal bacteria as they are harmless to human health in healthy conditions and benefit from the skin's environment. More precisely, both bacteria present a symbiotic relationship with the cutaneous system being mutual beneficial, as the skin supplements the bacteria with nutrients while both bacteria participate skin homeostasis by interacting with the extracellular matrix skin proteins of the human skin, such as type I collagen and toll-like receptors (TLR2 and 4) allowing the coordination of pathways between bacteria and skin cells [128].The relative abundance of both species did not reveal any significant changes (**Figure 1.4 E-F**). A similar result was obtained when comparing *Staphylococcus* sp/*Cutibacterium* sp and *S. epidermidis*/*C. acnes* ratios on both time points (**Supplementary table 4**), revealing that the application of Chaves' TSW does not impact the natural skin microbiome

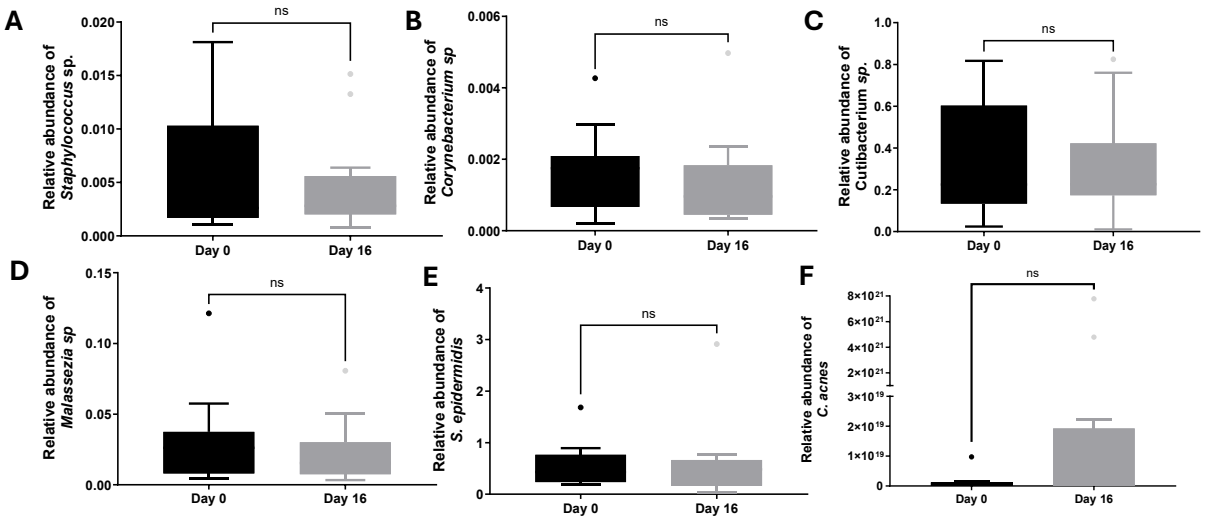

Figure 1.4 The relative abundances of (a) Staphylococcus sp. (b) Corynebacterium sp. (c) Cutibacterium sp. (d) Malassezia sp. (e) Staphylococcus epidermidis (d) Propionibacterium acnes determined by qPCR . Statistical analysis was performed using the one-way ANOVA with Tukey's multiple comparison. The results are represented as bar graphs (Average±SD). ns, not significant

Chapter II: Development of a Chaves' TSW based formulation and its properties on the hair fiber

Although TSWs have been a topic of discussion and research in the past two decades [6, 7, 129], their applications have predominantly been directed on skincare due to its well-documented anti-inflammatory [25, 130, 131] and skin barrier regeneration properties [15, 38]. This emphasis is largely justified by the significant revenue share that skincare products hold within the cosmetic market. Nonetheless, hair care cosmetics have been emerging as a key category experiencing growing demand from the consumers. According to the GVR market report of 2023 [63], the sector is projected to grow by 7% in coming years, being therefore promising for expanded applications of TSWs.

Despite such potential, the use of TSW as a cosmetic ingredient for hair care products has not yet been disclosed. Given its enrichment in dissolved minerals [1] such as sodium, calcium, zinc, selenium, magnesium, and silicates [6], TSW might play an important role in hair health and appearance. Hair, being a porous structure allows solutes to penetrate through transcellular channels of the cuticle cells and other intercellular pathways, allowing the adsorption and/or penetration of these compounds into the hair fiber [64].

The reported results in the previous chapter revealed that Chave's TSW might exhibit beneficial properties regarding skin health which might be translated to the scalp. However, its application in hair fiber remains unknown, which led to the opportunity of exploring its potential on hair application.

In addition to the TSW testing, based on the positive results of the previous chapter, Chaves' TSW was incorporated into a cosmetic formulation and promptly tested on the hair fiber.

Cosmetic formulations typically consist of a mixture of substances that are aimed at being placed in contact with external parts of the human body, with the objective of cleaning, perfuming and changing their appearance, keeping them in good condition. Formulations often offer advantages over the sole use of its active ingredient, due to the addition of other substances that can play a crucial role in enhancing its delivery, efficacy and safety [67]. Hair care formulated products like shampoos contain 10-30 ingredients in their composition. Amongst them surfactants facilitate the removal of environmental dirt by the reduction of surface tension between the water and the dirt; conditioners which include fatty substances aim at maintaining the natural condition of newly grown hair for a longer period of time preserving its lipidic coating [132]. Additionaly, additives are another combination of substances that further improve the functions of its main components. Some examples are preservatives that help protect the product against bacterial contaminations and chelating agents that help removing the interference of ions in the shampoos that could bind with the dirt and make it difficult to remove [132, 133].

Due to the presence of different compounds in the formulation, their interactions are not always predictable presenting both synergic and inhibitory properties towards the active ingredients [134-136]. Therefore, in addition to testing Chaves' TSW on hair fibers and developing a formulation, it was crucial to evaluate the formulation's interactions to identify any enhancing or inhibitory properties.

1. Materials and Methods

1.1. Development of the formulation

Chaves' TSW was developed considering not only the efficacy of its constituents, but also by searching for the ones that exhibited highest natural indexes. To achieve a high natural content, ISO 16128-2:2017 [137] was used to determine the exact percentage of natural composition using the following calculation:

$$Natural\ Content(\%) = \frac{\sum(Concentration \times Natural\ Origin\ Score)}{Total\ Concentration} \times 100$$

The products were then selected based on their natural origin score in order to obtain natural content over 90% exhibited in the table below (**Table 2.1**).

Chaves' TSW constitutes approximately 90% of the total constitution of the formulation being at the same time the solvent and its active compound. For the preparation of the formulation each of the selected components were weighed at the correspondent mass and dissolved in the water (**Table 2.1**). They were afterwards mixed by Turrax disperser (IKA, Germany). pH was then adjusted to be between 5,5 and 6

Table 2.1 Composition of Chaves' TSW-based formulation

Compound's name	Quantity (%(w/w))	Source
Chaves' TSW	89,87	Termas Chaves, Portugal
Glycerin	2,00	Acofarma, Spain
Sodium Phytate	0,10	Apollo Scientific, UK
Dexpanthenol	2,00	Thermo Scientific, USA
Natural Ectoin	1,00	TCI, Japan
Cocoamidopropyl betaine	4,00	Chimidroga, Portugal
Etanol 70%	0,03	LabChem, USA
Euxyl PE9010	1,00	LotionCrafter, USA

1.2. Hair Sample preparation

A total of 15 hair tresses of dark brown virgin hair (Kerling International, Germany) each measuring 25 cm in length and a weighting of 4 g were selected, for bleaching and subsequent analysis of their physical and chemical properties, both before and after applying thermal water.

1.3. Hair bleaching process

To access the TSW's reparative properties on the hair, a bleaching process was employed to induce deliberate damage to the hair fibers. The bleaching mixture was prepared by combining, Bleach and light powder (Lisap, Italy) in a 1:1 (w/w) ratio with an oxidizing emulsion containing 12% (v/v) H_2O_2.

For each hair tress, 16 g of the bleaching mixture (in a 1:4 (w/w) hair-to-mixture ratio) was applied by gently rubbing for 1 minute the hair fiber. Following application, the tresses were wrapped in aluminum foil and left at 25-35 ºC for 1 hour. Each hair tress was then subsequently washed in water for 1 min and

left to dry at 25 °C in 60 % Relative humidity (RH) for 24 hours. This complete process was iterated twice to ensure consistent bleached hair.

Following bleaching, each hair tress was washed for 1 minute with 4 mL of a 10% (m/v) sodium lauryl sulfate solution, followed by a 2-minute interval and a final rinse with water for another minute. The tresses were then dried at 25 °C at 60% RH until they were used for the thermal water application tests.

1.4. Product application

After the washing process, each tress was pre-moistened with 5 sprays of deionized water to facilitate the dispersion of the test compounds. Afterwards the test compounds were applied in a quantity of 40% the mass of each hair tress. With each tress weighing approximately 4 g, the mass of compound applied for each hair tress was 1,6 g.

For the application, the 15 tresses were separated into 5 groups each comprising triplicates denoted Control (Ctrl), Avène benchmark (Ave), Chaves' TSW (Chv), Formulation with the TSW (FChv) and a formulation with deionized water (F). Group Ctrl functioned as the negative control, devoid of any thermal water being treated with deionized water. Group Ave served as the positive control, subject to the application of commercially available thermal water (Avène, France). As for Chv group and FChv, they represented respectively the test triplicates where Chaves thermal water and its formulation were applied.

1.5. Analysis of Chaves' TSW impact on the hair physicochemical properties

1.5.1. Color and Gloss analysis

In order to analyze any potential change in the hair color after applying thermal water a colorimetric analysis using the CR-410 colorimeter (Minolta, Japan) was employed. In this analysis, CIELAB color space parameters, L*, a* and b* were used. To evaluate the color variation, the individual color parameters were compared as well as the obtained color when the CILAB parameters were converted to color. Additionally, the color variation was also calculated using the formula of ΔE_{ab}^{*} defined by the International Commission on Illumination (CIE) [138] as:

$$\Delta Eab* = \sqrt{(L^*_{ctrl} - L^*_{sample})^2 + (a^*_{ctrl} - a^*_{sample})^2 + (b^*_{ctrl} - b^*_{sample})^2}$$

Following the color analysis, gloss was also determined in order to verify if the TSW and its formulation has any potential effect on this hair physical property. For that reason, a TG 268 Gloss meter (Lovibond, Germany) was used to analyze this characteristic at 20°, 60° and 85°

The measures for each sample group were made in three distinct places along the hair tresses. Due to the thinness of the samples, to reduce the impact of the background each measurement was done with all the three hairs from each group clustered together, in order to cover all the full area of the sensor.

1.5.2. Texture analysis

Other physical properties of the hair involve its stiffness and its combability. To analyze such characteristics, TA.XTplusC texture analyzer (Stable Micro Systems, United Kingdom) was used.

1.5.2.1. Stifness test

For the stiffness analysis, TA.XTplusC texture analyzer (Stable Microsystems, United Kingdom) was assembled with the Three point Bending Rig accessory, in order to enable the analysis. The texture analyzer device was calibrated with a 5kg load. The hair tress for each analysis was held in the rig clamp and the test was run with the following parameters: Test type-cycle until count; Pre-test speed-1.00 mm/s; Test speed-0.5mm/s; Post-test speed-10 mm/s; Distance-10 mm; Count-5 cycles.

1.5.2.2. Combing test

As for the combing analysis, the hair combing rig of the texture analyzer was assembled in the device. Similar to the stiffness analysis, the device was calibrated with a 5 kg load cell in order to increase sensitivity on the device. For the test the hair tress was held on the hair tress clamp on the top of the texture analyser and the test was run under the following parameters: Test type-Compression, Test-comb force- -3800,0 g; Test speed-5 mm/s; Count-10 cycles; Return distance-10 mm; Return speed-20 mm/s; Contact force-50g; Height offset-0 mm.

For the height of the device the parameters were the following: Top height-75 mm, Bottom-140mm and Clamp-30mm

1.5.3. Analysis of the structural composition of the hair fibre

Hair's functional groups analysis was employed by for Attenuated Total Reflection Fourier-Transform Infrared Spectroscopy (ATR-FT-IR) through PerkinElmer Frontier™ MIR/FIR spectrometer (PerkinElmer, United States of America). Scans were conducted across a range of 550–4000 cm^{-1}, with 16 scans per sample at a spectral resolution of 4 cm^{-1}.

Hair overall structure integrity was employed through differential scanning calorimeter (DSC) using 204 F1 Phoenix® NETZSCH-Gerätebau GmbH (NETZSCH, Germany). The temperature and enthalpy calibration scale were carried out using indium/zinc standard. For the sample preparation, hair fibers were cut 5 cm below the top and 5 cm above the bottom of the hair tress and weighed in the DSC pan (weigh between 3-4 mg). Afterwards, the samples were hermetically sealed with pierced lids and heated over a range of 20-270 °C at a constant rate of 10 °C/min. An inert atmosphere was maintained by purging Nitrogen gas at a flow rate of 100 mL

2. Results and discussion

2.1. The formulation revealed a high natural index

The sole use of Chaves' TSW has already demonstrated potential beneficial effects on skin health, supporting its inclusion in a formulation designed to enhance dermatological benefits. Therefore, it was

a natural progression to develop a formulation that would not only maintain these properties but simultaneously enhance them.

Since nowadays there is a growing preference for more natural products [76], the following formulation was developed to achieve the highest possible level of natural composition.

Cosmetic formulations contain several components such as surfactants, humectant agents, fragrances and preservatives [67, 132, 139, 140]. To select these components, the natural index of each compound was analyzed through ISO 16128-2:2017 [137] ensuring the formulation aligns with the intended purpose while achieving the highest level of naturalness.

The main compound of this formulation is Chaves' TSW that works both as a solvent and as an active ingredient. Therefore, it is the most natural component being also the most present in the formulation.

For surfactant and cleansing agent, Cocoamidopropyl betaine (CAPB), a compound derived from coconut fatty acid [69], was selected for lowering the surface tension between ingredients and allowing for their mixture conferring also their cleansing properties [68, 69].

Glycerin and Dexpanthenol were selected as moisturizing agents. Glycerin naturally attracts moisture from the environment helping retain it in the skin and hair, which might potentiate the hydrating effects of the TSW [141]. As for Dexpanthenol a derivative of pantothenic acid (vitamin B5) also exhibits hydroscopic properties attracting and retaining moisture as well as enhancing skin barrier by increasing the mobility of molecular components [142, 143]. Additionally, to both components natural, ectoin has been used as an auxiliary compound. Ectoin is a water-binding organic osmolyte with low-molecular weight that has the capacity to improve skin hydration as well as skin barrier function possible further enhancing the hydration on the skin[144].

EDTA is a common chelating agent used in cosmetic and cleansing products such as Shampoos and Conditioners, helping binding metal ions such as calcium and magnesium [145]. However, due to its low natural index, sodium phytate was instead chosen as an alternative. Being derived from plants, sodium phytate has a higher natural index capable of chelating ions such as Ca^{2+} and Fe^{2+} allowing for a better antioxidant potential [146].

Many cosmetic products utilize fragrances in order to perfume the area where they are applied. To simulate the application of a fragrance in the formulation, an ethanol solution at 70% (v/v) was also applied in the formulation.

Preservatives in cosmetic products are crucial to maintain product quality and safety. Since this formulation, as well as many others, contains water and organic material, it is important to restrict microbial growth [147]. Euxyl PE9010, is a liquid cosmetic preservative that consists in the mixture of phenoxyethanol (PE) and ethylhexyglycerin (EHG). PE is the main antimicrobial agent that works by disrupting microbial cells leading to inhibitory and bactericidal activity. It's effects are potentiated by EHG, an additive that has surfactant properties, that is capable of inducing changes in the membrane surface tension properties of bacteria improving the contact between PE and the membrane [148].

Based on this composition, the calculation of the natural index of this Formulation revealed a total of 96% of natural content, achieving the high naturality desired for the product.

2.2. Bleaching

The primary focus of developing a cosmetic product derived from Chaves thermal water was to enhance the consumers' health and appearance upon applying such a product. To comprehensively evaluate the potential benefits of applying this water to the hair, it was crucial to first induce damage to the hair fiber. This step was necessary to gauge any type of recovery effect possibly caused by the cosmetic product.

The damaging process was done through an aggressive bleaching process employed in the12 test tresses of brown virgin hair. After two bleaching cycles, each tress presented an evident change in color, going from a dark brown to a platinum blonde (**Supplementary figure 5**). It was also possible to observe that the hair fibers were more brittle, with some of them breaking during the combing process.

This change of color occurs due to the oxidation of the melanin pigments present in the cortex of the hair fiber. The oxidative reaction is also responsible for the disruption of the cystine disulfide cross-links to cysteic acid residues which also affects the appearance of the hair, by turning its cuticles more porous and therefore giving it a more brittle structure [49, 149].

Based on these characteristics it is possible to conclude that the bleaching process was successfully performed, with the tresses ready to the subsequent analysis.

2.3. Chaves' TSW and its formulation did not reveal any visual impact on the hair color and gloss

After applying for the test, compounds color and gloss analysis of the hair samples was employed. As being some of the most visible characteristics of the hair, the impact of the water on these characteristics might determine already a possible product application.

The colorimetric analysis made use of CIELAB color space to compare the colors of each sample. This color space color space created by the International Commission on Illumination (CIE) [138], and was designed to be perceptual uniform, where a certain numerical change is directly related to a perceived change in color [150].

CIELAB expresses color through three coordinates, L*, a* and b*. In this color space, L* value represents the lightness value of the color, being mathematically limited between 0 and 100 [151]. This color coordinate is responsible for distinguishing the gray/light objects from the dark colored ones, being the polar axis of the 3D color space [151, 152]. For the a* coordinate, it represents one color axis that runs from cyan (a*<0) to magenta (a*>0), whereas the other coordinate axis b* runs from blue (b*<0) to yellow (b*>0) [152]. Each of these parameters were analyzed for each hair tress group, obtaining the results represented on **Table 2.2**.

Table 2.2 Colorimetric values for the hair test groups and their respective color variation (ΔE). Their color determined by Nix™ Color converter

Sample	L*	b*	a*	ΔE	Exhibited color
Ctrl	76,97 ± 0,24	3,45 ± 0,07	24,15 ± 0,23	———	
Ave	76,29 ± 0,21	3,60 ± 3,60	24,00 ± 0,19	0,63 ± 0,23	
Chv	75,72 ± 0,05	3,66 ± 0,13	23,21 ± 0,45	1,53 ± 0,22	
FChv	77,06 ± 0,04	3,69 ± 0,11	24,31 ± 0,59	0,59 ± 0,15	
F	75,57 ± 0,33	4,73 ± 0,03	26,31 ± 0,20	2,84 ± 0,05	

Comparing the samples with the control group, Ave and Chv test groups revealed significant differences in their L* parameter indicating a lighter color (**one-way ANOVA: p < 0,05**). Regarding the b* parameter, no significant differences were detected between the samples (**one-way ANOVA: p > 0,05**) and only Chaves' TSW formulation exhibited a significant difference regarding the a* parameter (**one-way ANOVA: p < 0,05**).

In addition to the individual color parameters comparison, the *ΔE*, which represents the total color difference between the control group and the test groups, was calculated. The *ΔE* scale varies from 0 to 100, and the value below one defines a color change that is not perceivable by the human eye. Both Ave and FChv groups revealed values below that threshold. However Chv and F groups revealed values above the 1 and 2 which represent slight color variations [153].

Although statistically significant, such variations might be derived from the natural heterogeneous composition of each hair fiber in the multiple hair tresses, conjugated with slight variations on the oxidation process during the bleaching. Nonetheless, by analyzing the sample colors, they did not exhibit any significant visible changes as by inserting CILAB coordinates in Nix™ Color converter (available at: https://www.nixsensor.com/free-color-converter) the colors obtained are not visible impactful.

Subsequent to the color analysis, gloss was also measured. Gloss is a parameter used to examine the smoothness of a surface through the amount of light it reflects in the same angle of the incidence light [154]. The measures were taken, first at a 60º angle to first determine what type of gloss the hair presented. This analysis revealed values bellow 10 SGU (Specular Gloss Units), classifying the samples as low gloss and therefore the most appropriate angle for the following analysis was 85º (**Table 2.3**) [155].

Table 2.3 Gloss analysis of the hair samples at an 85º angle

Sample	85º
Crt	0,23 ± 0,12
Ave	nd
Chv	0,033 ± 0,047
FChv	0,40 ± 0,34
F	0,47 ± 0,20

By comparing the hair samples treated Chaves' TSW and the formulation to the control group no significant differences were detected (**Kruskall-Wallis test: p > 0,5**), implying that the formulation did not significantly impact the natural gloss of the hair.

2.4. Chaves' TSW Formulation may impact the combing strength of the hair tress

Hair entanglement is a characteristic that arises from hair's topological properties, where individual strands twist and loop around each other which leads to the formation of tangles [156]. Hair is composed of thousands of fibers, with the scalp population density exceeding 200 hair fibers per square centimeter, which translates into approximately 170 000 fibers for a full head [157]. With a vast number of fibers located next to each other, interactions between them will occur frequently leading to the their entanglement [156]. Additionally, the friction between hair fibers influences how easily they align in parallel, a process largely determined by the condition of the cuticle. Due to bleaching and the progressive damage of the hair in the ageing process, the cuticle morphology changes, leading to more less defined scales and increasing its roughness, resulting in higher friction [158], which further impacts hair entanglement.

With an increase in hair entanglement, there is a necessary increase in the brushing force. Cosmetic products that reduce this necessary force are of interest to the consumer. For such reason, analyzing how Chaves's TSW might impact this property might reveal a possible product application.

The formulation contains several components that might impact the hair fibre's combing. Ingredients such as Glycerin and Dexpanthenol exhibit the capacity to hydrate and retain the moisture in the hair [143, 159]. Additionally, surfactants like Cocoamidopropyl betaine (CAPB) are present, which reduces water's surface tension, easing the cleansing of a surface and even presenting further moistening properties [68, 69]. The combination of these properties might impact on the force required for combing the hair and for that reason, this measurement was again performed for the hair tress submitted to the formulation.

For this study, five combing cycles were employed for each hair tress, and for each cycle, the top combing force was measured. When comparing these forces, it was possible to observe a prompt decrease in the measured force in the second cycle (**Figure 2.1**).

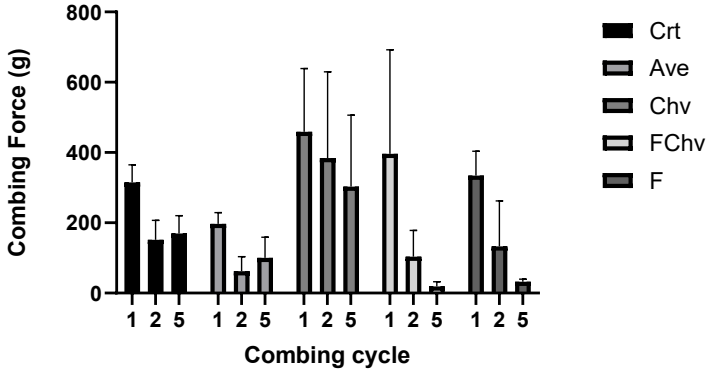

Figure 2.1 Combing forces at the first second and last combing cycle. Statistical analysis was performed using the one-way ANOVA with Tukey's multiple comparison. The results are represented as bar graphs (Average±SD). Control: Ctrl; Benchmark: Ave; Chaves's TSW: Chv; Chaves' TSW Formulation: FChv

The relative difference in the combing force was calculated using the first and last combing cycle forces revealing that the formulation indeed led to a significant decrease in the force necessary to comb the hair in the 5 cycles (**Figure 2.2**)

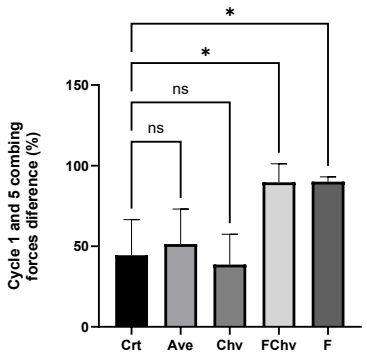

*Figure 2.2 Relative difference of the combing forces after the 5 cycles of combing. Statistical analysis was performed using the one-way ANOVA with Tukey's multiple comparison test. The results are represented as bar graphs (Average±SD). * stand for p < 0,05. ns, not significant*

From the pairwise comparison of the values obtained, it is possible to observe that indeed the formulation led to a decrease in the combability strength. However, such reduction is not caused by the TSW since the sole application of the water in the hair fiber did not lead to significant differences compared to the control and the F group, devoid of TSW (**Unpaired T-test: p > 0.05**). Therefore, this decrease in the combing force might be due to the components of the formulation.

This reduction can be associated with the presence of CAPB in the formulation, which acts as a surfactant [68, 69]. As reported by Kamath and Weigmann [160], wetted hair drastically increases midlength combing forces across the hair tress due to the surface tension forces involving the liquid film

between the fibres, which difficult their separation as the comb moves through the hair. As a surfactant, CAPB leads to the reduction of surface and interfacial tensions in the hair fiber [161] which might reduce the adherence between the hair fibers in the wet state. This results in more separated hair fibers facilitating the passage of the comb through the hair and therefore reducing the necessary force for the process.

2.5. Neither Chaves' TSW nor its formulation impacted the hair stifness

The primary content of the hair fiber is keratin, that through its conformation and chemical bonds, is responsible for hair stiffness, strength and insolubility [162]. Hair's cuticle protects the cortex of the fiber from its environment, and the structure and fraction of its constituents is associated with the hair's diameter which affects hair stiffness [163, 164].

When hair is in contact with water, it works as a plasticizer, reducing the interactions between the protein chains and swelling the keratin network, reducing stiffness. This effect occurs because water increases the spacing between the intermediate filaments that make up the cortex and also softens the amorphous matrix that surrounds these filaments [165].

The formulation contains moisturizing ingredients in its composition such as glycerin and dexpanthenol that retain water in the hair fiber which in turn might decrease its stifness. To assess this property, bending strength was measured, yielding the results shown in **Figure 2.3**. However, these measurements proved inconclusive, as no significant differences in bending strength were observed between the hair tresses. Therefore, it can be concluded that neither the formulation nor the TSW had a notable impact on the hair fiber.

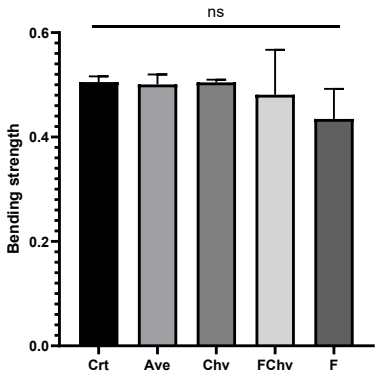

Figure 2.3 Bending strength of each hair tress. Statistical analysis was performed using the one-way ANOVA with Tuckey's multiple comparison test. The results are represented as bar graphs (Average±SD). ns, not significant

2.6. The application of the formulation revealed a decrease in the denaturation temperature of the hair tresses

Approximately 80% of the human hair is constituted by α-keratin that is mainly located into the cortex [166]. This protein is cysteine rich containing a significant amount of sulfur that is responsible for the formation of disulfide bonds between keratin chains that give the hair its characteristic shape, stability and texture [167].

With ageing and the use of cosmetic procedures such as hair dyeing, there is a structural decline of the hair keratin and keratin-associated proteins [166, 168]. Changes in these structures can lead to an alteration of the hair's thermal properties changing its denaturation temperature [167]. In practical terms, such alterations in its thermal properties might lead to the hair to be more/less susceptible to certain cosmetic processes like hair straightening through heat. Therefore, a cosmetic product that can protect against or reverse these effects could be advantageous. The assessment of the heat protection capacity was made using DSC.

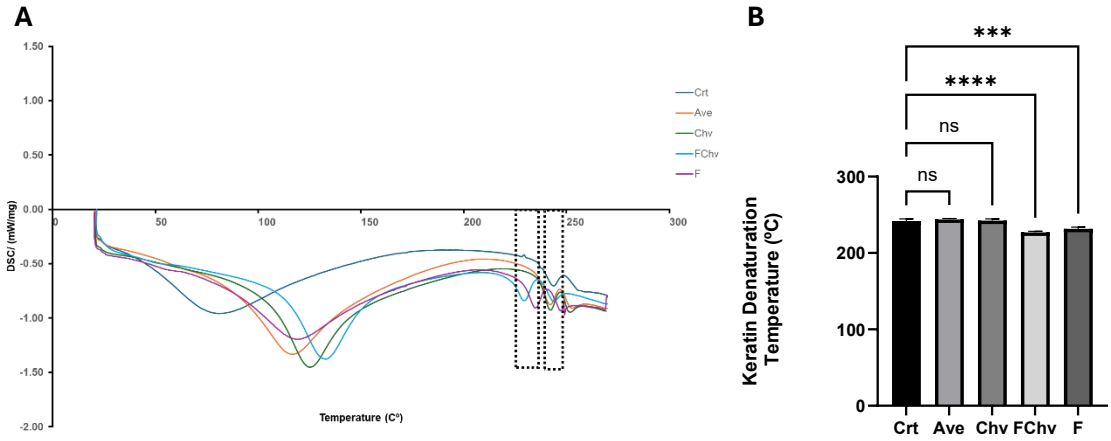

*Figure 2.4 Analysis of the thermal properties of the hair tresses. (A)DSC curve of each test group obtained at 10 ºC. min-1 under N2 atmosphere. Inside the boxes are market the thermal peaks that indicate keratin's thermal denaturation. (B) Keratin denaturation temperature. Statistical analysis was performed the one-way ANOVA with Tuckey's multiple comparison test. The results are represented as bar graphs (Average±SD). **** stands for p < 0,0001*

When comparing the DSC results between the test groups, it was possible to observe that the hair tresses that submitted to the treatment with the formulations exhibited a reduced keratin denaturation temperature (**Figure 2.4**). Denaturation temperature for these samples was 226,97 ± 2,10 ºC, a significant reduction from the other test groups that exhibited a denaturation temperature of 242,7 ± 2,2 ºC.

For the two test groups that did not differentiate from the control, such denaturation temperatures were expected and in agreement with the values reported in the literature for bleached hair. The bleaching process leads to an increase in cysteic acid due to the oxidation of the hair fiber. In turn, this increases the ionic interactions and stabilizes the keratin structure, resulting in an increase of its denaturation

temperature from 236 ºC (in a virgin hair) to approximately 245 ºC [167]. However, for the FChv test group, the registered temperature for keratin's denaturation is lower than that of virgin hair.

Protein denaturation depends on several factors such as chemical denaturants, environmental changes, and physical interactions, which are responsible for changing the original folding of the protein [169-171]. This folding is dependent on its amino acid sequence and the characteristics of its surrounding environment [169, 170].

Since the hair functional group might play an important role in its denaturation, ATR-FT-IR was employed to analyze any potential changes in the functional groups of the hair proteins and therefore its effects on the protein structure that might impact on its thermal behavior.

The structure of proteins, polypeptides and many other biological molecules exhibit peptide bond units, which are based on the amid bonds. These bonds can be observed in the ATR-FT-IR spectra of the samples with different wavelength depending on the type of amide region. The amide I band whose wavelength varies between 1600-1800 cm^{-1} [172], is related to the protein backbone conformation of the proteins providing important structural information. The location of this band is sensitive to changes in its secondary structure of the protein [173], and therefore its comparison might indicate any potential changes in the structure of keratin that might have led to the decrease of its denaturation temperature. However, when analyzing both spectra (**Figure 2.5-A**), both amide I bands seemed to overlap with each other, therefore not indicating any major backbone conformation change.

Nonetheless when comparing the full spectra of the hair samples, it is possible to observe that in the wavelength region 3000-2800 cm^{-1}, two peaks in the FChv and F groups are higher than all the previous samples (**Figure 2.5-B)**. These peaks are closely located in regions 2924 cm^{-1} and 2850 cm^{-1}, respectively corresponding to the asymmetric and symmetric C-H stretching of the methylene group of the lipids.

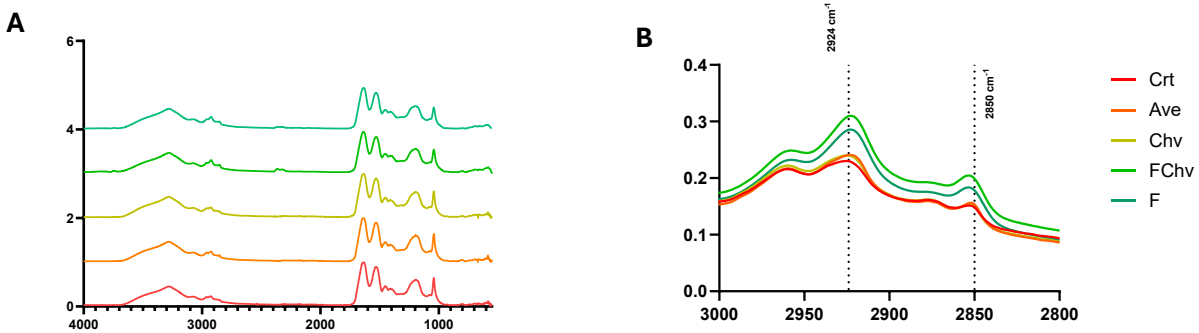

ATR-FT-IR can be used in a semiquantitative way whether the intensity of the peak represents the

Figure 2.5 Comparison of the infrared spectra of all test samples (A) Comparison of the full spectra (B) Comparison of the lipidic peak in the spectra 3000-2800 cm-1 region

absorption of a functional group at a specific wavelength. This intensity may vary according to the presence of the functional group absorbing in that region [174, 175], indicating that the hair tresses to which the formulation was applied had a higher lipidic content than the previous samples. By analyzing

the intensity of the peaks in **Figure 2.5-B**, it was possible to observe that as the peak intensity increases, the denaturation temperature exhibited by the hair tress decreases (**Figure 2.4**). In order to prove the observation, the relative level of lipids was determined according to the literature, by calculating the peak area ratio of 2850 and 2960 cm^{-1} bands (**Figure 2.6**), the latter representing the C-H stretching of the methyl groups of proteins [176]. Afterwards these results were crossed with the denaturation temperatures previously obtained revealing a negative correlation between both variables (Pearson's correlation coefficient: -0,830; $p < 0,01$), thus indicating that this increase on the relative level of lipids might be responsible for the decrease in the denaturation temperature of the hair's keratin.

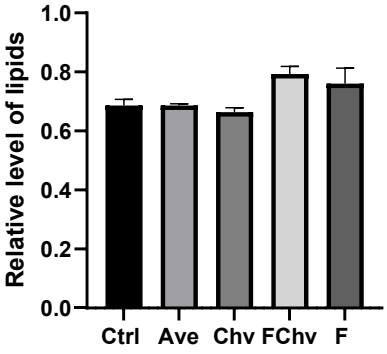

Figure 2.6 Relative level of lipids obtained through the ratio of the peak area of the bands 2850 and 2960 cm-1. The results are represented as bar graphs (Average±SD)

When analyzing the formulation's composition, it is possible to assume that this increase in the lipidic content might be caused by the presence of CAPB. CAPB is derived from coconut fatty acid [69], which might lead to an increased peak in the lipidic region of the ATR-FT-IR spectra. Being a surfactant, CAPB exhibits both anionic and cationic groups, being therefore, a zwitterion [177]. This characteristic confers them the capacity to bind with proteins electrostatically [178]. The binding to the positively or negatively charged parts of a protein, according to the literature, can lead to two different types of outcomes, in terms of protein thermal stability, destabilizing a protein by decreasing its melting temperature or stabilize it by increasing the protein folding cooperativity [178] . However, these effects are dependent on the specific protein involved.

It is possible that CAPB might be responsible for the decrease in thermal stability of the keratin by destabilizing its chain, which might ultimately restrict the use of this formulation previously to hair cosmetic procedures involving extreme heat such as hair straightening.

Chapter III: Enhancing Chaves Thermal Water formulation with bioactive natural extracts and its impact on skin's health

Despite its notable dermatological bioactivity - particularly its anti-inflammatory effects - its overall efficacy is constrained by a simplistic chemical composition derived from its mineral content. When additional active components were dissolved in Chaves' TSW, an enhancement of its beneficial properties was clearly observed, as demonstrated by the reduction in combing force.

Given that Chaves' TSW exhibited a more pronounced effect at the dermatological level compared to its limited impact on hair fibers, its incorporation into a topical formulation is expected to yield more substantial therapeutic outcomes. Prior to conducting further evaluation on the previously developed formulation, modifications were implemented to enhance its efficacy and broaden its bioactivity spectrum. To achieve this, two plant extracts were strategically incorporated, aiming to synergistically boost the functional properties of the TSW based formulation, hereby improving the formulation's dermatological benefits and overall therapeutic potential.

Plant extracts are one of the most used natural compounds in cosmetic formulations being used for centuries in the most diverse cultures across the world. Traditional Chinese medicine heavily relies on these extracts as these botanical ingredients are a rich source of bioactive molecules that compose the plant's secondary metabolites such as polyphenols, flavonoids, terpenes and many other molecules. These compounds act as potent antioxidants, neutralizing reactive oxygen species generated by UV exposure. They also exhibit anti-inflammatory, antimicrobial, photoprotective, moisturizing, wound healing, and anti-tyrosinase activities, making them multifunctional ingredients in formulations [179, 180].

In the formulation, two plant extracts, *Cucumis sativus* (Cucumber) and *Malva sylvestris* (Mallow) were incorporated for their documented anti-ageing properties. Cucumber extract is known for its antioxidant activity largely due to the presence of ascorbic acid and flavonoid content in its composition. Additionally, it also exhibits anti-elastase and anti-hyaluronidase activities contributing to skin elasticity and hydration [181]. Mallow extract, on the other hand, exhibits anti-inflammatory activity caused by the presence of malvidin 3-glucoside molecule. It also offers protection against oxygen radical species, attributed to the presence of phenolic compounds found in its leaves and has skin-whitening properties through the inhibition of the tyrosinase enzyme [182]. Additionally, to these properties *Malva sylvestris* is a native species across both mainland Portugal being present in Chaves' region (**Figure 3.1**). The plant is capable of striving in a variety of environments [183, 184] facilitating its obtention as a manufacturing product.

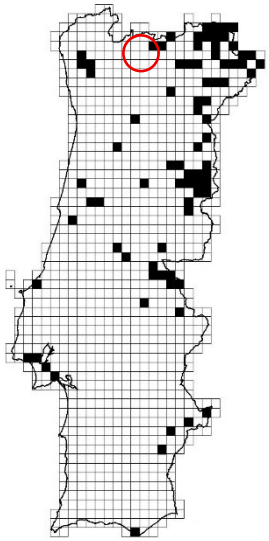

Figure 3.1 Malva sylvestris distribution across mainland Portugal. Circled in red is possible to observe Chaves' region where Malva sylvestris is a native plant. (Original image: Clamonte, et al. [191])

The extensive variety of plant extracts available on the market offers a range of beneficial properties for skin health including moisturizing, antioxidant and anti-inflammatory activities, therefore being a great choice for enhancing a formulation.

Given the reported positive impact of these extracts on skin health and the previously detailed beneficial effects of Chaves' TSW, this chapter explores whether these properties are retained in the final formulation and whether the plant extracts further enhance the bioactivities previously associated with TSW.

1. Materials and Methods

For this Chapter's methodology, a similar approach to the one employed in Chapter I was used with the results obtained being compared to the ones obtained with the sole application of Chaves TSW

1.1. Addition of Cucumber and Mallow extract to the formulation

Before beginning with the analysis of the formulation's bioactivities, three new variations incorporating plant extracts were prepared (**Table 3.1)**. The first formulation contained only cucumber extract (FP), the second contained only mallow (FM) and the third combined both extracts (FMP). Mallow and cucumber extracts (Crodarom, France) were used at the maximum recommended concentration of 5%, as specified by the manufacturer.

The preparation of the formulations followed the steps described in Chapter II (*See Chapter I: Material and Methods 1.1*).

Table 3.1 Composition of the Chaves' TSW-based formulation with the addition of the extracts (A) Formulation with only one of the extracts (B) Formulation with both extracts.

A

Ingredient name	Quantity (%(w/w))	Source
Chaves' TSW	84,87	Termas Chaves, Portugal
Mallow/Cucumber extract	5,00	Crodarom, France
Glycerin	2,00	Acofarma, Spain
Sodium Phytate	0,10	Apollo Scientific, UK
Dexpanthenol	2,00	Thermo Scientific, USA
Natural Ectoin	1,00	TCI, Japan
Cocoamidopropyl betaine	4,00	Chimidroga, Portugal
Etanol 70%	0,03	LabChem, USA
Euxyl PE9010	1,00	LotionCrafter, USA

B

Ingredient name	Quantity (%(w/w))	Source
Chaves' TSW	79,87	Termas Chaves, Portugal
Mallow extract	5,00	Crodarom, France
Cucumber extract	5,00	Crodarom, France
Glycerin	2,00	Acofarma, Spain
Sodium Phytate	0,10	Apollo Scientific, UK
Dexpanthenol	2,00	Thermo Scientific, USA
Natural Ectoin	1,00	TCI, Japan
Cocoamidopropyl betaine	4,00	Chimidroga, Portugal
Etanol 70%	0,03	LabChem, USA
Euxyl PE9010	1,00	LotionCrafter, USA

1.2. Antioxidant activity and enzymatic assays

Both ABTS and DPPH assays were conducted following the protocols described in Chapter I (*See Chapter I: Material and Methods 1.3.1 and 1.3.2*).

1.3. Fe^{2+} Chelating Activity

Chelating activity of the formulations was determined according to the protocol described in Ouahhoud, et al. [185]. In brief, to determine the chelating power of Fe^{2+} 250 µL of the sample were mixed with 1mL of acetate buffer (0,1M; pH 4,9) and $FeCl_2$ (2mM). The reaction was left incubating at room temperature for 30 minutes, afterwards added 0,1 mL of ferrozine (5mM). The reaction mixture was left incubating again for 30 min, the absorbance measured at 562 nm.

For negative control, distilled water was used in the same volume of the samples, while for positive control a 40 µg/mL solution was prepared and used. The percentage inhibition of Fe^{2+} ferrozine complex formation was then calculated according to the following formula:

$$Inhibition\ (\%) = \frac{A_0 - A_1}{A_0} \times 100$$

A_0: Absorbance of negative control

A_1: Absorbance of the sample of reference

1.4. Cell culture assays

The assays here employed were performed similarly to the ones described in chapter I (*See Chapter I: Material and Methods 1.3.3*)

1.5. Antimicrobial screening

1.5.1. Preparation of the media with the formulation components

For the antimicrobial screening, only the plant extracts and sodium phytate were used, to avoid interference from the surfactants and preservatives used in the formulation. The test components were mixed into TSW dissolved Muller Hinton broth (MHB), following the manufacturer instructions representing the formulation. After mixing the test media were filtered using a sterile 0.22 µm filter (Milipore, USA).

Different concentrations of the test compounds were prepared to evaluate their dose-dependent effects on microbial growth, enabling systematic screening of their antimicrobial activity. The highest tested concentration comprised 10% (w/w) plant extract and 0,20% (w/w) sodium phytate which was equivalent to twice the concentration of the base formulation concentration. Subsequent dilutions were then tested in series, down to the base-concentration of 5% (w/w) plant extract and 0,10% (w/w) sodium phytate. A detailed table containing the concentrations used can be observed in **supplementary table 1**

1.5.2. Antimicrobial activity time-growth curve screening

The antimicrobial activity of the formulation was screened using a time-growth inhibition curve, based on the CLSI-M07-A9 standard [186]. Previously to the execution of the assay, pure cultures of *Staphyloccus aureus* 209 and *Staphylococcus epidermidis* Fussel, were grown in Tryptic Soy Broth (TSB) (Bioakar, France) for two cycles of 24 hours, being afterwards platted into Tryptic Soy Agar (TSA) (Bioakar, France). Both TSB and TSA were supplemented with 3g/L of yeast extract (Sigma-Aldrich, Germany) and the incubations were performed at 37ºC under aerobic conditions. After incubation, the pre-inoculum was prepared by picking one colony from the plate and resuspend it in 10 mL of MHB being afterwards incubated for 24h at 37ºC under aerobic conditions. The inoculum was then prepared in the following day by adding 1mL of the inoculum to 9 mL of MHB, being left overnight at 37ºC. The working inoculum was prepared by adjusting the inoculum optical density (OD) at 625 nm until reaching a value of 0,08-0,1 being afterwards 10 times diluted in MHB. 20 µL of the work inoculum were inoculated into 980 µL of the test solutions and 200 µL of the suspension was transferred to a 96-well microtiter plat (Nunc, Germany). The growth was measured during 24 hours at 37ºC, and the OD measures were taken into hourly intervals at 625 nm, using a microplate reader (Epoch, USA). A positive control was drawn using inoculated MHB medium without the test components and a MHB medium with 20% DMSO was used as a negative control. Blanks of the samples were used to correct the sample color OD interference.

2. Results and Discussion

2.1. Chaves' Formulation exhibited enhanced antioxidant activity

Antioxidant activity similar to Chapter 1 was assessed by DPPH and ABTS assays. According to DPPH assay, none of the formulations tested showed antioxidant activity. However, according to ABTS assay it was possible to detect inhibitions above 60% in all the three formulations (**Table 3.2**).

To determine whether the plant extracts were responsible for the observed increase in antioxidant activity, we tested the original Chapter 2 formulation - containing none of these extracts - alongside the three extract-enriched formulations. Amongst the three variants the dual-extract formulation (FMP) exhibited a significant enhancement in ABTS radical scavenging (**one-way ANOVA: $p < 0,05$**).

Nevertheless, the absolute gain in radical-quenching capacity across all extract-containing samples was modest, indicating that the extracts may have produced a measurable effect although they did not induce a dramatic enhancement in $ABTS^{\bullet+}$ scavenging.

Table 3.2 ABTS and DPPH radical scavenging caused by the TSW formulations

	ABTS radical inhibition (%)	DPPH radical inhibition (%)
Formulation without extracts (FChv)	62,78 ± 11,29	nd
Cucumber Formulation (FP)	65,92 ± 3,39	nd
Mallow formulation (FM)	60,01 ± 7,78	nd
Mallow and cucumber formulation (FMP)	71,29 ± 5,25	nd

Plant extract's are recognized for their phenolic component. Originated from secondary metabolism pathways, the phenolic component of these extracts play a crucial role against oxidative stress, due to their capacity of donating hydrogen atoms or electrons and forming stable radical intermediates [187]. Both Mallow (M) and Cucumber (M) extracts, have both been reported to exhibit antioxidant effect [188, 189], although variable according to the part of the plant used.

To evaluate if these extracts were responsible for the increase antioxidant acitvity of FMP, the individual extracts and their mixture, were tested through ABTS assay at a concentration of 5%, dissolved in deionized water (**Table 3.3**). In oposition to the literature the cucumber extract revealed a minimal ABTS radical inhibition whereas both the mallow extract and its combination with cucumber demonstrated clear antioxidant activity.

Table 3.3 ABTS radical scavenging of the plant extracts present in the formulations

	ABTS radical inhibition (%)
Cucumber extract (P)	0,25 ± 0,57
Mallow extract (M)	5,44 ± 0,82
Mallow and Cucumber extract mixture (MP)	4,91 ± 1,01

Such an outcome was not expected and therefore the deviation from the reported antioxidant activities was hypothesized as being caused by the composition of the plant extract. CRODAROM Phytexcell™ Cucumber extract is obtained from *Cucumis sativus*, being advertised as an ingredient for improving skin moisture. The extract also contains a high glycerin concentration, well known as a powerfull moisturizer [190]. Glycerin is used during the extraction process due to its capacity of dissolving compounds that are not miscible in water [191], the amount of the compound present during the extraction represents a key element by regulating the amount of polyphenols that are dissolved in the final extract. It has been reported by Anis and Ahmed [191], that during the extraction process, there is an optimal glycerin extraction concentration that allows the dissolution of the polyphenols from the plant material. The glycerol content makes the solvent more viscous which slows down the process of diffusion, hindering the extraction of polyphenols. Glycerol content is variable depending on the plant

extract, and therefore higher glycerol content during extraction process might be the factor that hindered the antioxidant activity of the Cucumber extract at a 5% concentration.

Since the mixture of mallow and cucumber yielded a higher antioxidant activity, there is the possibility that the mallow extract could play a role in improving the antioxidant properties of the formulation. Nevertheless, the antioxidant capacity of the complete formulation significantly exceeds the activity of the individual extracts indicating a pronounced synergistic interaction among its components rather than merely an additive effect.

It has been supported by the literature that the antioxidant activity of the phenolic content of plant extracts might be the result of two mechanisms of action, the capacity of scavenging free radicals and chelation of iron ions. All the three formulations contain sodium phytate as its chelating agent, which might play a role in its potential chelating activity. In addition, flavonoids, a group of polyphenols composed by two benzene rings with phenolic hydroxyl groups connected through three central carbon atoms, may also present chelating activity being essential for both metal binding and radical quenching [192, 193].

Faced with this possibility, the chelating potential of the formulation was accessed.

2.2. Antioxidant activity of the formulations might be a product of the combination of a significant chelating activity and free radical scavenging

Chelating agents are substances whose molecules are able to form several bonds to a specific metal ion, effectively creating a stable complex [194]. Chelating agents are commonly incorporated into cosmetic formulations due to their ability to bind heavy metal ions—such as iron—thereby facilitating their removal and minimizing the damage they can induce [195, 196]. Flavonoids present in plant extracts are capable of chelating metal ions and form complexes with them. For instance, the interaction of a flavonoid with Fe^{2+} catalyzes its oxidation to Fe^{3+}, forming a chelation ring with the metal. The catechol groups in the flavonoid ring B (**Figure 3.2**) as well as the 3-OH/4-C=O in ring C and 5-OH/4-C=O in rings AC are responsible for the coordination reaction with iron metals. During the coordination that leads to the complex formation some OH or C=O sites remain transiently free to donate H• or e^- to incoming radicals. Upon donation, the flavonoid radical is stabilized lowering the bond-dissociation enthalpy for H-atom transfer. This accelerates the electron transfer kinetics, augmenting the capacity of the flavonoid to trap the radical. Such type of reaction is mostly observed in the chelation of Cu^{2+} ions, however it has been reported that Fe^{2+} reaction with flavonoids, might enhance the performance of the flavonoid against antioxidant tests such as DPPH and ABTS [197].

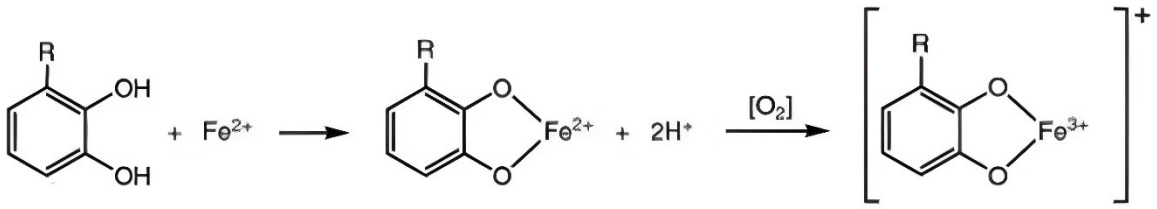

Figure 3.2 Polyphenol ring B coordination of Fe2+ and subsequent electron transfer reaction in the presence of oxygen, forming the flavonoid-Fe3+ complex (figure obtained from Walencik, et al. [212] – Figure 5-C)

Fe^{2+} also represents an important agent in regulation of the reactive oxygen species homeostasis (ROS) of the organism. Being necessary in several metabolic pathways, ferrous ions also play a crucial role in the formation ROS due to its ability to transfer single electrons [196].

Iron-induced peroxidation, for example, is responsible for the wrinkling that occurs as result of chronic photodamage to the skin [198]. The exposure to UVA radiation, leads skin cells to release loosely bound iron which is responsible to catalyze the production of highly toxic hydroxyl radical through Fenton reaction which further leads to an enhanced production of metalloproteases and lipid peroxidation [195].

Therefore, due to such impact on skin health, the capacity of chelating agents to protect skin's integrity might present itself as an effective therapeutic approach by reducing the amount of available free iron that could catalyze ROS producing reactions [195, 196], working as an indirect way of reducing ROS levels.

For the ferrous ion chelating activity assay, the complete formulation with Cucumber extract (FP), Mallow extract (FM) and Mallow and Cucumber extract (FMP) were used. To identify the key contributor to any potential antioxidant activity, the individual components – including the extracts (P, M, MP), the water (TSW) and the main chelating agent, sodium phytate (Fit) - were also tested separately. Each was assessed at the same concentration used in the formulation but dissolved in deionized water to isolate their individual effects. EDTA, one of the most widely used chelating agents in the cosmetic industry due to its strong metal ion-binding capacity [145], was included as a positive control.

By analyzing the chelating activity of the formulations, it was possible to observe a significant increase in iron chelating percentage when compared to the sole use of Chaves' TSW (**one-way ANOVA: p < 0,0001**). None of the individual components exhibit a drastic Fe^{2+} iron chelating activity, however it is possible to observe that all the three formulations demonstrated a high capacity to chelate iron. Such behavior could be explained by the conjugated action of these components, that synergistically increase the capacity to chelate this ion, since every component exhibits chelating capacity (**Figure 3.3)**

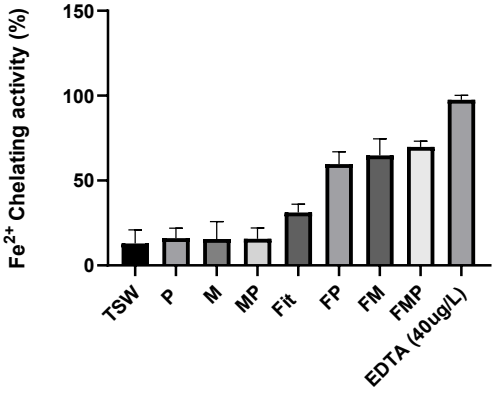

*Figure 3.3 Comparative chelating activity of the formulation and its constituents. Statistical analysis was performed using the one-way ANOVA with Tukey's multiple comparison. The results are represented as bar graphs (Average±SD). TSW: Thermal Spring Water P: Cucumber extract; M: Mallow extract; MP: Mallow and Cucumber extract; FP: Cucumber extract formulation; FM: Mallow extract formulation; FMP: Mallow and Cucumber extract formulation. *, **, **** stand for F*

The major chelating component of the formulation is sodium phytate, which its sole use at a concentration of 0,10% revealed a significant difference in the chelating activity when compared with Chaves' TSW (**one-way ANOVA: p < 0,0005**). However, when compared with the results obtained with the formulations, sodium phytate alone does not justify the increase in chelating activity, being the chelation activity of the three formulations significantly different (**one-way ANOVA: p < 0,0001**).

When analyzing their chelating capacities, it's possible to observe that the extracts did also exhibit Fe^{2+} chelating potential, although at a lower magnitude than sodium phytate. Extract polyphenols such as Flavonoids and water-soluble pigments such as Anthocyanins are mainly present in the CRODAROM Phytexcell® Mallow are known for their chelating capacities which might be responsible for the chelating activity exhibited by the compound [185, 199]. However, regarding the CRODAROM Phytexcell® Cucumber extract, the technical sheet does not detail the presence of the aforementioned polyphenol components and therefore its chelating activity was not expected. However, literature, details that such extracts contain also other types of flavonoids in their composition which as mentioned, are capable of forming complexes with iron ions due to the presence of hydroxyl groups in its chemical structure [200]. This could justify the fact that the extract exhibited some chelating activity.

Chaves' TSW also exhibited the capacity to chelate iron as it revealed a 12,96 ± 7,94% Fe^{2+} activity possibly due to interactions between the HCO_3^- and the ferrous ion. Although the characterization of Chaves' TSW in chapter I did not include the quantification of HCO_3^-, *Termas Chaves* SPA, has previously described that the water contains a concentration of 1762 mg/L of the hydrogencarbonate ion [201]. It has been reported that the presence of elevated bicarbonate concentration promotes ferrous iron transformation facilitating Fe-CO_3 synthesis. By reacting with HCO_3^{2-} some of the free Fe^{2+} could not react with ferrozine during the assay and was therefore not detected leading to some chelating potential.

Since every single tested component exhibited a Fe^{2+} chelating capability, and the formulation does not contain any other known potential chelating agent, it is possible to assume that the major increase in chelating activity observed in the formulations might be due to the synergistically effects of all the tested constituents. By combining different iron chelators such synergistic effect was expected as such approaches have been already described in literature [202].

Although exhibiting significantly lower chelating activity than EDTA (**one-way ANOVA: $p < 0,001$**), the formulations, nonetheless, present a significant chelating activity. Due to the fact that ions such as Fe^{2+} are key elements in the formation of ROS on the organism [195, 196], and the chelation of Iron by the polyphenol content of the plant extracts might improve its ROS scavenging potential [197], the observed results in ABTS might be a result from these factors.

2.3. An enhanced inhibition of age-related enzymes was observed after Chave's TSW application

Additional to the enhanced antioxidant potential, previously study skin enzymes could exhibit completely distinct behavior when interacting with the formulation and its compounds. MMP-1 (a collagenase enzyme), Elastase and Tyrosinase were once again selected for their respective enzyme inhibition assays due to their important role in skin ageing.

The reported results revealed a much more positive landscape regarding the inhibitory properties of Chaves' based formulations, with at least the formulation containing both mallow and cucumber extract inhibiting all the 3 enzymes with a significant activity (**Table 3.3**).

Table 3.4 Evaluation of Chaves' TSW based formulation and their potential to inhibit age related enzymes

	Enzyme relative inhibition		
	Collagenase (MMP-1)	**Tyrosinase**	**Elastase**
Cucumber Formulation (FP)	11,55 ± 5,09	21,85 ± 3,25	nd
Mallow formulation (FM)	12,83 ± 4,32	30,74 ± 6,29	nd
Mallow and cucumber formulation (FMP)	24,34 ± 7,87	21,90 ± 0,87	44,01 ± 0,06

Regarding collagenase activity, it has been reported in the literature how zinc is an essential cofactor to the activity of the MMP-1 enzyme. Zn^{2+} plays an essential role in various catalytical process, being the family of Matrix metalloproteinases (MMPs) dependent of this ion. Such enzymes contain two sites for the ion, one catalytic site where Zn^{2+} binds and another that contributes to the overall structural stability of the enzyme [203]. It has been reported that some inhibitors of the collagenase activity disrupt this interaction of the zinc with its active sites on MMP-1 [204]. Due to the chelating capacity of the formulations, it is possible that its active ingredients incapacitate the binding of Zn^{2+} [205, 206] by chelating it and therefore lead to an increased inhibition of the enzyme's activity.

This type of interaction may also explain the increased anti-tyrosinase activity of the formulation. Tyrosinase belongs to the type 3 copper protein family capable of catalyzing the ortho-hydroxylation of phenolic substrates and the two-electron oxidation of catecholic substrates to quinones, being the latter responsible for the formation of melanin. In order for the enzyme to work properly, similar to collagenase it requires a cofactor. In the case of tyrosinase, binuclear copper atoms (Cu^{2+}) are essential for the correct catalytic activities of the enzyme, which turn copper chelation a possible responsible for suppressing its activity [207].

Regarding elastase, this enzyme is a serine protease that is involved in the degradation of the ECM degrading elastin but also with capacity to cleave collagen, fibronectin and other ECM proteins. Several reports on anti-Elastase activity from whole plant extracts detailed that a wide variety of polyphenols such as flavonoids, tocopherols, phenolic acids and tannins have the capacity to inhibit this enzyme [205, 208, 209]. Flavonoids are composed of two benzene rings and one heterolytic pyran ring and can be divided into subgroups depending on the point of attachment of the β-carbon ring to the C-carbon ring and the degree of its oxidation and according to their chemical substitution. Several characteristics on the chemical structure of flavonoids are responsible for the different inhibitory capacities of these compounds. For example. The presence of catechol groups (with contiguous phenolic hydroxyl groups at position 3' and 4') reveal a notable elastase inhibition enabling a better binding with the enzyme [205]. When analyzing the results we can observe that among the 3 formulations only the one containing the mixture of both extracts revealed a visible inhibition of the elastase enzyme. Separated cucumber or mallow extracts seem to cause an inhibition of the enzyme. Such phenomenon could be due to the flavonoid content in the formulation. It was reported that many flavonoids exhibit a concentration-dependent inhibition of elastase. Since the extracts are present at a concentration of 5% the flavonoid content in each extract might not be sufficient to inhibit the elastase activity. By adding the two extracts together, we increase the amount and variety of flavonoids in the formulation possibly inhibiting the enzyme.

In chapter I it was observed that the sole application of Chaves' TSW did not significantly impact on the majority of age-related enzymes, with only Elastase being inhibited by the TSW. By incorporating other bioactive compounds dissolved in the TSW, it was possible to observe a potentiator effect, making the formulation much more valuable in terms of bioactive and age-related effects.

Among the three formulations, the dual-extract formulation (FMP), seems to comprise the combined benefits of both the cucumber (FP) and mallow (FM) formulations. Therefore, in the subsequent cell culture assays, both extracts were used in combination as a mixture.

2.4. Although inhibiting collagenase, the formulation does not promote the synthesis of collagen

Prior to testing the formulation in cell cultures some adjustments were taken into account. Due to the presence of agents like CAPB that act as surfactants and therefore might lead to cell membrane solubilization and destabilization [210, 211], and the presence of a preservatives that can lead to changes in cell growth and gene expression of basic molecular processes [212, 213], the complete formulation could not be tested.

Therefore, since the full usage of the formulation could lead to elevated cytotoxic levels, only key components studied, such as the plant extracts and sodium phytate were mixed in the TSW cell media for further testing.

Cytotoxicity assessment was conducted before the quantification of pro-collagen. Both Mallow and Cucumber extracts did not reveal any negative impact on cell viability, at the base concentration of 5% (**Supplementary Figure 6 - A**). In opposition, sodium phytate revealed a cytotoxic effect when incubated with the nHDF cells. Therefore, different concentrations were tested, and the highest non-cytotoxic concentration was chosen to proceed with pro-collagen quantification (**Supplementary Figure 6 - B**). A TSW cell culture medium (DMEM 11885084) was supplemented with 5% mallow and cucumber extracts with 0,025% sodium phytate and incubated for 24 hours with the cells. Following treatment, the levels of pro-collagen I α1 were quantified by ELISA using lysates obtained from the cell pellet of nHDF cultures. The results were normalized considering the protein content of the cells to allow comparison of the different conditions.

As demonstrated in **Figure 3.4**, the reported levels of collagen were not significantly different from the cells exposed to the TSW, which was previously reported on chapter I. Therefore, the integration of both plant extracts and sodium phytate did not significantly impact collagen synthesis.

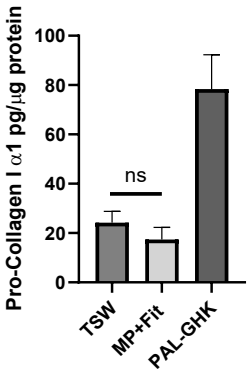

Figure 3.4 Quantification of pro-collagen 1α1 in nHDF cells treated with Chaves thermal spring water (Chaves TSW). Palmitoyl Tripeptide-1 (Pal-GHK) was used as positive control. Statistical analysis was performed using the one-way ANOVA with Tukey's multiple comparison. The results are represented as bar graphs (Average±SD). Ns, not significant

2.5. The formulation's composition may mitigate the heightened inflammatory response induced by exposure to pollution particles

PP are known for their capacity to stimulate the inflammatory response in skin cells. This stimulus is mainly due to the increased production of ROS in the cells due to the binding of the PP with the Toll-like receptor 5 (TLR5), which in turn interacts with the NADPH oxidase, NOX4, producing increased levels of ROS. These ROS leads to the phophorilation of Ser536 of the NF-kB subunit p65 that then translocate to the nucleus and binds to form the transcription factor NF-kB promoting the expression of inflammatory cytokines like IL-6 [214]. Additionally, to NOX4 induced ROS production and IL-6 expression, these PPs can also lead to increasing intracellular Iron levels due to their internalization causing iron overload and redox imbalance which in turn leads to ferroptosis [215, 216].

Oxidative stress is a critical mediator in the cellular inflammatory response, with iron also contributing significantly to this process. The previously conducted assays demonstrated the formulation's ability to chelate iron and its antioxidant potential, suggesting the possibility of an enhanced anti-inflammatory effect. Based on this hypothesis, the effect of the formulation's components on cells subjected to PP exposure was subsequently assessed.

The maximal non-cytotoxic concentrations were established before evaluating anti-inflammatory effects in HaCaT cells. The base formulation concentrations - 5% cucumber and mallow extracts, 0.10% sodium phytate - exhibited significant cytotoxicity after 24 hours, whereas lower concentrations - 0.625% extracts and 0.0125% sodium phytate - were identified as the highest tolerated levels (**Supplementary Table 7**) and used in subsequent pollution-induced inflammation assays.

As in Chapter 1, the cells were incubated for 24 hours with or without PP dispersed in the supplemented test media. Following 24-hour incubation, the supernatants were collected and used for for IL-6 and IL-1α quantification via ELISA. The correspondent cell pellets were lysed and afterwards used to quantify the total protein content in order to normalize the IL-6 and IL-1α allowing the correct comparison across different conditions.

The IL-6 levels observed for the formulation components did not demonstrate a significant difference in comparison to TSW (**Figure 3.5 - A**), thereby indicating the preservation of its anti-inflammatory potential as established in Chapter 1. However, a significant difference was observed in IL-1α levels between TSW and the formulation components, both with and without PP (**Figure 3.5 - B**).

Although demonstrating increased levels of IL-1α compared to TSW under conditions without PP stimulation, the application of the inflammatory stimulus did not lead to a significant increase in IL-1α (**Supplementary figure 8**), as was observed in the TSW control group.

IL-1α is a constitutively expressed cytokine present inside the keratinocytes which has long been associated as having a role of alarmin. This cytokine is a constitutively expressed in higher levels within and upon cellular damage or cell death, IL-1α is released into the extracellular environment, where it contributes to inflammation by activating key transcription factors such as NF-κB [108, 217].

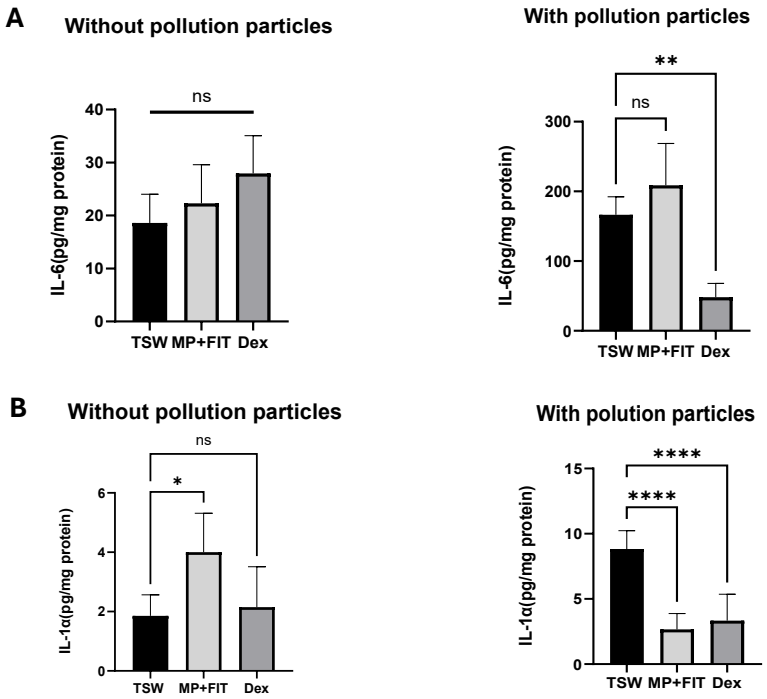

*Figure 3.5 Evaluation of anti-inflammatory potential of the formulation's key components. Quantification of IL-6 (A) and IL-1α (B) levels in supernatants of HaCaT cells with and without urban air pollution. Statistical analysis was performed using the one-way ANOVA with Tukey's multiple comparison. The results are represented as bar graphs (Average±SD). ** and *** stand for p < 0,001 and p <0,0001*

The use of PPs to induce an inflammatory response promotes the generation of significant concentrations of ROS. Iron, a major metallic component of SRM 1648a PPs, plays a key role in this process. Its internalization by keratinocytes increases intracellular iron levels, leading to redox imbalance and subsequent cell death [215, 216]. This in turn results in the release of IL-1α further amplifying the inflammatory response [108, 217].

Given the strong iron-chelating activity exhibited by the formulation's components—particularly sodium phytate—it is likely that the formulation conferred protection to HaCaT cells against ROS-induced

oxidative damage and subsequent cell death. This protection minimized the release of IL-1α. Therefore, the formulation not only preserved its anti-inflammatory activity in terms of IL-6 modulation but also exhibited superior antioxidant properties compared to TSW by mitigating IL-1α-driven inflammation through cellular protection against iron- and ROS-induced cytotoxicity.

2.6. The formulation visibly impacted the growth of S.aureus and S.epidermidis

Both *S. aureus* and *S. epidermidis* are two of the most common bacteria reported in the skin microbiome. *S. epidermidis* is a widely recognized as one of the most abundant and ubiquitous bacterial colonizers of healthy human skin, contributing to the maintenance of the skin integrity and homeostasis. As an example, *S.epidermidis* can activate distinct innate immune signaling from human keratinocytes augmenting the antimicrobial peptide (AMP) that can be used to mediate the levels of other microorganisms such as *S. aureus*, preventing the colonization of pathogenic microorganisms [218].

S. aureus on the other hand is a highly versatile and opportunistic pathogen, that is responsible for a wide variety of infections in humans. Nonetheless, approximately 20-30% of the population is permanently, although, asymptomatically colonized in the nose, while other 30% may carry the bacterium intermittently [219]. This bacterium is recognized by its association with AD, since its capability to adapt into different niches permits it to colonize the afflicted skin [219-222]. In more severe cases, *S. aureus* is able to penetrate the dermis and stimulate the production of proinflammatory cytokines, further exacerbating the AD symptoms [222].

Skin across the lifetime accumulates an excessive number of senescent cells, leading to the gradual loss of cellular functions. With the progressive loss of cellular functions, immunological alterations can lead the immunological system to become hyperresponsive, with increased levels of pro-inflammatory cytokines leading to an imbalance between inflammatory and anti-inflammatory responses [22]. Conjugated with the progressive deterioration of the epidermal skin barrier, the ageing process can cause the emergence of conditions such as AD [22-24].

In the skin, the balance between *S. aureus* and *S. epidermidis* is highly dynamic and context dependent. In situations where the skin barrier integrity is disrupted the protection against *S. aureus* opportunistic infections conferred by *S. epidermidis* can be compromised, allowing *S. aureus* to colonize the skin. The increase of *S.aureus* colonization in AD afflicted skins is correlated with the progress of the condition characteristic flares [221]. However, it's important to notice that *S. epidermidis* role is also dynamic and although capable of combating *S. aureus* growth and colonization, it has been also observed at increase density on lesional skin in AD, often, although not always together with *S. aureus* [223].

Disrupting this equilibrium can bring undesirable health outcomes and therefore validate how the formulation impacts the growth of this bacteria is important. For that reason, an antimicrobial test was employed to analyze if the formulation may represent an anti-microbial agent that could drastically affect one bacterium relative to the other.

For both bacterial species, the OD was measured 24 hours in hourly intervals, and it was possible to observe that at this time interval, the test medium with double the plant extract and sodium phytate inhibited the growth of *S. aureus* and *S. epidermidis* (**Figure 3.6**). As the concentration decreased it was possible to observe that the growth of the microorganism started to increase until reaching the standard concentration used in the formulation with 5% mallow and cucumber extract and 0,10% sodium phytate. At this concentration, the growth inhibition of both bacteria becomes less sever larger exponential phases but with a significant 10-hour delay on the lag phase. Such a delay could prove beneficial in flares of atopic dermatitis AD, since it's mostly impacted by microbial growth.

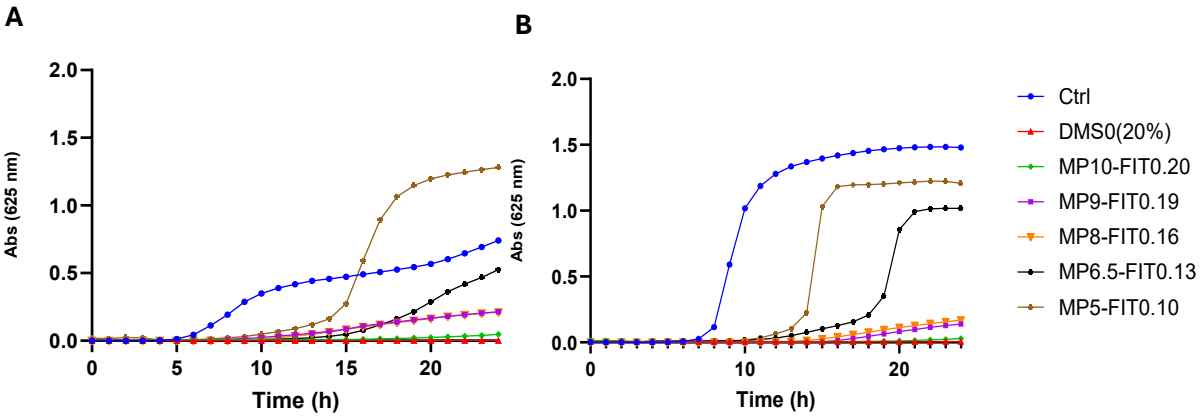

Figure 3.6 Inhibition curves of (A) S. aureus and (B) S. epidermidis

Byrd, et al. [221], reported that most severe cases of AD flares were visibly accompanied with an increase in *S. aureus* relative abundance. *S. epidermidis* relative abundance was also analyzed and also revealed an increase. Nevertheless, no correlation with the severity of the skin condition was traced. *S. epidermidis,* nonetheless, can predominate in less severe cases of AD [221]. It has been shown that strains from *S. epidermidis* that populate lesional skin of AD exhibit a distinct phenotype compared with those from healthy skin. These strains exhibited higher protease activity and produced less metabolites capable of inducing the Aryl Hydrocarbon Receptor (AhR). This reduction in AhR ligands undermines the AhR/OVOL 1 signaling axis responsible for regulating skin barrier balance and immunintegrity and immune homeostasis [224].

By similarly prolonging the lag phase of both microbial strains, the formulation could help mitigate both severe and less severe flares of atopic dermatitis by promoting a more gradual - and therefore less intense - onset of symptoms. Moreover, because aged skin is particularly prone to microbial imbalances and subsequent inflammation, regular application of this formulation may help delay dysbiosis and curb the propagation of pathogenic species, thereby preserving a healthier, more balanced skin microbiome.

Conclusion and future work

The use of TSW throughout the centuries has been continuously supported by their observed and, more recently, scientifically validated health benefits. The composition of every water differs depending on the geographical location where it is extracted, and therefore this factor shapes their therapeutic effects.

The objective of this work aimed at investigating the properties of the TSW and assess its potential integration into cosmetic formulations targeted at mitigating signs of aging in both the skin and hair—two of the most visibly features during the aging process.

Initially, Chaves' TSW therapeutic potential was assessed for cutaneous application. Amongst the various assays conducted, its anti-inflammatory properties represented a significant highlight, with TSW being able to reduce the amount of IL-6 produced by the cells when in contact with PP as inflammatory stimulus. Such an outcome was hypothesized as being a key action of the chemical composition of this water, through the presence of immunoregulatory ions such as Mg^{2+} [113, 114] that are prevalent in the water's composition. A population study was also employed revealing that the water was capable of improving the skin barrier by reducing TEWL and improving skin hydration on the volunteers that exhibited dry skin. These effects are attributed, at least in part, to the presence of Ca^{2+}, which plays a critical role in keratinocyte proliferation and differentiation [15].

While these results underscore the promise of Chaves' TSW as a cosmetic ingredient, it is important to notice that its benefits are inherently limited by the simplicity of its chemical composition, since its activity is constrained to its mineral composition. To enhance its functional capabilities, the water was integrated into a pilot cosmetic formulation comprising surfactants, chelating agents, moisturizers, and preservatives.

Upon development of the formulation, the second phase of the study aimed at the hair fibers aspect and health condition. With the pilot formulation developed in Chapter 2, it was possible to compare the water and its derived pilot formulation's properties. Through side-by-side evaluation of pure TSW and the pilot formulation, it became clear that TSW alone did not significantly impact the hair's physical properties. Given that hair is composed of non-living keratinized cells the results were expected. The minerals present in the water's composition are normally beneficial due to their physiological role in living tissues and therefore its action could not drastically change the physical properties of the hair fiber. Nonetheless, the research here conducted allowed us to observe how integrating other components into a complex cosmetic formulation might expand its properties and applications. With the incorporation of surfactants such as CAPB – an amphoteric molecule - it was possible to observe a reduction in the force needed for combing the hair tresses due to its impact in reducing water's surface tension [161] allowing for a lower adherence between hair fibers. Additionally, changes in keratin denaturation temperature suggested an influence on hair protein stability, hypothesized to result from CAPB's interaction with the hair fiber [178].

Although these results are consistent with expectations, further research is required to validate them. Future work should rely on testing each of the ingredients of the formulation to isolate its contribution.

Moreover, the inherent variability introduced by the heterogenicity of hair tresses – despite being used standardized commercial samples – poses challenges both in reproducibility and statistical analysis. With thousands of hair fibers interacting with each other, both the entanglement of the fibers and their special arrangement might hinder an even application of the test product across all hair fibers and impact the measurements taken with the texturometer. Enhanced sampling strategies with a larger number of hair tresses may be necessary for future studies.

Building in the formulation's potential, in Chapter 3, the pilot formulation was further enhanced by incorporating plant extracts derived from cucumber and mallow and its dermocosmetic potential was assessed. Initial antioxidant testing promptly revealed a significant improvement in the antioxidant activity of the formulations with the mixture of both plant extracts exhibiting a higher ABTS scavenging potential than the pilot formulation. This increase was although hypothesized as being mainly caused by the significant Fe^{2+} chelating activity of the formulation as the two extracts and their mixture did not exhibit an ABTS radical scavenging activity high enough to justify such an outcome [197]. Enzymatic assays further revealed an improved performance of the formulations as they were capable of inhibiting all three skin enzymes – Elastase, Collagenase and Tyrosinase. These inhibitory activity might be due to the extracts' polyphenolic content and their chelating activity which likely interfere with metallic ions such as Zn^{2+} and Cu^{2+} used as cofactors by MMP-1 and tyrosinase [203, 205, 207].

Nevertheless, these assays, being purely chemical and synthetic in nature, have limited biological relevance. For instance, ABTS radical is a chemically synthetized and stable radical [93], which in some cases may not accurately represent *in vivo* oxidative stress, since biologically produced ROS have different redox potentials, half-lives, and reactivities [225]. Additionally, antioxidant potential can act both directly and indirectly by inhibiting agents responsible for producing ROS, such as free Fe^{2+} capable of catalyzing ROS formation through Fenton reaction [195]. Future work should incorporate cell-based models to better assess bioavailability, intracellular iron chelation, and ROS modulation.

It is also important to highlight the discrepancies between the antioxidant activity of the cucumber extract and the reported values in the literature, as the used extract did not reveal the capacity to scavenge the ABTS radical. It is hypothesized here, that the phenolic composition of the extract was reduced due to the high amount of glycerol used in the extraction of the plant material, but such claim needs further testing. The optimal amount of glycerin used to extract the cucumber flavonoid content is not discussed in the work of Anis and Ahmed [191], and the optimal values could vary according to the plant and region of the plant used. Additionally, the manufacturer does not disclose information either about the polyphenolic content or concentration in both extracts and therefore claims about these components in the formulations are also hypothesized. Therefore, future work should prioritize compositional analysis of these extracts or optimize the extract by manually manufacturing the extract.

Among the different formulations tested, the mixture of both extracts yielded the most beneficial outcomes inhibiting all three target skin enzymes. Therefore, this formulation was selected for further assessment of collagen synthesis and anti-inflammatory properties via *in vitro* cell culture assays.

Although collagen synthesis in nHDF cells did not show a significant improvement with the addition of the extracts and sodium phytate, the formulation demonstrated enhanced anti-inflammatory potential. It not only preserved the anti-inflammatory properties of the TSW but also protected cells from ROS-induced damage caused by the PPs, which are responsible for the release of IL-1α cytokines. Although the results are promising, further evaluation in more complex cellular models, comprising multiple skin cell types is necessary to better replicate an *in vivo* environment.

Finally, a preliminary antimicrobial activity screening of the formulation was assessed for both *S. aureus* and *S. epidermidis*, two of the most common bacteria reported in the skin microbiome. *S. aureus* is typically the primary bacterium associated with opportunistic infections [219] with its growth in AD lesions being associated with increase in the severity of AD [221]. Its growth can be prevented by *S. epidermidis,* capable of stimulating human keratinocytes' capacity to secrete AMP [218]. However the balanced between both species is dynamic and context dependent, and less severe cases of AD lesion are vastly populated by this specie [221]. The screening revealed that at a concentration of 10% cucumber and mallow extract with 0,20% sodium phytate in a TSW dissolved MHB, the growth of *S. aureus* and *S. epidermidis* was fully inhibited for 24 hours. This inhibition is progressively lost as the concentration of the active ingredients is progressively diminished, however it is possible to observe that at a concentration equal to the formulation's base concentration, there is a prolonged lag phase, with an approximately 10-hour increase compared to the control. Nonetheless, the reported assay represents a screening of the bacterial growth in the presence of the formulation components and does not fully explore how the equilibrium from both bacteria might change. However, as optical density measurements cannot distinguish living from dead cells, these findings are therefore limited. Accurate CFU quantification will be essential in future studies to assess differential microbial responses and elucidate the severity of the inhibition for each bacterium [226].

In conclusion, this work demonstrates that Chaves' TSW exhibits modest but meaningful benefits for skin health, alleviating some of the agents responsible for ageing. It's integration on a formulation allowed to expand its action spectra, significantly enhancing its properties providing an effective cosmetic product. These findings provide a foundation for future studies aimed at refining formulation composition and validating efficacy in biologically relevant models.

Bibliographic references

1. Hategekimana, F., et al., *Geochemical Characterization of Nyamyumba Hot Springs, Northwest Rwanda*. AppliedChem, 2022. **2**(4): p. 247-258.
2. Sun, V.Z. and R.E. Milliken, *Characterizing the mineral assemblages of hot spring environments and applications to Mars orbital data*. Astrobiology, 2020. **20**(4): p. 453-474.
3. Hou, W., et al., *A comprehensive census of microbial diversity in hot springs of Tengchong, Yunnan Province China using 16S rRNA gene pyrosequencing*. PloS one, 2013. **8**(1): p. e53350.
4. Gaur, N., et al., *Evaluation of water quality index and geochemical characteristics of surfacewater from Tawang India*. Scientific Reports, 2022. **12**(1): p. 11698.
5. Taweelarp, S., et al., *Geochemical modeling of scale formation due to cooling and CO 2-degassing in San Kamphaeng Geothermal Field, Northern Thailand*. Chiang Mai Univ. J. Nat. Sci., 2021. **20**: p. e2021049.
6. Figueiredo, A.C., et al., *Thermal Spring Waters as an Active Ingredient in Cosmetic Formulations*. Cosmetics, 2023. **10**(1): p. 27.
7. Cacciapuoti, S., et al., *The role of thermal water in chronic skin diseases management: a review of the literature*. Journal of clinical medicine, 2020. **9**(9): p. 3047.
8. Quattrini, S., B. Pampaloni, and M. Brandi, *Natural mineral waters: chemical characteristics and health effects*. *Clin Cases Miner Bone Metab 13: 173–180*. 2016.
9. Lewis, R.E. and H.W. Young, *Thermal springs in the Payette River basin, west-central Idaho*. Vol. 80. 1980: US Department of the Interior, Geological Survey.
10. Pandarinath, K., *Solute geothermometry of springs and wells of the Los Azufres and Las Tres Virgenes geothermal fields, Mexico*. International Geology Review, 2011. **53**(9): p. 1032-1058.
11. Aires-Barros, L., J. Marques, and R. Graça, *Elemental and isotopic geochemistry in the hydrothermal area of Chaves, Vila Pouca de Aguiar (northern Portugal)*. Environmental Geology, 1995. **25**: p. 232-238.
12. Mormile, I., et al., *The Benefits of Water from Nitrodi's Spring: The In Vitro Studies Leading the Potential Clinical Applications*. International Journal of Molecular Sciences, 2023. **24**(18): p. 13685.
13. Zajac, D., *Inhalations with thermal waters in respiratory diseases*. Journal of Ethnopharmacology, 2021. **281**: p. 114505.
14. Simon, N., et al., *Physico-chemical characterisation and potential health benefit of the Hulu Langat Hot Spring in Selangor, Malaysia*. Sains Malaysiana, 2019. **48**(11): p. 2451-62.
15. Cauche, V., et al., *Jonzac Thermal Spring Water Reinforces Skin Barrier Function of Human Skin and Presents a Soothing and Regenerating Effect*. Journal of Cosmetics, Dermatological Sciences and Applications, 2023. **13**(4): p. 247-268.
16. Gilaberte, Y., et al., *Anatomy and Function of the Skin*, in *Nanoscience in dermatology*. 2016, Elsevier. p. 1-14.
17. Surbek, M., S. Sukseree, and L. Eckhart, *Iron Metabolism of the Skin: Recycling versus Release*. Metabolites, 2023. **13**(9): p. 1005.

18. Tarnowska, M., et al., *The effect of vehicle on skin absorption of Mg2+ and Ca2+ from thermal spring water*. International Journal of Cosmetic Science, 2020. **42**(3): p. 248-258.
19. Salsberg, J., et al., *A review of protection against exposome factors impacting facial skin barrier function with 89% mineralizing thermal water*. Journal of Cosmetic Dermatology, 2019. **18**(3): p. 815-820.
20. Krutmann, J., et al., *The skin aging exposome*. Journal of dermatological science, 2017. **85**(3): p. 152-161.
21. Ahmed, I.A., et al., *Natural anti-aging skincare: role and potential*. Biogerontology, 2020. **21**: p. 293-310.
22. Bocheva, G.S., R.M. Slominski, and A.T. Slominski, *Immunological aspects of skin aging in atopic dermatitis*. International journal of molecular sciences, 2021. **22**(11): p. 5729.
23. Williamson, S., J. Merritt, and A. De Benedetto, *Atopic dermatitis in the elderly: a review of clinical and pathophysiological hallmarks*. British Journal of Dermatology, 2020. **182**(1): p. 47-54.
24. Yang, F., et al., *Differences in clinical characteristics of rosacea across age groups: A retrospective study of 840 female patients*. Journal of cosmetic dermatology, 2023. **22**(3): p. 949-957.
25. Eliasse, Y., et al., *Effect of thermal spring water on human dendritic cell inflammatory response*. Journal of Inflammation Research, 2019: p. 181-194.
26. da Silva Lima, M., et al., *Anti-inflammatory effects of carvacrol: evidence for a key role of interleukin-10*. European journal of pharmacology, 2013. **699**(1-3): p. 112-117.
27. Moore, K.W., et al., *Interleukin-10 and the interleukin-10 receptor*. Annual review of immunology, 2001. **19**(1): p. 683-765.
28. Stumpf, C., et al., *Atorvastatin enhances interleukin-10 levels and improves cardiac function in rats after acute myocardial infarction*. Clinical Science, 2009. **116**(1): p. 45-52.
29. Stefanache, A., et al., *Understanding how minerals contribute to optimal immune function*. Journal of Immunology Research, 2023. **2023**.
30. Patel, R.H. and S.S. Mohiuddin, *Biochemistry, Histamine*. 2020.
31. Aries, M.-F., et al., *Anti-inflammatory and immunomodulatory effects of Aquaphilus dolomiae extract on in vitro models*. Clinical, Cosmetic and Investigational Dermatology, 2016: p. 421-434.
32. Song, Z.Q., et al., *Bacterial and archaeal diversities in Y unnan and T ibetan hot springs, C hina*. Environmental microbiology, 2013. **15**(4): p. 1160-1175.
33. Wang, X. and L. Pecoraro, *Diversity and co-occurrence patterns of fungal and bacterial communities from alkaline sediments and water of Julong high-altitude hot springs at Tianchi Volcano, Northeast China*. Biology, 2021. **10**(9): p. 894.
34. Tang, J., et al., *Temperature-controlled thermophilic bacterial communities in hot springs of western Sichuan, China*. BMC microbiology, 2018. **18**: p. 1-14.
35. Li, L. and Z. Ma, *Global microbiome diversity scaling in hot springs with DAR (diversity-area relationship) profiles*. Frontiers in Microbiology, 2019. **10**: p. 118.

36. Wang, S., et al., *Greater temporal changes of sediment microbial community than its waterborne counterpart in Tengchong hot springs, Yunnan Province, China*. Scientific reports, 2014. **4**(1): p. 7479.
37. Tabarzad, M., V. Atabaki, and T. Hosseinabadi, *Anti-inflammatory activity of bioactive compounds from microalgae and cyanobacteria by focusing on the mechanisms of action*. Molecular biology reports, 2020. **47**(8): p. 6193-6205.
38. Pernet, I., et al., *Calcium triggers β-defensin (hBD-2 and hBD-3) and chemokine macrophage inflammatory protein-3α (MIP-3α/CCL20) expression in monolayers of activated human keratinocytes*. Experimental dermatology, 2003. **12**(6): p. 755-760.
39. Velnar, T., T. Bailey, and V. Smrkolj, *The wound healing process: an overview of the cellular and molecular mechanisms*. Journal of international medical research, 2009. **37**(5): p. 1528-1542.
40. Hoover, E., M. Alhajj, and J.L. Flores, *Physiology, hair*, in *StatPearls [Internet]*. 2023, StatPearls Publishing.
41. Natarelli, N., N. Gahoonia, and R.K. Sivamani, *Integrative and mechanistic approach to the hair growth cycle and hair loss*. Journal of clinical medicine, 2023. **12**(3): p. 893.
42. Yousef, H., et al., *Histology, skin appendages*, in *StatPearls [Internet]*. 2023, StatPearls Publishing.
43. Zhang, H.-L., X.-X. Qiu, and X.-H. Liao, *Dermal Papilla Cells: From Basic Research to Translational Applications*. Biology, 2024. **13**(10): p. 842.
44. Andl, T., L. Zhou, and Y. Zhang, *The dermal papilla dilemma and potential breakthroughs in bioengineering hair follicles*. Cell and tissue research, 2023. **391**(2): p. 221-233.
45. Yang, C.-C. and G. Cotsarelis, *Review of hair follicle dermal cells*. Journal of dermatological science, 2010. **57**(1): p. 2-11.
46. Cedirian, S., et al., *The exposome impact on hair health: etiology, pathogenesis and clinical features—Part I*. Anais Brasileiros de Dermatologia, 2024.
47. Rogers, G.E., *Known and unknown features of hair cuticle structure: a brief review*. Cosmetics, 2019. **6**(2): p. 32.
48. Yang, F.-C., Y. Zhang, and M.C. Rheinstädter, *The structure of people's hair*. PeerJ, 2014. **2**: p. e619.
49. Fernandes, C., et al., *On hair care physicochemistry: from structure and degradation to novel biobased conditioning agents*. Polymers, 2023. **15**(3): p. 608.
50. Rouse, J.G. and M.E. Van Dyke, *A review of keratin-based biomaterials for biomedical applications*. Materials, 2010. **3**(2): p. 999-1014.
51. Kaisheva, E., *Microscopic Characteristics for Human Hair Identification*. Acta morphologica et anthropologica. **28**: p. 3-4.
52. He, Y., et al., *Mechanisms of impairment in hair and scalp induced by hair dyeing and perming and potential interventions*. Frontiers in Medicine, 2023. **10**: p. 1139607.
53. Trüeb, R.M., et al., *Scalp condition impacts hair growth and retention via oxidative stress*. International journal of trichology, 2018. **10**(6): p. 262-270.
54. Grymowicz, M., et al., *Hormonal effects on hair follicles*. International journal of molecular sciences, 2020. **21**(15): p. 5342.

55. Bertoli, M.J., et al., *Female pattern hair loss: A comprehensive review*. Dermatologic therapy, 2020. **33**(6): p. e14055.
56. Hickey, M., R.A. Szabo, and M.S. Hunter, *Non-hormonal treatments for menopausal symptoms*. Bmj, 2017. **359**.
57. Ioannides, D. and E. Lazaridou, *Female pattern hair loss*. Alopecias-practical evaluation and management, 2015. **47**: p. 45-54.
58. Chen, J., et al., *Hair graying regulators beyond hair follicle*. Frontiers in Physiology, 2022. **13**: p. 839859.
59. Adav, S.S. and K.W. Ng, *Recent omics advances in hair aging biology and hair biomarkers analysis*. Ageing Research Reviews, 2023. **91**: p. 102041.
60. Baltenneck, F., et al., *Age-associated thin hair displays molecular, structural and mechanical characteristic changes*. Journal of Structural Biology, 2022. **214**(4): p. 107908.
61. Tokunaga, S., H. Tanamachi, and K. Ishikawa, *Degradation of hair surface: Importance of 18-MEA and epicuticle*. Cosmetics, 2019. **6**(2): p. 31.
62. Trüeb, R.M., *Pharmacologic interventions in aging hair*. Clinical interventions in aging, 2006. **1**(2): p. 121-129.
63. Research, G.-G.V. *Cosmetics Market Size, Share & Trends Analysis Report By Product (Skin Care, Hair Care), By End-user (Men, Women), By Distribution Channel (Offline, Online), By Region (North America, Europe), And Segment Forecasts, 2024 - 2030*. 2023 [cited 2024 14th May]; Available from: https://www.grandviewresearch.com/industry-analysis/cosmetics-market.
64. Li, L. and J. Qin, *Advances in Permeation of Solutes into Hair: Influencing Factors and Theoretical Models*. Applied Sciences, 2023. **13**(9): p. 5577.
65. Cruz, C.F., et al., *Human hair and the impact of cosmetic procedures: a review on cleansing and shape-modulating cosmetics*. Cosmetics, 2016. **3**(3): p. 26.
66. Srinivasan, G. and S. Chakravarthy Rangachari, *Scanning electron microscopy of hair treated in hard water*. International Journal of Dermatology, 2016. **55**(6): p. e344-e346.
67. Wiechers, J.W., et al., *Formulating for efficacy 1*. International journal of cosmetic science, 2004. **26**(4): p. 173-182.
68. Jacob, S.E. and S. Amini, *Cocamidopropyl betaine*. DERM, 2008. **19**(3): p. 157-160.
69. Herrwerth, S., et al., *Highly concentrated cocamidopropyl betaine–the latest developments for improved sustainability and enhanced skin care*. Tenside Surfactants Detergents, 2008. **45**(6): p. 304-308.
70. O'goshi, K.-i., M. Iguchi, and H. Tagami, *Functional analysis of the stratum corneum of scalp skin: studies in patients with alopecia areata and androgenetic alopecia*. Archives of dermatological research, 2000. **292**: p. 605-611.
71. Kim, J.Y. and H. Dao, *Physiology, integument*. 2020.
72. Blakely, K. and M. Gooderham, *Management of scalp psoriasis: current perspectives*. Psoriasis: targets and therapy, 2016: p. 33-40.
73. Akarsu, S., et al., *Efficacy of the addition of salicylic acid to clindamycin and benzoyl peroxide combination for acne vulgaris*. The Journal of dermatology, 2012. **39**(5): p. 433-438.
74. Huang, A., S. Seité, and T. Adar, *The use of balneotherapy in dermatology*. Clinics in dermatology, 2018. **36**(3): p. 363-368.

75. Antunes, J.d.M., et al., *Hydrotherapy and crenotherapy in the treatment of pain: integrative review.* BrJP, 2019. **2**: p. 187-198.
76. Alves, T., et al., *Applications of natural, semi-synthetic, and synthetic polymers in cosmetic formulations. Cosmetics, 7 (4), 75*. 2020.
77. Vaz, M., et al., *The importance-satisfaction matrix as a strategic tool for Termas de Chaves thermal spa priority improvements.* Journal of Tourism, Sustainability and Well-Being, 2023. **11**(1): p. 52-65.
78. Chaves, T.d. 2025 [cited 2025 17 june]; Available from: https://www.termasdechaves.com/historia.
79. Clesceri, L.S., *Standard methods for examination of water and wastewater*. American public health association, 1998. **9**.
80. Standardization, I.O.f., *Water quality — Enumeration of culturable micro-organisms — Colony count by inoculation in a nutrient agar culture medium*. 1999.
81. Gonçalves, B., et al., *Effects of elevated CO2 on grapevine (Vitis vinifera L.): volatile composition, phenolic content, and in vitro antioxidant activity of red wine.* Journal of agricultural and food chemistry, 2009. **57**(1): p. 265-273.
82. Standardization, I.O.f., *Biological evaluation of medical devices; Part 5: Tests for in vitro cytotoxicity.* 2009.
83. Carvalho, M.J., et al., *Anti-Aging Potential of a Novel Ingredient Derived from Sugarcane Straw Extract (SSE).* International Journal of Molecular Sciences, 2023. **25**(1): p. 21.
84. Carvalho, M.J., et al., *Impact of a novel sugarcane straw extract-based ingredient on skin microbiota via a new preclinical in vitro model.* The Microbe, 2023. **1**: p. 100017.
85. Ahuja, K. and P. Lio, *The role of trace elements in dermatology: A systematic review.* Journal of Integrative Dermatology, 2023.
86. Ali, S.M. and G. Yosipovitch, *Skin pH: from basic science to basic skin care.* Acta dermato-venereologica, 2013. **93**(3): p. 261-267.
87. Carneiro, J., G.M. Marques, and P.A. Vicente, *Development and Evaluation of an Anti-aging Cosmetic Formulation Exploring Antioxidant Potential of Vitis vinifera L.* International journal of pharmaceutical compounding, 2020. **24**(6): p. 515-518.
88. Kusumawati, I. and G. Indrayanto, *Natural antioxidants in cosmetics.* Studies in natural products chemistry, 2013. **40**: p. 485-505.
89. Rembiesa, J., et al., *The Impact of Pollution on Skin and Proper Efficacy Testing for Anti-Pollution Claims.* Cosmetics, 2018. **5**(1): p. 4.
90. Joly, F., J.-E. Branka, and L. Lefeuvre, *Thermal Water from Uriage-les-Bains Exerts DNA Protection, Induction of Catalase Activity and Claudin-6 Expression on UV Irradiated Human Skin in Addition to Its Own Antioxidant Properties.* Journal of Cosmetics, Dermatological Sciences and Applications, 2014. **04**(02): p. 99-106.
91. Knott, A., et al., *Corrigendum to "Decreased fibroblast contractile activity and reduced fibronectin expression are involved in skin photoaging" [J. Dermatol. Sci. 58 (2010) 75–77].* Journal of Dermatological Science, 2010. **58**(3): p. 232.
92. Sun, W., et al., *Comprehensive functional evaluation of a novel collagen for the skin protection in human fibroblasts and keratinocytes.* Bioscience, Biotechnology, and Biochemistry, 2023. **87**(7): p. 724-735.

93. Nenadis, N., et al., *Estimation of scavenging activity of phenolic compounds using the ABTS•+ assay.* Journal of agricultural and food chemistry, 2004. **52**(15): p. 4669-4674.
94. Juang, K.-W., Y.-J. Lo, and B.-C. Chen, *Modeling Alleviative Effects of Ca, Mg, and K on Cu-Induced Oxidative Stress in Grapevine Roots Grown Hydroponically.* Molecules, 2021. **26**(17): p. 5356.
95. Golshani-Hebroni, S., *Mg++ requirement for MtHK binding, and Mg++ stabilization of mitochondrial membranes via activation of MtHK & MtCK and promotion of mitochondrial permeability transition pore closure: A hypothesis on mechanisms underlying Mg++'s antioxidant and cytoprotective effects.* Gene, 2016. **581**(1): p. 1-13.
96. Baud, S., et al., *Elastin peptides in aging and pathological conditions.* Biomolecular concepts, 2013. **4**(1): p. 65-76.
97. Gosselin, L.E., *Skeletal muscle collagen: age, injury and disease.* Sarcopenia–Age-Related Muscle Wasting and Weakness: Mechanisms and Treatments, 2011: p. 159-172.
98. Hariri, R., M. Saeedi, and T. Akbarzadeh, *Naturally occurring and synthetic peptides: Efficient tyrosinase inhibitors.* Journal of Peptide Science, 2021. **27**(7): p. e3329.
99. Widelski, J., et al., *Extracts from European propolises as potent tyrosinase inhibitors.* Molecules, 2022. **28**(1): p. 55.
100. Shim, J.H., *Prostaglandin E2 induces skin aging via E-prostanoid 1 in normal human dermal fibroblasts.* International Journal of Molecular Sciences, 2019. **20**(22): p. 5555.
101. Tanaka, T., et al., *Visualized procollagen Iα1 demonstrates the intracellular processing of propeptides.* Life Science Alliance, 2022. **5**(5).
102. Grether-Beck, S., et al., *Bioactive molecules from the Blue Lagoon: in vitro and in vivo assessment of silica mud and microalgae extracts for their effects on skin barrier function and prevention of skin ageing.* Experimental Dermatology, 2008. **17**(9): p. 771-779.
103. Araújo, L.A.d., F. Addor, and P.M.B.G.M. Campos, *Use of silicon for skin and hair care: an approach of chemical forms available and efficacy.* Anais brasileiros de dermatologia, 2016. **91**: p. 0331-0335.
104. Eliasse, Y., D. Redoules, and E. Espinosa, *Impact of Avène Thermal Spring Water on immune cells.* Journal of the European Academy of Dermatology and Venereology, 2020. **34**: p. 21-26.
105. Lee, H.-P., et al., *Effect of spa spring water on cytokine expression in human keratinocyte HaCaT cells and on differentiation of CD4+ T cells.* Annals of Dermatology, 2012. **24**(3): p. 324-336.
106. Guilloteau, K., et al., *Skin inflammation induced by the synergistic action of IL-17A, IL-22, oncostatin M, IL-1α, and TNF-α recapitulates some features of psoriasis.* The Journal of Immunology, 2010. **184**(9): p. 5263-5270.
107. Tsai, M.-H., et al., *Urban particulate matter enhances ROS/IL-6/COX-II production by inhibiting microRNA-137 in synovial fibroblast of rheumatoid arthritis.* Cells, 2020. **9**(6): p. 1378.

108. Macleod, T., et al., *The immunological impact of IL-1 family cytokines on the epidermal barrier*. Frontiers in Immunology, 2021. **12**: p. 808012.
109. Jarlborg, M. and C. Gabay, *Systemic effects of IL-6 blockade in rheumatoid arthritis beyond the joints*. Cytokine, 2022. **149**: p. 155742.
110. da Silva Lima, F., et al., *An insight into the role of magnesium in the immunomodulatory properties of mesenchymal stem cells*. The Journal of nutritional biochemistry, 2018. **55**: p. 200-208.
111. Weyh, C., et al., *The role of minerals in the optimal functioning of the immune system*. Nutrients, 2022. **14**(3): p. 644.
112. Steward, C.J., et al., *One week of magnesium supplementation lowers IL-6, muscle soreness and increases post-exercise blood glucose in response to downhill running*. European journal of applied physiology, 2019. **119**: p. 2617-2627.
113. Sugimoto, J., et al., *Magnesium decreases inflammatory cytokine production: a novel innate immunomodulatory mechanism*. The Journal of Immunology, 2012. **188**(12): p. 6338-6346.
114. Bernstein, H., et al., *823: Magnesium decreases inflammatory cytokine production: A novel innate immunomodulatory mechanism*. American Journal of Obstetrics & Gynecology, 2012. **206**(1): p. S361.
115. Naji, A.A. and H.M. Mousa, *Evaluation of Interleukin6 (IL-6) levels in Atopic Dermatitis Patients in Thi-Qar province*. University of Thi-Qar Journal of Science, 2022. **9**(1): p. 49-51.
116. Toshitani, A., et al., *Increased interleukin 6 production by T cells derived from patients with atopic dermatitis*. Journal of investigative dermatology, 1993. **100**(3): p. 299-304.
117. Parke, M.A., et al., *Diet and skin barrier: The role of dietary interventions on skin barrier function*. Dermatology Practical & Conceptual, 2021. **11**(1).
118. Proksch, E., J.M. Brandner, and J.M. Jensen, *The skin: an indispensable barrier*. Experimental dermatology, 2008. **17**(12): p. 1063-1072.
119. Berardesca, E., et al., *The revised guidance for the in vivo measurement of water in the skin*. Skin Research and Technology, 2018. **24**(3): p. 351-358.
120. Almeida, C., et al., *Monfortinho thermal water-based creams: effects on skin hydration, psoriasis, and eczema in adults*. Cosmetics, 2019. **6**(3): p. 56.
121. Heinrich, U., et al., *Multicentre comparison of skin hydration in terms of physical-, physiological-and product-dependent parameters by the capacitive method (Corneometer CM 825)*. International journal of cosmetic science, 2003. **25**(1-2): p. 45-53.
122. Montero-Vilchez, T., et al., *Skin Barrier Function in Psoriasis and Atopic Dermatitis: Transepidermal Water Loss and Temperature as Useful Tools to Assess Disease Severity*. Journal of Clinical Medicine, 2021. **10**(2): p. 359.
123. Nikam, V.N.M., Rochelle C.; Dandakeri, Sukumar; Bhat, Ramesh M., *Transepidermal Water Loss in Psoriasis A Case-control Study*. Indian Dermatology Online Journal. **10**(3): p. 267-271.
124. Weyrich, L.S., et al., *The skin microbiome: Associations between altered microbial communities and disease*. Australasian journal of dermatology, 2015. **56**(4): p. 268-274.

125. Borrego-Ruiz, A. and J.J. Borrego, *Microbial dysbiosis in the skin microbiome and its psychological consequences*. Microorganisms, 2024. **12**(9): p. 1908.
126. Byrd, A.L., Y. Belkaid, and J.A. Segre, *The human skin microbiome*. Nature Reviews Microbiology, 2018. **16**(3): p. 143-155.
127. Whiting, C., S. Abdel Azim, and A. Friedman, *The skin microbiome and its significance for dermatologists*. American journal of clinical dermatology, 2024. **25**(2): p. 169-177.
128. Fournière, M., et al., *Staphylococcus epidermidis and Cutibacterium acnes: two major sentinels of skin microbiota and the influence of cosmetics*. Microorganisms, 2020. **8**(11): p. 1752.
129. Inaka, K. and T. Kimura, *Comfortable and dermatological effects of hot spring bathing provide demonstrative insight into improvement in the rough skin of Capybaras*. Scientific Reports, 2021. **11**(1): p. 23675.
130. Bajgai, J., et al., *Balneotherapeutic effects of high mineral spring water on the atopic dermatitis-like inflammation in hairless mice via immunomodulation and redox balance*. BMC complementary and alternative medicine, 2017. **17**(1): p. 1-9.
131. Karagülle, M.Z., et al., *In vitro evaluation of natural thermal mineral waters in human keratinocyte cells: a preliminary study*. International journal of biometeorology, 2018. **62**: p. 1657-1661.
132. Trüeb, R.M., *Shampoos: ingredients, efficacy and adverse effects*. JDDG: Journal der Deutschen Dermatologischen Gesellschaft, 2007. **5**(5): p. 356-365.
133. Im, S.H., *Shampoo compositions*. Handbook of hair in health and disease, 2012: p. 434-447.
134. Rahim, N.F.A., et al., *Synergistic effect of polyherbal formulations on DPPH radical scavenging activity*. Journal of Science and Technology, 2018. **10**(2).
135. Kircik, L.H., *Synergy and its clinical reievance in topical acne therapy*. The Journal of Clinical and Aesthetic Dermatology, 2011. **4**(11): p. 30.
136. Mountfield, R.J., et al., *Potential inhibitory effects of formulation ingredients on intestinal cytochrome P450*. International journal of pharmaceutics, 2000. **211**(1-2): p. 89-92.
137. Standardization, I.O.f., *Cosmetics — Guidelines on technical definitions and criteria for natural and organic cosmetic ingredients*. 2017.
138. (CIE), I.C.o.I. *CIE 1976 (L*, a*, b*) colorspace (CIELAB)*. 1976.
139. Senthilkumar, K., et al., *Preparation of self-preserving personal care cosmetic products using multifunctional ingredients and other cosmetic ingredients*. Scientific Reports, 2024. **14**(1): p. 19401.
140. Mérat, E., et al., *Sensory evaluation of cosmetic functional ingredients*, in *Nonfood sensory practices*. 2022, Elsevier. p. 197-216.
141. Roussel, L., N. Atrux-Tallau, and F. Pirot, *Glycerol as a skin barrier influencing humectant*, in *Treatment of dry skin syndrome*. 2012, Springer. p. 473-480.
142. Porto Ferreira, V.T., et al., *Topical dexpanthenol effects on physiological parameters of the stratum corneum by Confocal Raman Microspectroscopy*. Skin Research and Technology, 2023. **29**(9): p. e13317.
143. Proksch, E., et al., *Topical use of dexpanthenol: a 70th anniversary article*. Journal of Dermatological Treatment, 2017. **28**(8): p. 766-773.

144. Hon, K.L., et al., *Testing an ectoin containing emollient for atopic dermatitis*. Current Pediatric Reviews, 2019. **15**(3): p. 191-195.
145. Lanigan, R.S. and T.A. Yamarik, *Final report on the safety assessment of EDTA, calcium disodium EDTA, diammonium EDTA, dipotassium EDTA, disodium EDTA, TEA-EDTA, tetrasodium EDTA, tripotassium EDTA, trisodium EDTA, HEDTA, and trisodium HEDTA*. International journal of toxicology, 2002. **21**: p. 95-142.
146. Graf, E., K.L. Empson, and J.W. Eaton, *Phytic acid. A natural antioxidant*. Journal of Biological Chemistry, 1987. **262**(24): p. 11647-11650.
147. Halla, N., et al., *Cosmetics preservation: a review on present strategies*. Molecules, 2018. **23**(7): p. 1571.
148. Langsrud, S., et al., *Ethylhexylglycerin impairs membrane integrity and enhances the lethal effect of phenoxyethanol*. PloS one, 2016. **11**(10): p. e0165228.
149. Robbins, C.R. and C.R. Robbins, *The physical properties of hair fibers*. Chemical and physical behavior of human hair, 2012: p. 537-640.
150. Cheung, T.L.V., *Uniform Color Spaces*. 2012, Springer, Berlin, Heidelberg.
151. Durmus, D., *CIELAB color space boundaries under theoretical spectra and 99 test color samples*. Color Research & Application, 2020. **45**(5): p. 796-802.
152. Hernández, B., et al., *CIELAB color coordinates versus relative proportions of myoglobin redox forms in the description of fresh meat appearance*. Journal of food science and technology, 2016. **53**: p. 4159-4167.
153. Zschuessler. *Delta E 101*. 2019; Available from: https://zschuessler.github.io/DeltaE/learn/.
154. Zhang, L., P. Yu, and X.-Y. Wang, *Surface roughness and gloss of polished nanofilled and nanohybrid resin composites*. Journal of Dental Sciences, 2021. **16**(4): p. 1198-1203.
155. Hanson, A., *Good practice guide for the measurement of gloss*. 2006.
156. Plumb-Reyes, T.B., N. Charles, and L. Mahadevan, *Combing a double helix*. Soft Matter, 2022. **18**(14): p. 2767-2775.
157. EM, C., *Observation of female scalp hair population, distribution and diameter*. J Soc Cosmet Chem, 1977. **28**: p. 219-229.
158. Thieulin, C., R. Vargiolu, and H. Zahouani, *Effects of cosmetic treatments on the morphology, biotribology and sensorial properties of a single human hair fiber*. Wear, 2019. **426**: p. 186-194.
159. Becker, L.C., et al., *Safety assessment of glycerin as used in cosmetics*. International journal of toxicology, 2019. **38**(3_suppl): p. 6S-22S.
160. Kamath, Y. and H.-D. Weigmann, *Measurement of combing forces*. Journal of the Society of Cosmetic Chemists, 1986. **37**(3): p. 111-124.
161. Singh, A., J.D. Van Hamme, and O.P. Ward, *Surfactants in microbiology and biotechnology: Part 2. Application aspects*. Biotechnology advances, 2007. **25**(1): p. 99-121.
162. Barreto, T., et al., *Straight to the Point: What Do We Know So Far on Hair Straightening?* Skin Appendage Disorders, 2021. **7**(4): p. 265-271.
163. Ezawa, Y., et al., *Stiffness of human hair correlates with the fractions of cortical cell types*. Cosmetics, 2019. **6**(2): p. 24.
164. Rogers, G., *Known and Unknown Features of Hair Cuticle Structure: A Brief Review. Cosmetics 2019*.

165. Feughelman, M. and M. Robinson, *The relationship between some mechanical properties of single wool fibers and relative humidity1*. Textile research journal, 1967. **37**(6): p. 441-446.
166. Tinoco, A., et al., *Keratin-based particles for protection and restoration of hair properties*. International journal of cosmetic science, 2018. **40**(4): p. 408-419.
167. Lima, C.R.R.d.C., et al., *DSC measurements applied to hair studies*. Journal of Thermal Analysis and Calorimetry, 2018. **132**: p. 1429-1437.
168. Giesen, M., et al., *Ageing processes influence keratin and KAP expression in human hair follicles*. Experimental dermatology, 2011. **20**(9): p. 759-761.
169. England, J.L. and G. Haran, *Role of solvation effects in protein denaturation: from thermodynamics to single molecules and back*. Annual review of physical chemistry, 2011. **62**(1): p. 257-277.
170. Anson, M., *Protein denaturation and the properties of protein groups*, in *Advances in protein chemistry*. 1945, Elsevier. p. 361-386.
171. Dissanayake, M., et al., *Denaturation of whey proteins as a function of heat, pH and protein concentration*. International Dairy Journal, 2013. **31**(2): p. 93-99.
172. Ji, Y., et al., *DFT-calculated IR spectrum amide I, II, and III band contributions of N-methylacetamide fine components*. ACS omega, 2020. **5**(15): p. 8572-8578.
173. Ghosh, A., *Vibrational coupling on stepwise hydrogen bond formation of amide I*. The Journal of Physical Chemistry B, 2019. **123**(37): p. 7771-7776.
174. Henry, D.G., J.S. Watson, and C.M. John, *Assessing and calibrating the ATR-FTIR approach as a carbonate rock characterization tool*. Sedimentary geology, 2017. **347**: p. 36-52.
175. Bellamy, M.K., *Using FTIR-ATR spectroscopy to teach the internal standard method*. Journal of chemical education, 2010. **87**(12): p. 1399-1401.
176. Mcmullen, R.L., G. Zhang, and T. Gillece, *Quantifying hair shape and hair damage induced during reshaping of hair.* J Cosmet Sci, 2015. **66**(6): p. 379-409.
177. Erfani, A., et al., *Effect of zwitterionic betaine surfactant on interfacial behavior of bovine serum albumin (BSA)*. Journal of Molecular Liquids, 2020. **318**: p. 114067.
178. Kisley, L., et al., *Soluble zwitterionic poly (sulfobetaine) destabilizes proteins*. Biomacromolecules, 2018. **19**(9): p. 3894-3901.
179. McMullen, R.L. and G. Dell'Acqua, *History of natural ingredients in cosmetics*. Cosmetics, 2023. **10**(3): p. 71.
180. Michalak, M., *Plant extracts as skin care and therapeutic agents*. International journal of molecular sciences, 2023. **24**(20): p. 15444.
181. Mansoor, K., et al., *Plants with cosmetic uses*. Phytotherapy Research, 2023. **37**(12): p. 5755-5768.
182. Paul, Z.A., et al., *Phytochemistry and pharmacological activity of Malva sylvestris L: a detailed insight*. Comb Chem High Throughput Screen, 2023. **10**(011386207326933623100911031 3).
183. Biodiversidade, M.V.d. *Malva sylvestris*. 2020; Available from: https://www.museubiodiversidade.uevora.pt/elenco-de-especies/biodiversidade-actual/plantas/angiospermicas/malva-sylvestris?utm_source=chatgpt.com.
184. F. Clamonte, C.A., P.V Araújo, M. Porto, D.T. Holyoak, A. Amado, J. Lourenço, J.D. Almeida, T. Monteiro-Henriques, A. Carapeto, P. Cardose, E. Marabuto. *Flora-on:*

Malva sylvestris. 2020 [cited 2025 23 June]; Available from: https://flora-on.pt/#1Malva+sylvestris.
185. Ouahhoud, S., et al., *Antioxidant activity, metal chelating ability and dna protective effect of the hydroethanolic extracts of crocus sativus stigmas, tepals and leaves*. Antioxidants, 2022. **11**(5): p. 932.
186. Institute, C.L.S., *CLSI M07*. 2024.
187. Chaves, N., A. Santiago, and J.C. Alías, *Quantification of the antioxidant activity of plant extracts: Analysis of sensitivity and hierarchization based on the method used*. Antioxidants, 2020. **9**(1): p. 76.
188. Attar, U. and S. Ghane, *Proximate composition, antioxidant activities and phenolic composition of Cucumis sativus forma hardwickii (Royle) WJ de Wilde & Duyfjes*. Int. J. Phytomed, 2017. **9**: p. 101-112.
189. Benso, B., et al., *Anti-inflammatory, anti-osteoclastogenic and antioxidant effects of Malva sylvestris extract and fractions: in vitro and in vivo studies*. PLoS One, 2016. **11**(9): p. e0162728.
190. SpecialChem. *Phytexcell™ Cucumber*. 2025 [cited 2025 22nd February]; Available from: https://cosmetics.specialchem.com/product/i-croda-phytexcell-cucumber.
191. Anis, N. and D. Ahmed, *Modelling and optimization of polyphenol and antioxidant extraction from Rumex hastatus by green glycerol-water solvent according to response surface methodology*. Heliyon, 2022. **8**(12).
192. van Acker, S.A., et al., *Influence of iron chelation on the antioxidant activity of flavonoids*. Biochemical pharmacology, 1998. **56**(8): p. 935-943.
193. Chen, Z., et al., *Exploring the correlation between the molecular structure and biological activities of metal–phenolic compound complexes: research and description of the role of metal ions in improving the antioxidant activities of phenolic compounds*. International Journal of Molecular Sciences, 2024. **25**(21): p. 11775.
194. Aaseth, J., G. Criponi, and O. Andersen, *Chelating Agents as Therapeutic Compounds—Basic Principles*. Chelation Therapy in the Treatment of Metal Intoxication, 2016: p. 36-37.
195. Juzeniene, A., et al., *Topical applications of iron chelators in photosensitizationBased on work presented at the 11th World Congress of the International Photodynamic Association in Shanghai, China, March 2831, 2007*. 2007.
196. Adjimani, J.P. and P. Asare, *Antioxidant and free radical scavenging activity of iron chelators*. Toxicology reports, 2015. **2**: p. 721-728.
197. Walencik, P.K., et al., *Metal–Flavonoid Interactions—From Simple Complexes to Advanced Systems*. Molecules, 2024. **29**(11): p. 2573.
198. Valacchi, G., *Chelating Agents in Skincare: Comprehensive Protection Against Environmental Aggressors*. JOURNAL OF DRUGS IN DERMATOLOGY, 2023. **22**(5): p. s5-s10.
199. Guo, B., et al., *Fruit extracts from Phyllanthus emblica accentuate cadmium tolerance and accumulation in Platycladus orientalis: A new natural chelate for phytoextraction*. Environmental Pollution, 2021. **280**: p. 116996.

200. Kejík, Z., et al., *Iron complexes of flavonoids-antioxidant capacity and beyond*. International journal of molecular sciences, 2021. **22**(2): p. 646.
201. Chaves, T.d. *As Águas Termais-Composição Química*. 2025; Available from: https://www.termasdechaves.com/as-aguas-termais.
202. Vlachodimitropoulou Koumoutsea, E., M. Garbowski, and J. Porter, *Synergistic intracellular iron chelation combinations: mechanisms and conditions for optimizing iron mobilization*. British journal of haematology, 2015. **170**(6): p. 874-883.
203. Varghese, A., et al., *Effects of the Nature of Metal Ion, Protein and Substrate on the Catalytic Center in Matrix Metalloproteinase-1: Insights from Multilevel MD, QM/MM and QM Studies*. ChemPhysChem, 2022. **23**(4): p. e202100680.
204. Kim, Y.-J., H. Uyama, and S. Kobayashi, *Inhibition effects of (+)-catechin–aldehyde polycondensates on proteinases causing proteolytic degradation of extracellular matrix*. Biochemical and biophysical research communications, 2004. **320**(1): p. 256-261.
205. Thring, T.S., P. Hili, and D.P. Naughton, *Anti-collagenase, anti-elastase and anti-oxidant activities of extracts from 21 plants*. BMC complementary and alternative medicine, 2009. **9**: p. 1-11.
206. Pientaweeratch, S., V. Panapisal, and A. Tansirikongkol, *Antioxidant, anti-collagenase and anti-elastase activities of Phyllanthus emblica, Manilkara zapota and silymarin: An in vitro comparative study for anti-aging applications*. Pharmaceutical biology, 2016. **54**(9): p. 1865-1872.
207. Yap, P.-G. and C.-Y. Gan, *Multifunctional tyrosinase inhibitor peptides with copper chelating, UV-absorption and antioxidant activities: Kinetic and docking studies*. Foods, 2021. **10**(3): p. 675.
208. Jakimiuk, K., et al., *Flavonoids as inhibitors of human neutrophil elastase*. Journal of enzyme inhibition and medicinal chemistry, 2021. **36**(1): p. 1016-1028.
209. Wittenauer, J., et al., *Inhibitory effects of polyphenols from grape pomace extract on collagenase and elastase activity*. Fitoterapia, 2015. **101**: p. 179-187.
210. Sharma, J., D. Sundar, and P. Srivastava, *Biosurfactants: potential agents for controlling cellular communication, motility, and antagonism*. Frontiers in Molecular Biosciences, 2021. **8**: p. 727070.
211. Aguirre-Ramírez, M., et al., *Surfactants: physicochemical interactions with biological macromolecules*. Biotechnology letters, 2021. **43**(3): p. 523-535.
212. Tani, H., et al., *Effect of methyl p-hydroxybenzoate on the culture of mammalian cell*. Drug Discoveries & Therapeutics, 2017. **11**(5): p. 276-280.
213. Neville, R., et al., *Preservative cytotoxicity to cultured corneal epithelial cells*. Current eye research, 1986. **5**(5): p. 367-372.
214. Ryu, Y.S., et al., *Particulate matter induces inflammatory cytokine production via activation of NFκB by TLR5-NOX4-ROS signaling in human skin keratinocyte and mouse skin*. Redox biology, 2019. **21**: p. 101080.
215. Wang, Y. and M. Tang, *PM2. 5 induces ferroptosis in human endothelial cells through iron overload and redox imbalance*. Environmental pollution, 2019. **254**: p. 112937.

216. Piao, M.J., et al., *Particulate matter 2.5 damages skin cells by inducing oxidative stress, subcellular organelle dysfunction, and apoptosis*. Archives of toxicology, 2018. **92**: p. 2077-2091.
217. Cavalli, G., et al., *Interleukin 1α: a comprehensive review on the role of IL-1α in the pathogenesis and treatment of autoimmune and inflammatory diseases*. Autoimmunity reviews, 2021. **20**(3): p. 102763.
218. Brown, M.M. and A.R. Horswill, *Staphylococcus epidermidis—Skin friend or foe?* PLoS pathogens, 2020. **16**(11): p. e1009026.
219. Gehrke, A.-K.E., C. Giai, and M.I. Gómez, *Staphylococcus aureus Adaptation to the Skin in Health and Persistent/Recurrent Infections*. Antibiotics, 2023. **12**(10): p. 1520.
220. Akiyama, H., et al., *Antimicrobial effects of acidic hot-spring water on Staphylococcus aureus strains isolated from atopic dermatitis patients*. Journal of dermatological science, 2000. **24**(2): p. 112-118.
221. Byrd, A.L., et al., *Staphylococcus aureus and Staphylococcus epidermidis strain diversity underlying pediatric atopic dermatitis*. Science translational medicine, 2017. **9**(397): p. eaal4651.
222. Ogonowska, P., et al., *Colonization with Staphylococcus aureus in atopic dermatitis patients: attempts to reveal the unknown*. Frontiers in microbiology, 2021. **11**: p. 567090.
223. Abdurrahman, G., et al., *The extracellular serine protease from Staphylococcus epidermidis elicits a type 2-biased immune response in atopic dermatitis patients*. Frontiers in Immunology, 2024. **15**: p. 1352704.
224. Chen, Z., et al., *The AhR-Ovol1-Id1 regulatory axis in keratinocytes promotes epidermal and immune homeostasis in atopic dermatitis-like skin inflammation*. Cellular & Molecular Immunology, 2025: p. 1-16.
225. D'Autréaux, B. and M.B. Toledano, *ROS as signalling molecules: mechanisms that generate specificity in ROS homeostasis*. Nature reviews Molecular cell biology, 2007. **8**(10): p. 813-824.
226. Kesisoglou, I., et al., *Discerning in vitro pharmacodynamics from OD measurements: A model-based approach*. Computers & chemical engineering, 2022. **158**: p. 107617.

Supplementary material

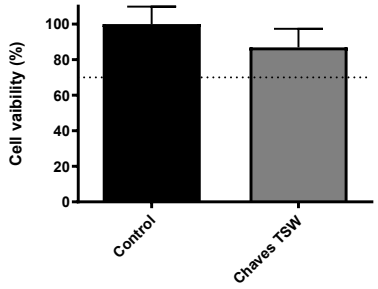

Supplementary Figure 1 Effect of Chaves thermal spring water on cellular viability in human keratinocytes (nHDF) after 24 hours incubation

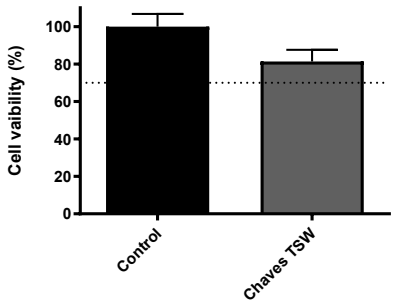

Supplementary Figure 2 Effect of Chaves thermal spring water on cellular viability in human dermal fibroblasts (HaCaT) after 24 hours incubation

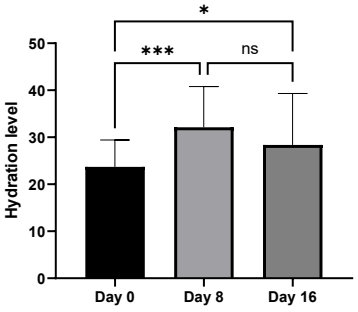

*Supplementary Figure 3 Hydration level of dry skin individuals up to 15 days of Chaves' TSW application. The results are represented as bar graphs (Average±SD). * and *** stand for $p < 0.05$ and $p < 0.0005$, respectively. ns, not significant ($p > 0.05$).*

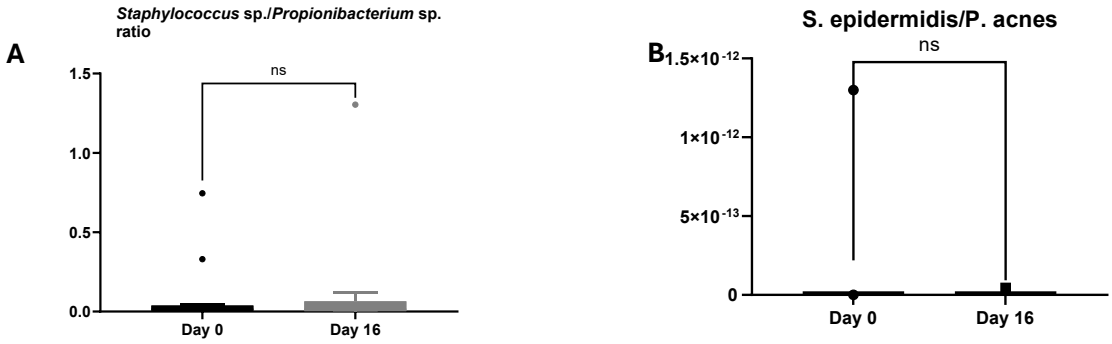

Supplementary Figure 4 (A) Staphylococcus sp/Propioniobacterium sp and (B) and S. epidermidis/P. acnes ratios when comparing both time-points of collection. The results are represented as bar graphs (Average±SD). NS, not significant (p > 0.05). Statistical analysis was performed using Mann-Whitney non-parametric test. NS, not significant (p>0.05)

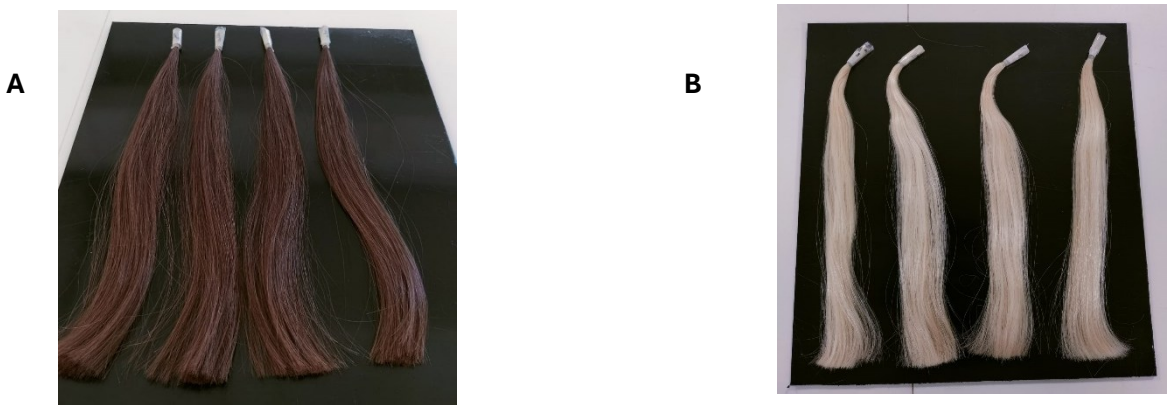

Supplementary Figure 6 Effect of the (A) Plant extracts and (B) Sodium Phytate on cellular viability in human dermal fibroblasts (nHDF) after 24 hours incubation. MP-Mallow and Cucumber extract; Fit-Sodium Phytate

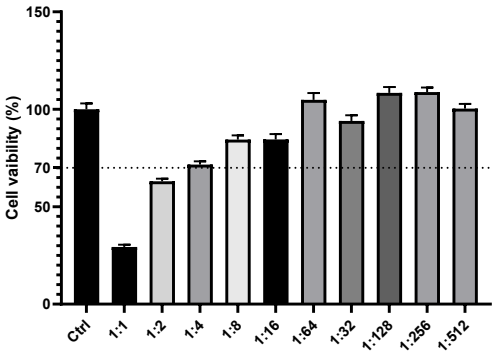

Supplementary Figure 5 Hair tresses (A) before and (B) after bleaching

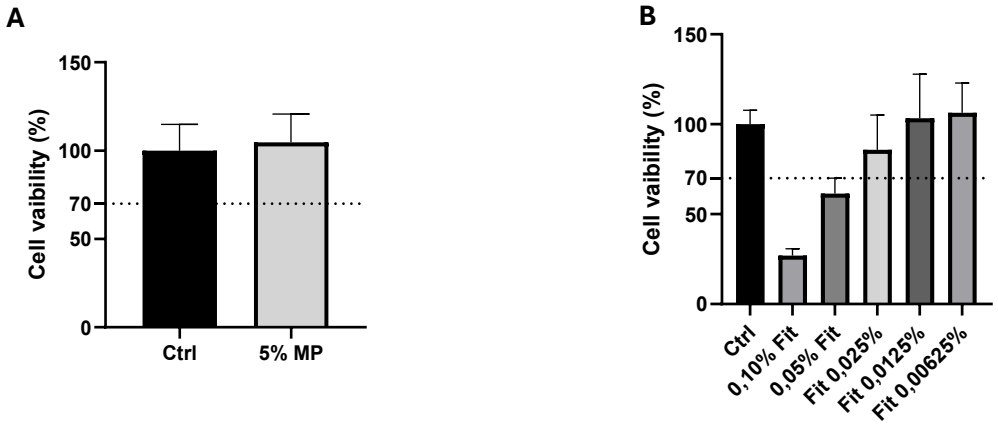

Supplementary Figure 7 Effect of the cucumber and mallow extract mixture (A) and sodium phytate (B) on cellular viability of Human keratinocytes. The values represent the dilutions of the supplemented medium. The dilution 1:8 that represents a concentration of 0,625% plant extract mixture and 0,0125% sodium phytate was selected for further testing

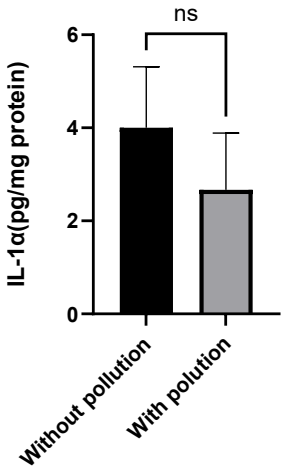

Supplementary Figure 8 Comparison between the IL-1 levels between the cells with and without the polution particles stimuli. The results are represented as bar graphs (Average±SD). NS, not significant ($p > 0.05$). Statistical analysis was performed using unpaired t-test. NS, not significant ($p>0.05$)

Supplementary Table 1 Test concentrations tested for the antimicrobial activity screening

Test Media	**Mallow and Cucumber Quantity (%(w/w))**	**Sodium Phytate (%(w/w))**
MP10-FIT0.20	10	0,20
MP9-FIT0.19	9	0,19
MP8-FIT0.16	8	0,16
MP6.5-FIT0.13	6,5	0,13
MP5-FIT0.10	5	0,10